UiA University of Agder

Master

Market Spillovers in the EU Emissions Trading System and Energy markets: A Connectedness Approach

REX TIM MATTHEW A. FONACIER

SANDER ØSTBY NORDBOTTEN

SUPERVISOR

JOCHEN A. JUNGEILGES

University of Agder, 2024

Faculty of Business and Law

Department of Economics and Finance

Acknowledgements

This thesis serves as the final part of our Master's degree in Business and Administration with a specialization in Analytical Finance at the University of Agder. We would like to express our sincere appreciation to our supervisor, Professor Jochen Jungeilges, for his guidance, knowledge, and feedback throughout this semester. We also want to thank him for allowing us to work independently on our thesis, to some extent, which greatly contributed to our learning and personal growth.

We would also like to express our gratitude to fellow students, family, and friends for their support throughout this incredible academic journey. Their encouragement and assistance have been invaluable, and we are deeply grateful for their unwavering belief in us.

Abstract

We analyzed the information spillover between carbon allowances, industries within the European Union Emissions Trading System, and global energy commodities from July 3, 2017, to February 1, 2024, using a generalized vector autoregression framework proposed by Diebold and Yilmaz (2012, 2014). Our findings suggest that carbon prices were primarily the recipients of shocks originating from other assets, with the Chemical index being the main driver in both the returns and volatility spillovers. The COVID-19 pandemic and the ongoing Russia-Ukraine war significantly influenced the interconnectedness of the assets in this study.

Keywords: Carbon credits, Emissions Trading System, Energy Markets, Dynamic Connectedness, Vector Autoregressive, Geopolitical Risk

JEL Classification C32, C58, G15, Q54

Contents

List of Figures

List of Tables

Chapter 1

Introduction

The Intergovernmental Panel on Climate Change urges us to limit global warming to 1.5 degrees Celsius. Achieving carbon neutrality by the mid-21st century is now a critical mission for all 194 nations and the European Union (EU) that pledged their commitment under the Paris Agreement (EuropeanParliament, 2023).

In 2015, an international agreement was established in Paris with the aim of limiting *"the increase in the global average temperature to well below 2°C above pre-industrial levels"* and pursue efforts *"to limit the temperature increase to 1.5°C above pre-industrial levels"* (UNFCC, 2024). This marked the first instance of a binding treaty designed to unite all participating nations in combating climate change. The agreement also outlined a framework for countries to facilitate the economic and social transformations necessary to achieve carbon neutrality.

The Kyoto Protocol, established in 1997, was an international agreement between 37 industrialized countries and the European Community aimed at reducing carbon dioxide (CO_2) emissions and other greenhouse gases (Newell et al., 2013). One of the key features derived from this agreement is the allocation of maximum carbon emission levels to participating countries for a given period. Any country exceeding its assigned emission limit incurs penalties in the following period. Moreover, the Protocol facilitates a carbon allowance trading system among nations. Over time, the total allocated carbon allowances are systematically reduced, putting pressure on businesses to find ways to reduce their carbon footprint (Newell et al., 2013; UnitedNations, 2024).

The European Union Emissions Trading System (EU ETS) is a part of EU's policy to re-

duce greenhouse gas emissions. It is the first major carbon market in the world and remains the largest. This system is a key tool for reaching the goals set under the Kyoto Protocol. The EU ETS is divided into four phases, Phase I of the EU ETS lasted from 2005 to 2007. This pilot project aimed to prepare and become more effective for Phase II. In Phase I, the focus was specifically on CO_2 emissions, targeting energy-intensive industries and power generators identified as major sources of greenhouse gas emissions. Initially, almost all emission allowances were allocated to businesses at no cost. A penalty of 40 euros per tonne was imposed on any businesses that exceeded their allocated allowances. The EU ETS succeeded in establishing a price for carbon as an economic tool to reduce greenhouse gas emissions. It facilitated free trade in emission allowances across the European Union, enabling a market-driven approach to control and reduce emissions effectively and efficiently. Critical to the success of the EU ETS was the development of a comprehensive infrastructure to monitor, report, and verify emissions from the businesses covered, ensuring transparency and accountability in the system (EuropeanCommission, 2024a).

Phase II of the EU ETS, spanning from 2008 to 2012, featured several key developments. Notably, there was a 6.5% reduction in the cap on allowances compared to 2005, signaling a stricter approach to emissions control. The phase welcomed Iceland, Liechtenstein, and Norway into the scheme and expanded its environmental scope by including nitrous oxide emissions from certain industries. The allocation of free allowances slightly decreased to about 90%, and several countries began auctioning allowances, marking a shift towards market-driven distribution. To reinforce compliance, the non-compliance penalty was raised to 100 euros per tonne. Businesses were given the option to purchase international credits, integrating the EU ETS more closely with global carbon markets. Administrative changes included the introduction of the Union registry and the European Union Transaction Log (EUTL) for enhanced emissions tracking. Additionally, the aviation sector was incorporated into the scheme from 2012, although some regulations were initially suspended for flights connected to non-European countries. The economic crisis in 2008 also played an important role on the demand of carbon allowances. This is because companies in distress prioritized other initiatives such as cutting costs over their climate commitments. Recessions reduce consumption, leading to overall lower market activity. This led to a surplus of allowances and credits, which influenced carbon prices heavily throughout Phase II (EuropeanCommission, 2024a).

Phase III, covering the period 2013-2020, introduced a new framework that changed the system considerably compared to Phases I and II. The total allowances were set based on the average total quantity of allowances issued annually in Phase II. The new framework in Phase III introduced five key changes to enhance its effectiveness. First, national caps within each nation were replaced by a single EU cap on emissions. Second, free allocation was largely replaced with an auction-based system. Third, there was a move towards harmonized allocation rules for the distribution of free allowances. Fourth, the framework added more sectors and gases. Finally, it supported the development of innovative renewable energy technologies and carbon capture and storage by allocating 300 million allowances to the New Entrants Reserves (EuropeanCommission, 2024a).

Phase IV of EU ETS, stretching from 2021 to 2030, is similar to Phase III but includes a few changes to further reduce greenhouse gas emissions. This period is also critical in terms of EU's goal of achieving climate neutrality by 2050, and a target of at least a 55% net reduction in greenhouse gas emissions by 2030. One of the key changes is the linear reduction factor of 2.2% annually, compared to phase III's 1.74%. The Union-Wide cap was kept; however, the fixed rule was employed in the ETS directive for phase IV (EuropeanCommission, 2024b).

Since the 1997 Kyoto Protocol and the Paris Agreement of 2015, many international carbon trading markets have emerged (CarbonCredits, 2024b). This development has transformed CO_2 emissions into a tradable, transferable right known as carbon credits. Carbon credits or carbon allowances give the holder permission to produce 1 metric tonne of CO_2 emissions. This transformation of CO_2 emissions can almost be traded like a commodity and follows a *'cap-and-trade'* system, where parties are permitted to trade with the carbon emission allowances provided by the authorities (Newell et al., 2013; UnitedNations, 2024). The pricing of carbon credits is primarily influenced by the market dynamics of supply and demand within regulatory frameworks. There are two pricing mechanisms for carbon pricing: carbon taxes and emissions trading systems. (1) A carbon tax imposes a rate on greenhouse gas emissions or on the carbon content of fossil fuels. (2) Companies that emit less than these caps are allowed to sell carbon credits to those exceeding their limits. The price of carbon credits can fluctuate based on factors such as policies, economic conditions, and technological advancements in emissions reduction. Additionally, there is also a voluntary carbon market where companies can purchase allowances to offset their emissions (CarbonCredits, 2024a).

The EU ETS specifically targets certain greenhouse gases from specific activities, emphasizing emissions that can be precisely reported and measured. Carbon dioxide is monitored in sectors such as electricity and heat generation, aviation within the European Economic Area, and maritime transport, including 100% of emissions within EU ports and 50% for those starting or ending outside EU ports. This approach is similarly applied for energy-intensive sectors like chemicals, acids, oil refineries, and the production of industrial materials. The EU ETS also tracks nitrous oxide (N_2O) from production of glyoxal, nitric, adipic and glyoxylic acids, as well as perfluorocarbons (PFCs) from aluminum production. Participation in the EU ETS is mandatory for these sectors (EuropeanCommission, 2024c).

Given the comprehensive coverage and mandatory participation, it is crucial to explore how carbon credits influence the sectors within the EU ETS and identify the main drivers of the returns and volatility in this system. This thesis is motivated by several papers on carbon dynamics. Research papers such as Batten et al. (2021), Ji et al. (2018), Jiang et al. (2024), Meng et al. (2024), and Wen et al. (2022) have primarily explored drivers of carbon allowances, price determination, and lead-lag relationships using energy commodities in their models.

Our study differs from previous research through the definition of *drivers*. We define these drivers as industries with high emissions participating in the Emissions Trading Scheme, and we also include global energy commodities. Our aim is to understand the interconnected dynamics within this framework. Thus, we investigate information spillovers from these industries and global energy commodities to the EU ETS carbon credits using the same methodology as Ji et al. (2018) and Jiang et al. (2024). We therefore expect parts of our results to be relatively similar to theirs. Furthermore, our study can provide decision-makers with insights into which industries are potentially the main drivers of sectors covered by EU ETS during periods of tranquility and crises. To this end, our thesis will utilize the Diebold and Yilmaz (2012) Connectedness framework and apply it to a sample that covers the COVID-19 pandemic and Russia's invasion of Ukraine. It is reasonable to expect that stocks in the same industry are correlated some degree, and some might even "share" their volatility. The purpose of this methodology is to evaluate and monitor these shares through the impact of shocks in one asset's risks on other assets.

This approach will allow us to measure the total interdependence or "connectedness" in a

dynamic system of random variables, such as the EU ETS, which covers several industries and is related only to producing greenhouse gas emissions. We will be able to identify and quantify the spillover effects of volatility among stocks within the EU ETS. This will also help us determine which industries are the main drivers and recipients of volatility, providing a clear picture of how interconnected these industries are, especially during periods of crises.

This study is also interested in testing three hypotheses. The first hypothesis centers around carbon credits. We wish to investigate whether carbon allowances contribute to connecting these energy-intensive sectors through carbon trading in terms of returns and volatility. The second hypothesis concerns energy commodities. Based on Ji et al. (2018), we expect Brent crude oil to play a pivotal role in driving carbon credits dynamics. The third hypothesis is that connectedness in volatility exceeds that in returns, also based on Ji et al. (2018).

Our contribution to the existing literature is twofold. First, we are the first to examine the influence of carbon credits on industries participating in the Emissions Trading Scheme using the connectedness approach supplied by Diebold and Yilmaz (2012). Second, we identified that the index for chemical commodities in Europe is the main driver of information spillover between assets in the system. This finding could potentially be of significant interest to EU policymakers and portfolio managers interested in diversification.

This thesis will continue by presenting previous literature on the intricate interplay between carbon markets, energy markets, geopolitical risk, and other markets in Chapter 2. In Chapter 3, we present our data base, encompassing both returns and volatility, and explain historical events, provide descriptive statistics and detailed data modification. The methodology will be detailed in Chapter 4, where we first introduce VAR, before deriving connectedness measures supplied by Diebold and Yilmaz (2012, 2014). In Chapter 5, we present our results, with tables and figures illustrating the connectedness measures. The discussion section in Chapter 6 will interpret and discuss our findings, compare them to other related studies and evaluate the adequacy of the underlying approximation model. Finally, Chapter 7 will summarize the conclusions of our thesis and suggest avenues for further research.

Chapter 2

Literature Review

Since greenhouse gas emissions became a concern and carbon markets had been established, carbon allowances have attracted several researchers seeking to determine the reasons behind carbon price fluctuations and their driving forces. Naturally, investigations have focused on the primary sources of greenhouse gas emissions, such as those from burning fossil fuels for transportation, given that over 94% of the fuel used for transportation is petroleum-based and consists of a mixture of Brent crude oil and natural gas (Agency, 2024; Britannica, 2024). Accordingly, this thesis collected research papers that examine the driving factors of carbon credits, the assets/commodities explaining the variations in carbon prices, and variables significantly influencing the determination and prediction of carbon credits prices.

Adekoya (2021), motivated by the predictive role of energy prices in forecasting EU carbon allowances, applied a Feasible Quasi Generalized Least Squares estimator to EU carbon allowance future prices and three energy commodities: Brent crude oil price, natural gas price, and coal price. These commodities are among the largest sources of energy consumption globally. This study, along with Aatola et al. (2013), underscores that the futures market for EU carbon market had a higher volume of investors than the spot market, making it less volatile. The findings reveal that all energy prices considered significantly predicted carbon allowance prices. Specifically, the asymmetric models for oil and coal prices had better forecast performance than their symmetric counterparts. For natural gas, the results appear mixed. This aligns with Alberola et al. (2008), who studied the daily price fundamentals of European Union Allowances (EUAs) in Phase I, along with the disclosure of a stricter Phase II. The findings reveal that natural gas and clean spark positively impacted EUA price changes, whereas coal and clean dark had negative effect. The study concludes by clearly identifying three types of carbon price fundamentals: institutional design issues,

energy prices and temperature events. However, the regression models utilized in the study exhibited low explanatory power (R-squared) between 13.27% and 36.94%. Batten et al. (2021), utilizing the same method, delved into the extent to which key energy prices (coal, gas, oil, and electricity) and weather explain carbon prices in the EU ETS. The results show that energy prices impact the carbon prices in Phase III. However, their model shows that only 12% of carbon price variation was explained. Weather variables did not affect the carbon prices except for unanticipated temperature changes. Extreme weather events, such as unusually cold winters, increased energy demand for heating, which leads to energy producers requiring additional EUAs and forcing the carbon price upwards.

Aatola et al. (2013), motivated by determining the prices of EU carbon allowances from 2005 to 2010, developed a theoretical equilibrium price model for the emissions trading market, in which risk-averse firms maximize their expected profits in the presence of an uncertain permit price. The model was tested empirically using daily carbon forward prices along with EU-related commodities and employed several econometric models (regression, instrumental variables, and VAR models) with multiple stationary time series. The findings show that approximately 40% of the price changes in carbon prices are explained by German electricity prices and gas and coal prices. Although their results are robust, they do not consider the non-linear characteristics of the carbon data, as highlighted by Alberola et al. (2008), Y. Liu et al. (2024), and Wang et al. (2023). Additionally, their results indicate that independent variables such as paper and steel have no significant effect on carbon prices on average.

Other papers, such as Chen et al. (2023) and Sousa et al. (2014), utilized the non-parametric thermal optimal path method and multivariate wavelet analysis to investigate lead-lag relationships between carbon allowances with other indices. Sousa et al. (2014) used spot data on EU ETS carbon prices, including prices for natural gas, coal, and electricity in Europe. The findings suggest that carbon spot prices lead the energy variables. Additionally, there is a simultaneous relationship between carbon and FTSE, with the FTSE slightly leading carbon. In contrast, Chen et al. (2023) found that the stock market leads the carbon prices in China on most trading days, but this relationship reverses when the carbon market returns are negative.

Following one of the objectives of this thesis, which is to uncover the interconnected dynamics across EU carbon allowances, EU-related industries, and energy commodities, we utilized the

Diebold and Yilmaz (2012) framework through a generalized variance decomposition (GVD), following Ji et al. (2018) and Wen et al. (2022) to help identify information spillovers. Ji et al. (2018) found that the biggest information receiver in the system is electricity prices. The study also found that the volatility system demonstrated a higher total connectedness than the returns system. In contrast, the findings in Wen et al. (2022) suggested that only 3-5% of volatility spillover comes from the stock market, coal, and oil prices, electric power index, market sentiment, economic and policy uncertainty, air quality, and extreme temperature. The main driving factors were market sentiment and air quality. The dynamic analysis suggested the main driving factors were heterogeneous and varied over the whole sample period.

The Diebold and Yilmaz (2012) approach is nonstructural and can have several underlying approximating models. For instance, Jiang et al. (2024) examined time-frequency connectedness by incorporating the Bahruník and Krehlik (2018) method to investigate the link between carbon markets, energy commodities, and geopolitical risk. The findings suggest that in the medium and long term, geopolitical risk displays positive net connectedness, but fluctuates in the short run. Total connectedness is higher during periods of high geopolitical risk, such as during COVID-19 and the Russia-Ukraine war. Additionally, in the short term, the carbon market influences geopolitical risk more than it is affected by it.

Similarly, Meng et al. (2024), using the same approach combined with Vine Copula function and TVP-VAR-DY, investigated the spillover effects and dynamic connectedness between international markets, carbon markets, and energy markets in China. The findings indicate a strong interdependence between the carbon and energy commodities. Brent crude oil plays an important role in impacting the other markets. Moreover, the time-varying characteristics of economic conditions and extreme events tend to correspond with the significant volatility spillover effects between the carbon and energy markets. Furthermore, the Chinese carbon emissions trading market reduces risk spillover in traditional energy markets during high volatility.

However, the connectedness framework has its drawbacks, as pointed out by Caloia et al. (2019) and Lastrapes and Wiesen (2021). First, Caloia et al. (2019) conducted a replication study of the Diebold and Yilmaz (2012) paper. The study recalculated the directional connectedness/spillover measures by applying them to the commodity market along with three financial markets, based on the generalized forecast error variance decomposition (GFEVD).

The results suggest that net spillover derived from the directional spillover is sensitive to the normalization method used in the framework when evaluating the contribution of one market to overall risk in the system. The paper also illustrates that for data processes with varying persistence and variance scalar-based normalization for GFEVD is better than the row normalization by Diebold and Yilmaz. This approach avoids ranking errors in net spillovers. Second, Lastrapes and Wiesen (2021) proposed an alternative approach to the total connectedness measure to avoid cross-correlation across variables. The study approached the replication through joint conditional forecast to decompose the forecasts error variance. The findings suggest that the connectedness framework overestimates information spillovers.

To summarize, several papers conducted in the past two decades have defined drivers according to their specific research problems. However, the majority of the research papers primarily focused on energy commodities as drivers of the EU carbon allowances, with the exception of Aatola et al. (2013), which utilized EU-related indices in his model. Furthermore, recent literature indicates that carbon exhibits non-linear characteristics, carbon future prices are better than spot prices in representing EU carbon allowances, and energy commodities play a role in driving carbon prices, including crises such as the COVID-19 pandemic and the Russia-Ukraine war. Lastly, the existing literature finds clear evidence supporting the notion that Chinese and European carbon markets function in different ways.

Chapter 3

Data

This chapter will begin by presenting the raw data, then outline the alterations made to obtain two sets of transformed data: returns and volatility, before implementing the statistical analysis in the methodology chapter. Finally, it will characterize the data through various tests to ensure robustness.

3.1 Data Description

Daily carbon prices are represented by Carbon Emissions Futures - Dec 24, which expire in December 2024 (hereafter carbon prices) and are traded on the Intercontinental Exchange (ICE). The decision to use EU carbon futures instead of spot prices was influenced by Adekoya (2021), who argued that the EU carbon futures market demonstrated superiority over the spot market in terms of trade volume and stability.

The driving factors[1] of the carbon price are selected by examining the EU ETS to identify specific activities from industries that are included and measurable and by reviewing other research mentioned in the literature review in Chapter 2 (EuropeanCommission, 2024c).

The following variables will represent the energy commodities. Brent Oil futures - Apr 24 represent the oil price in our data, and are future contracts that expire in April 2024. The prices represent one barrel of Brent Crude oil. Brent crude was selected because it is the leading global price benchmark for Atlantic crude oils. Natural Gas futures - Mar 24 (NG prices), future contracts that expire in March 2024, and one unit is measured in million British thermal units (MMBtu), reflecting how much energy the natural gas contains. Rotterdam Coal futures - Feb 24 (Coal prices) represent the price for one metric tonne of Rotterdam coal at a given time. The S&P Global Clean Energy Index (CE prices) tracks

[1]Electricity prices were excluded due to the inaccessibility of data.

the performance of companies worldwide involved in the clean energy sector.

The following index and stock prices will represent a type of driving factors that are highly influenced by carbon credits through the EU ETS. The STOXX Europe Total Market Airlines index (Aviation price) will represent the aviation sector in our analysis, as the index provides investors with a benchmark to track the performance of European airline stocks. The STOXX Europe 600 Food & Beverage PR (Food price) is a benchmark index that tracks the performance of European food and beverage companies. The STOXX Europe 600 Chemicals (Chemicals price) will represent chemical companies engaged in production, distribution, and other related services within the industry. The London Metal Exchange (Metal price) serves as the global hub for trading industrial metals, facilitating the majority of all futures transactions involving non-ferrous metals on its platforms. Finally, Cementir Holding is a multinational company that offers innovative building solutions. The company produce building materials and are one of the global leaders in white cement production. Table 3.1 provides an overview of these commodities.

Table 3.1: Price series from investing.com.

Commodity	Specification	Ticker	Length
Carbon	EUA ETS allowance, future price (EUR)	CFI2Z4	1694
Oil	Brent Crude Oil, future price (USD)	LCOJ4	1701
Aviation	Airlines index in Europe (EUR)	T5751P	1692
Natural Gas	Natural Gas, future prices (USD)	NGJ4	1739
Coal	Rotterdam Coal, future price (USD)	ATWMc1	1693
Clean Energy	Global Clean Energy index (EUR)	SPGTCTRE	1710
Chemicals	Index for chemical commodities in Europe (EUR)	SX4PEX	1672
Metal	Index for production of metal (EUR)	.LMEX	1664
Food	Index for production of food and beverage (EUR)	SX3P	1692
Cement	Cementir Holding, leading producer of cement in Denmark (EUR)	CEMI	1675

The frequency of all *Close*[2] prices is daily, ranging from July 3, 2017, to February 1, 2024. All prices were obtained from investing.com. Due to varying trading days, each price series has a different number of observations (see Table 3.1). Upon constructing the dataset to establish a common index date for all assets, a total of 508 missing observations were removed. This involved the exclusion of 109 dates accompanied by missing observations, which are listed

[2]investing.com labels Close prices as *Price*.

in Tables 8.3 and 8.4 in the appendix. Finally, the dataset comprised 1,634 observations for each asset.

3.2 Log Return

Following the approach of recent literature, we address the non-stationarity of price data. Financial data often exhibits right-skewed distributions, unstable variances, and statistical procedures later in the analysis require data with relatively constant mean levels and variances (Mills, 2019). To achieve these characteristics, we transformed all price series into natural logarithmic returns. The transformation involves taking the first difference of the price asset i at time t with its previous price at time *t-1*. Equation 3.1 illustrates this transformation and expresses the results in percentages.

$$R_{it} = \ln\left(\frac{\text{price}_{i,t}}{\text{price}_{i,t-1}}\right) * 100. \tag{3.1}$$

The sections below will explain each commodity, detailing the evolution of the price series, analyzing trends in the transformed data with time series plots, and illustrating the distribution of returns through histogram plots.

3.2.1 Carbon

The carbon prices increased from 2017 to 2020. According to Batten et al. (2021), the increased prices were due to the introduction of gradually full auctioning of allowances in the EU ETS Phase III, which started in 2013. The yearly allowance cap decrease of 1.74% in Phase III contributed to the increased prices. In 2020, carbon prices dropped due to COVID-19 but increased again as restrictions were eased. In 2021, the annual allowance cap was decreased by 2.2% instead of 1.74%, contributing to higher carbon prices. The conflict between Russia and Ukraine in 2022, caused a disruption in the supply of natural gas to Europe, prompting a resurgence in coal power generation. The revival of coal-fired power plants subsequently drove up the demand for carbon allowances (Su et al., 2023). Due to macroeconomic uncertainty and reduced volatility in global gas and power markets, carbon prices declined in the latter half of 2023, a trend that continued into the beginning of 2024 (CarbonCredits, 2024b).

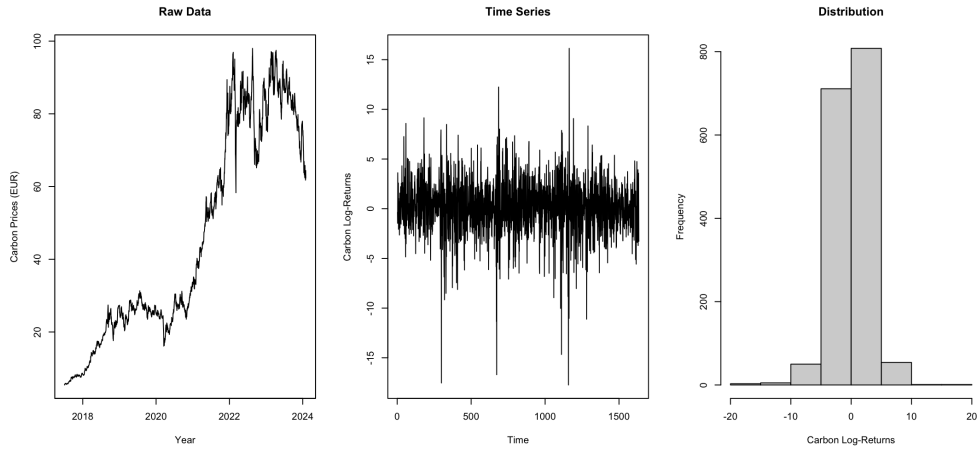

Figure 3.1: Carbon price series (left), time series plot (center), and the marginal log return distribution (right)

3.2.2 Oil

The prices of Brent crude oil increased in the second half of 2017, but 2018 turned out to be its worst year since 2015, with prices declining by 25% at the end of the year. The trade war between the US and China, rising interest rates, and a stock market plunge played pivotal roles in the price fall. Additionally, the sanctions imposed in November 2018 by former US President Donald Trump on Iran influenced the price, causing it to fall even further (DiChristopher, 2019). At the beginning of 2019, oil prices recovered from 2018 and remained relatively constant with some minor fluctuations. The price dropped significantly at the start of 2020, due to COVID-19 and significant economic uncertainty. Oil prices recovered, as it steady increased to minor fluctuations throughout 2020.

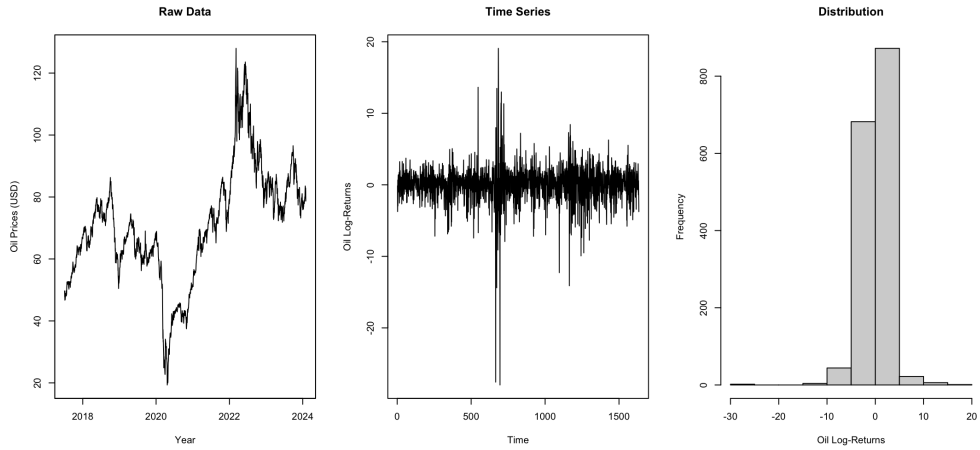

Figure 3.2: Oil price series (left), time series plot (center), and the marginal log return distribution (right).

According to Eia (2022a), higher vaccination rates from COVID-19, the loosening of pandemic-related restrictions, and a growing global economy resulted in increased oil prices during

2021 due to global petroleum demand grew faster than the supply. In the first half of 2022, prices peaked following Russia's invasion of Ukraine and low global crude oil inventories, resulting in low supply. The observed decrease in oil prices in the latter part of 2022 was predominantly attributed to diminishing demand, driven by escalating concerns regarding an impending economic recession (Eia, 2023). The EU's import ban of Russian crude oil and products, caused price fluctuations in the first half of 2023. In the second half of 2023, geopolitical tension and concerns about crude oil demand resulted in more price fluctuations (Eia, 2024a).

3.2.3 Aviation

The STOXX Europe Total Market Airlines Index began 2017 at a high price level and continued to increase throughout the year. As 2017 gave way to 2018, the index experienced record-breaking prices following a year of notable success (LufthansaGroup, 2018). However, the price index decreased during 2018 due to higher fuel costs and irregularities in flight operations (LufthansaGroup, 2019). The aviation industry faced numerous challenges in 2019. During the initial months, the industry saw a decline in prices attributed to sluggish economic expansion, uncertainties surrounding Brexit, and ongoing trade conflicts. However, as the year progressed, the industry's index rallied back, nearly reaching the same levels as those at the beginning of 2019 by the year's end (LufthansaGroup, 2020).

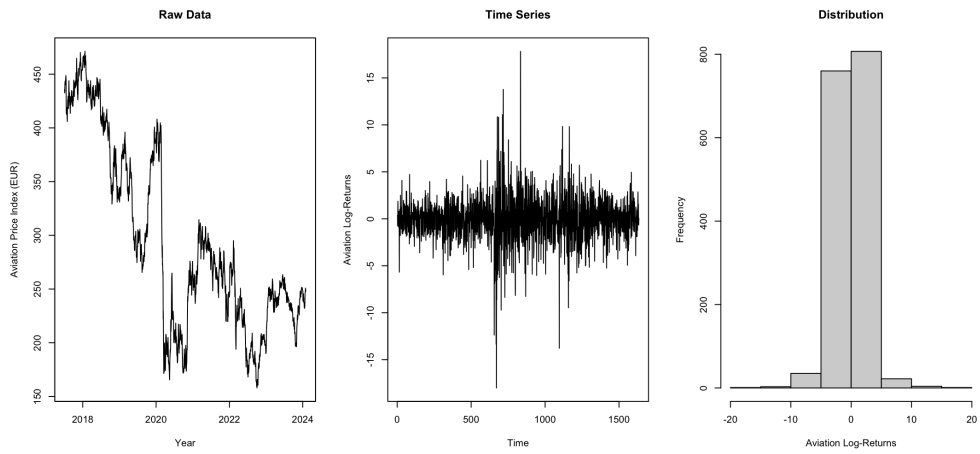

Figure 3.3: Aviation price series (left), time series plot (center), and the marginal log return distribution (right)

The outbreak of COVID-19 made 2020 a challenging year for the airline industry, and the price dropped significantly due to strict restrictions and market uncertainty. At the end of 2020, the easing of restrictions helped the index recover from the significant price drop (LufthansaGroup, 2021). During 2021, prices increased significantly as a result of ris-

ing vaccination rates and relaxation of travel restrictions drove demand for flights higher (LufthansaGroup, 2022). The beginning of 2022 was still influenced by COVID-19, and the prices dropped before recovering in the latter half of 2022 due to higher demand (LufthansaGroup, 2023). Throughout 2023, as the world gradually recovered from the pandemic, demand for flights increased. This led to a significant increase in prices, particularly during the summer months (LufthansaGroup, 2024).

3.2.4 Natural Gas

Natural Gas prices exhibited relative stability from mid-2017 to the end of 2018, with occasional fluctuations. A significant price spike was observed during the winter of 2018/2019 due to increased demand driven by cold temperatures (Eia, 2020). Prices declined through 2019, reaching an all-time low amid the COVID-19 pandemic in 2020. In 2021, prices rebounded due to tighter demand and supply balances and cold weather (Eia, 2022b). The ongoing conflict between Ukraine and Russia further increased the prices, peaking in 2022 as the supply of natural gas was tightened (Su et al., 2023). Throughout 2023, natural gas prices declined, reaching their lowest point since 2020 due to overproduction and milder winters (Eia, 2024b).

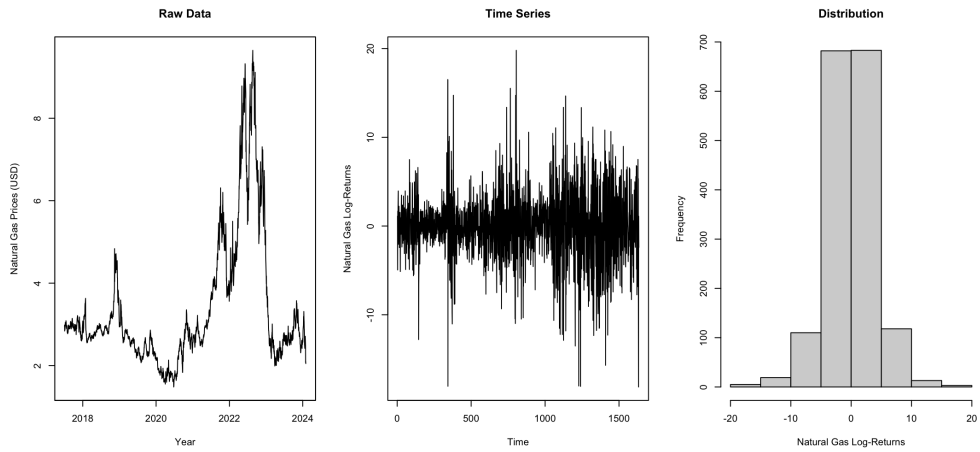

Figure 3.4: Natural Gas price series (left), time series plot (center), and the marginal log return distribution (right)

3.2.5 Coal

From 2015 to 2020, the transshipment of coal decreased by 44%, causing the prices to decline from 2017 through the COVID-19 pandemic in 2020. Due to rising gas prices in 2021, coal was used as an alternative for electricity production (PortofRotterdam, 2024). This increased

use of coal led to an all-time high in October 2021. However, due to swift policy actions from China the market was balanced by the end of 2021 (IEA, 2021). As the war between Ukraine and Russia caused even higher gas prices, more coal was used to produce electricity. Consequently, the demand for coal rose, pushing prices to their peak in 2022. Lower gas prices and a higher supply of coal led to a decline in coal prices in 2023 (IEA, 2023).

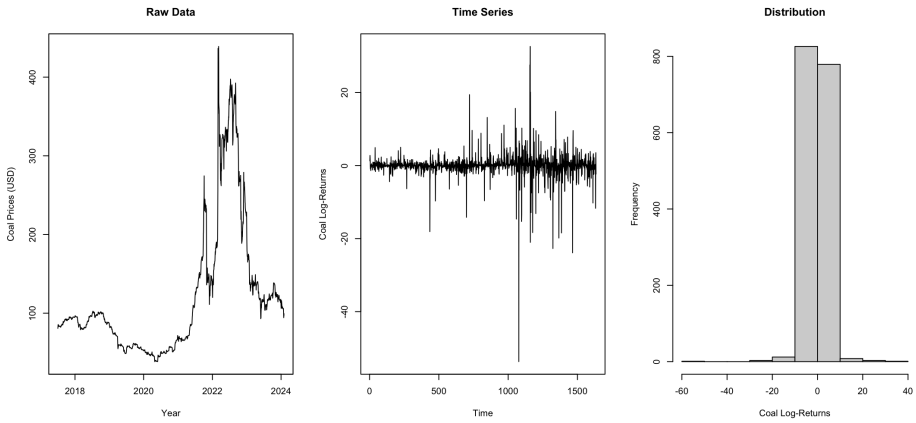

Figure 3.5: Coal price series (left), time series plot (center), and the marginal log return distribution (right)

3.2.6 Clean Energy

Clean energy prices remained constant through the second half of 2017 and 2018, with some minor fluctuations. Prices increased slightly in 2019, except for a minor decrease at the end of the year (Tiwari et al., 2023). In early 2020, reduced demand for energy and

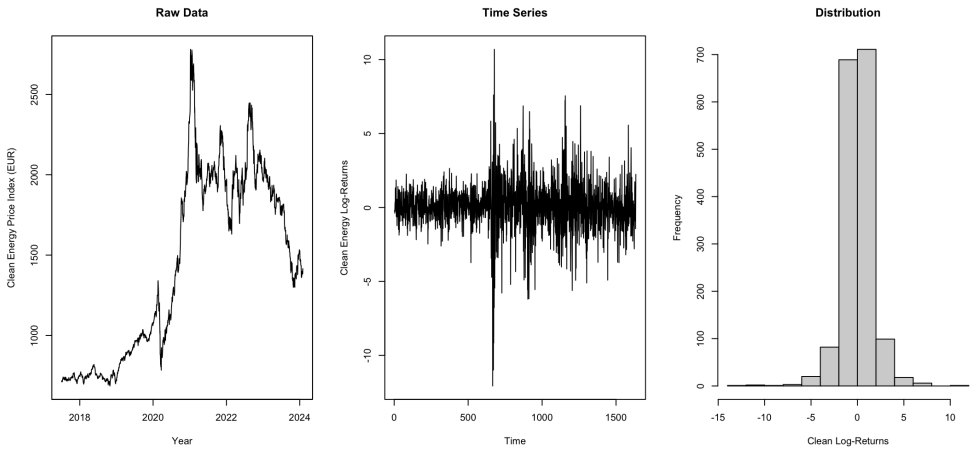

Figure 3.6: Clean Energy price series (left), time series plot (center), and the marginal log return distribution (right)

market uncertainty due to COVID-19 caused the prices to fall. Prices recovered in the latter half of 2020 as the international demand grew. The energy prices in the EU doubled from

December 2020 to December 2021. Increased import prices on energy in 2021 caused higher prices further into 2021 (EuropeanCouncil, 2024a). The Russia-Ukraine war pushed the gas prices to an all-time high in 2022, which led to higher clean energy prices. Heatwaves during summer 2022 pushed the prices even higher as demand for energy for cooling grew. Later in 2022 prices fell due to EU's transition away from dependency on Russian fossil fuels and a shift towards more clean energy sources (EuropeanCouncil, 2024a). Through 2023, the prices remained relatively stable with minor fluctuations and continued to do so at the beginning of 2024 (EuropeanCouncil, 2024b).

3.2.7 Chemicals

The price of the STOXX Europe 600 Chemicals index rose at the end of 2017, driven by strong economic growth in Europe and increased private consumption (Cefic, 2018). In 2019, prices fell compared to 2018 due to economic and political uncertainty affecting the chemical prices globally, as well as the Europe 600 Chemicals index (Cefic, 2020). The index decreased significantly in the first half of 2020 due to COVID-19 as chemical output was down 4.4% from January 2020 to September 2020 compared to 2019. At the end of the year, the price almost recovered from this price decreases (Cefic, 2021). The index continued to rise through 2021, recovering to pre-COVID-19 pandemic levels. High energy prices and economic uncertainty pushed the prices down in 2022, close to those of 2021 (Cefic, 2022). During 2023, the index was still influenced by high energy prices and geopolitical disruption. The price remained relatively stable, with some fluctuations through 2023 and in the first two months of 2024 (Cefic, 2024).

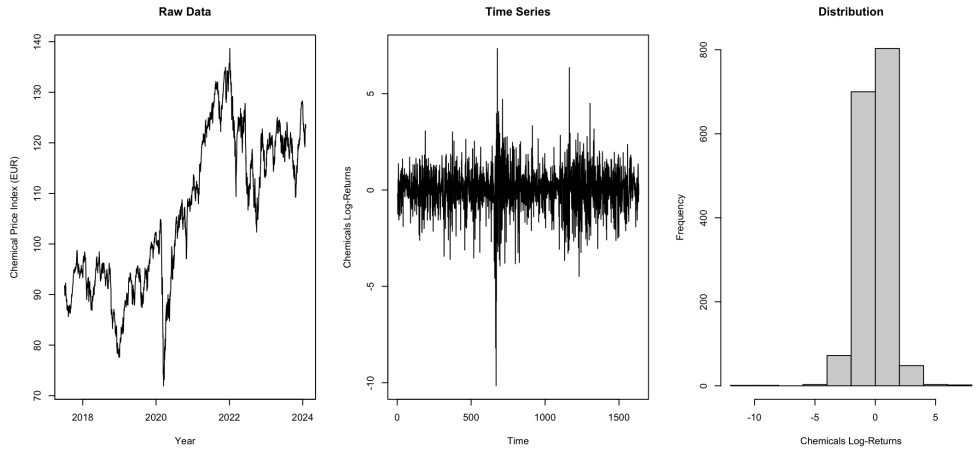

Figure 3.7: Chemicals price series (left), time series plot (center), and the marginal log return distribution (right)

3.2.8 Metal

Prices increased in the second half of 2017 due to higher total metal prices and sales prices for aluminum (Hydro, 2018). In 2018, prices decreased compared to 2017 due to higher raw material costs, which were partly offset by the higher all-in metal price (Hydro, 2019). Throughout 2019, prices slightly decreased but remained stable with small variations. This was due to reduced prices of aluminum and alumina, partially mitigated by reduced raw material expenses (Hydro, 2020). The COVID-19 pandemic of 2020 caused a considerable decrease in prices during the first half of the year. Despite these economic uncertainties, by the year's end prices had returned to pre-pandemic levels (Hydro, 2021). As global demand outpaced the metal supply, prices increased throughout the whole year in 2021 (Hydro, 2022). Prices increased even further in the beginning of 2022, but due to the Russia-Ukraine war, inflation, energy crisis, and global economic slowdown, the demand for metal significantly decreased. The price recovered at the end of 2022 (Hydro, 2023). In 2023 the prices on the index decreased due to war, inflation, and geopolitical rivalry, making it a difficult market to operate in (Hydro, 2024). At the start of 2024, the prices experienced fluctuations, but remained constant.

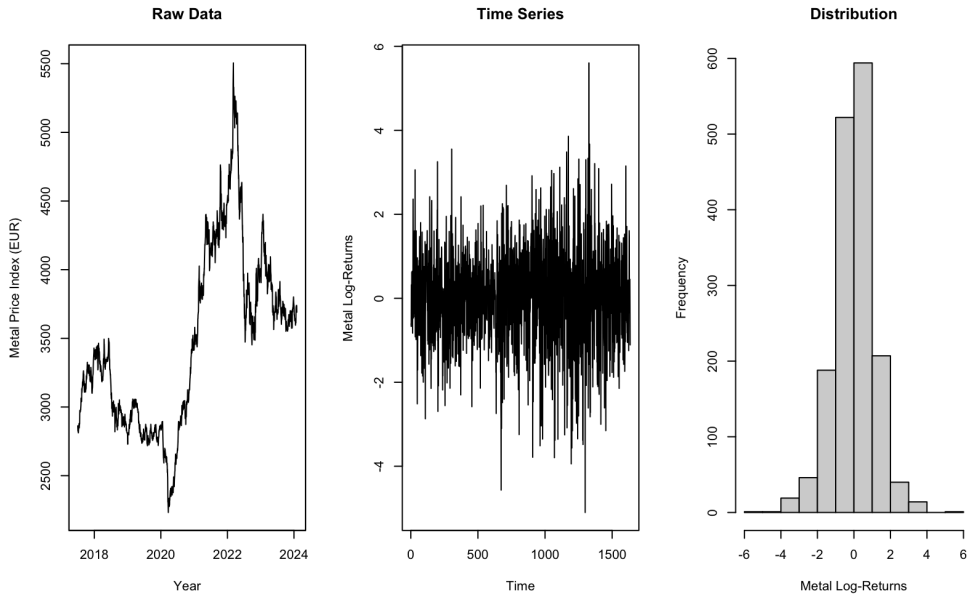

Figure 3.8: Metal price series (left), time series plot (center), and the marginal log return distribution (right)

3.2.9 Food

In the second half of 2017, prices for the STOXX 600 Food & Beverage index experienced a period of gradual increase, punctuated by minor fluctuations. However, at the beginning of

2018, prices decreased before rebounding in mid-2018, only to face another decrease towards the year's end. Throughout 2019, the index showed steady growth driven by rising demand outpacing supply, accelerated innovation, adoption of new technologies, and an increased focus on sustainability (Nestle, 2020).

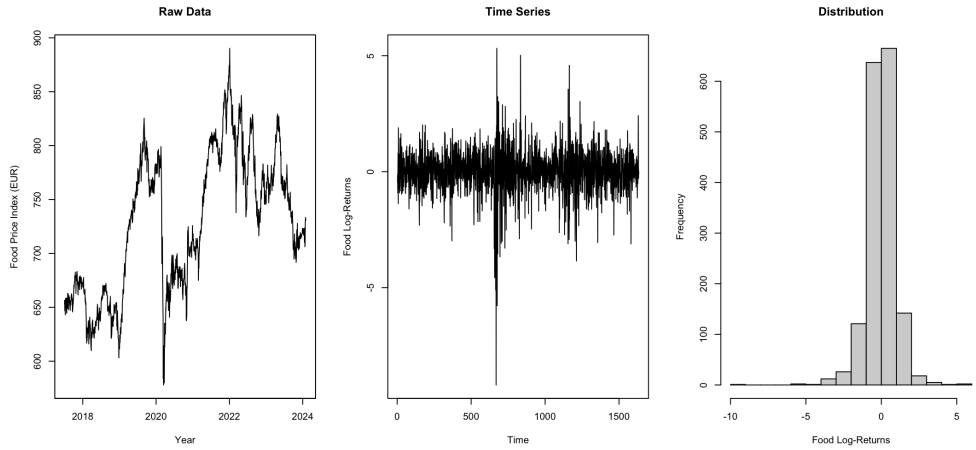

Figure 3.9: Food price series (left), time series plot (center), and the marginal log return distribution (right)

The onset of the COVID-19 pandemic in early 2020 caused a significant decline in prices due to market uncertainty. However, prices began to recover in the latter half of 2020 and continued to rise into 2021. By 2022, prices reached all-time highs but became increasingly volatile due to the Russia-Ukraine war (Benton et al., 2023). The year 2023 saw continued instability in prices, marked by fluctuations and an eventual decline towards the year's end. As of the beginning of 2024, prices have remained relatively stable, though with minor fluctuations.

3.2.10 Cement

The trajectory of Cementir Holding's stock price exhibited an upward trend from mid-2017, followed by a subsequent decline in early 2018. This fluctuation can be attributed to a confluence of factors, notably an enhancement in earnings in China, the United Kingdom, Norway, and Sweden. These positive developments in key regions served to counterbalance the diminished earnings observed in Turkey, Egypt, and Malaysia (CementirHolding, 2018). Throughout 2018, prices decreased due to worsening results in Egypt, caused by the war in Sinai, Turkey's economic situation and issues in Malaysia. The economic situation in Turkey influenced the performance of Cementir Holding in the second half of 2018 (CementirHolding, 2019). In 2019, prices recovered from the 2018 decline due to improved economic conditions in Turkey, offset by performance in other countries like Belgium, the Nordic and Baltic regions,

and Egypt (CementirHolding, 2020). In 2020, prices fell due to the COVID-19 pandemic but recovered to earlier levels. Prices increased significantly in 2021 due to markets recovering from COVID-19 and favorable weather conditions (CementirHolding, 2022). In 2022, the overall volume of cement decreased by 6% compared to the previous year. The export of white cement declined by 29% due to a redistribution in the United States, which was one of the main reasons for the price decrease in 2022 (CementirHolding, 2023). During 2023, prices increased following improved results in all geographical areas except the United States (CementirHolding, 2024).

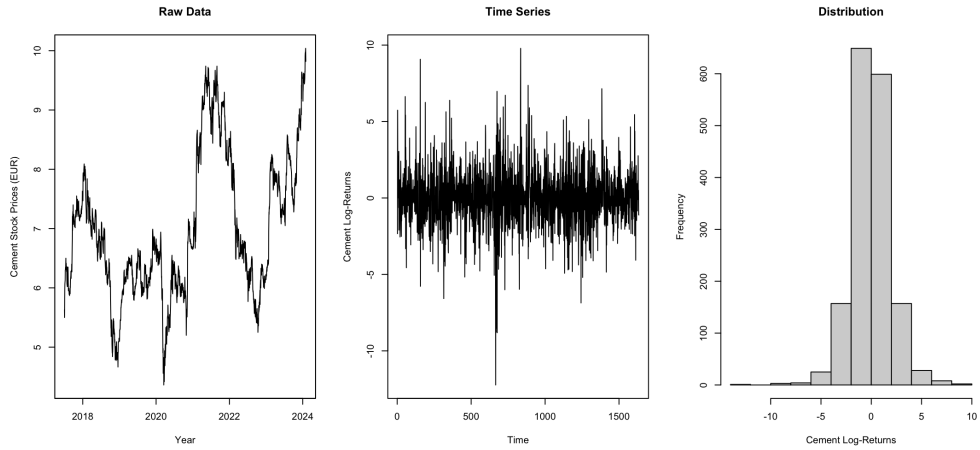

Figure 3.10: Cement price series (left), time series plot (center), and the marginal log return distribution (right)

3.3 Log Volatility

The daily volatility of the data was computed using Equation 3.2. The formula is revised, building upon several papers on range volatility, as summarized by Chou et al. (2015). Our paper employs logarithmic volatility, which approximates a standard Gaussian distribution (Chou et al., 2015). The formula is based on the method dating back to Parkinson (1980). However, since the retrieved prices from investing.com have the same values for *Price* (*Close*), *Open*, *High*, and *Low* prices, reflecting the specific price of a given financial metric over a defined period, proceeding with the same method would yield zero volatility. Therefore, we used the same method as calculating returns, taking the first differences for price i at time t with its previous price at time *t-1* to estimate the day-to-day price variation. Consequently, daily log standard deviation was calculated using Equation 3.3 in percentages.

$$\sigma_{it}^2 = \frac{1}{4 \ln 2} * (\ln \text{price}_{i,t} - \ln \text{price}_{i,t-1})^2 \tag{3.2}$$

$$\sigma_{it} = \sqrt{\sigma_{it}^2} * 100 \tag{3.3}$$

3.3.1 Carbon

Carbon daily log volatility had at least three periods with significant spikes, during the sample period. In 2017, carbon volatility hovered around 2%, punctuated by occasional larger fluctuations until 2019, attributed to a decrease in carbon allowances. Amid the COVID-19 pandemic in 2020, volatility surged to approximately 3%, characterized by substantial variation, before reverting to around 2% due to the easing of restrictions and reduced economic uncertainty. During 2021, carbon volatility remained relatively stable with minor fluctuations, only to experience higher spikes in 2022 as the carbon allowance cap decreased by 2.2% annually. From 2023 until 2024, carbon volatility remained around 2%.

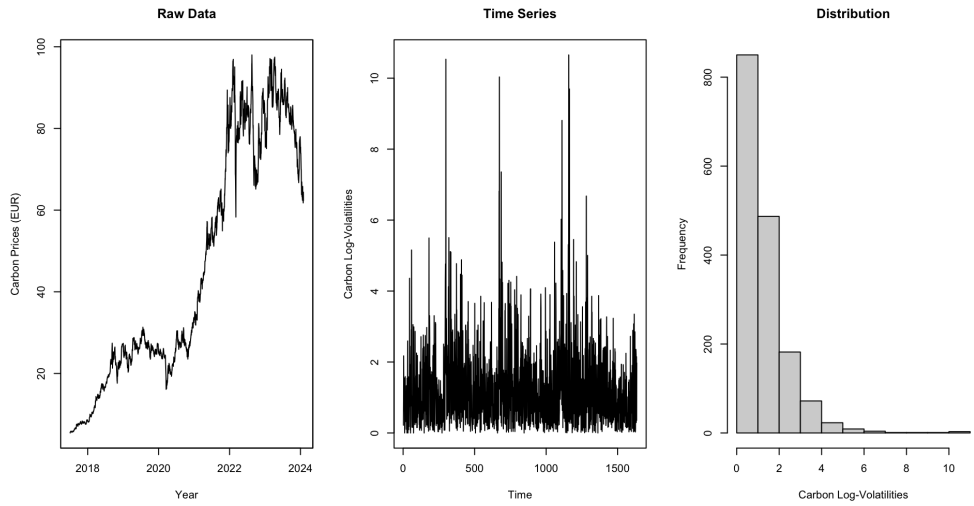

Figure 3.11: Carbon price series (left), time series plot (center), and the marginal log volatility distribution (right)

Figure 3.11 (right) illustrates the frequency of carbon volatility. The distribution of the carbon volatility is right-skewed, supported by Table 3.4 where the skewness is positive at 2.508 for carbon volatility. We note a high frequency of lower carbon volatility, evident from the tall bars on the left side of the histogram, while fewer occurrences of high volatility are observed on the right side of the histogram, though they do exist.

3.3.2 Oil

Oil volatility remained relatively stable around 1% between 2017 and 2018, with some minor variation. However, by the end of 2018, volatility increased to approximately 2.5% due to

restrictions imposed by the United States on Iran. Throughout 2019, oil volatility remained at a similar level to that of 2018. However, the onset of the COVID-19 pandemic in 2020 resulted in significant volatility spikes, pushing volatility to nearly 8%. After recovering from the pandemic, oil volatility remained at approximately 1% throughout 2021. In 2022, the outbreak of the war in Ukraine caused larger spikes and oil volatility reaching levels close to 4%. Subsequently, oil volatility decreased back to its 1% level with some minor spikes observed in 2023.

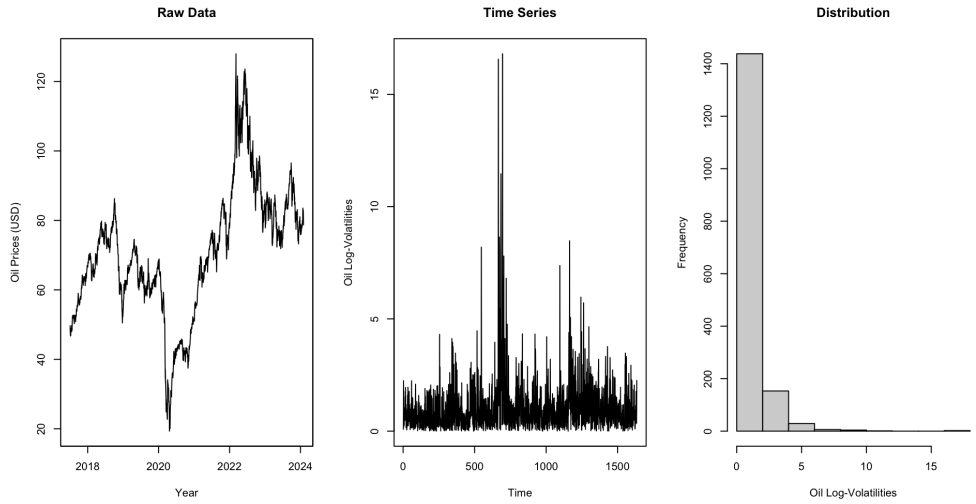

Figure 3.12: Oil price series (left), time series plot (center), and the marginal log volatility distribution (right)

3.3.3 Aviation

During 2017 and 2018, the volatility for aviation remained relatively stable at 1%, with minor fluctuations. In 2019, the aviation volatility increased to roughly 2% due to factors like slow economic growth, trade disputes and uncertainty surrounding Brexit. However, in 2020 the outbreak of COVID-19 increased aviation volatility to around 5% with large volatility spikes. Throughout 2021, the aviation volatility was decreased to around 1% as vaccination rates were growing and demand rising. In 2022, volatility increased to 3% with some higher spikes due to high demand in the market. The aviation volatility decreased to its previous level of 2% during 2023.

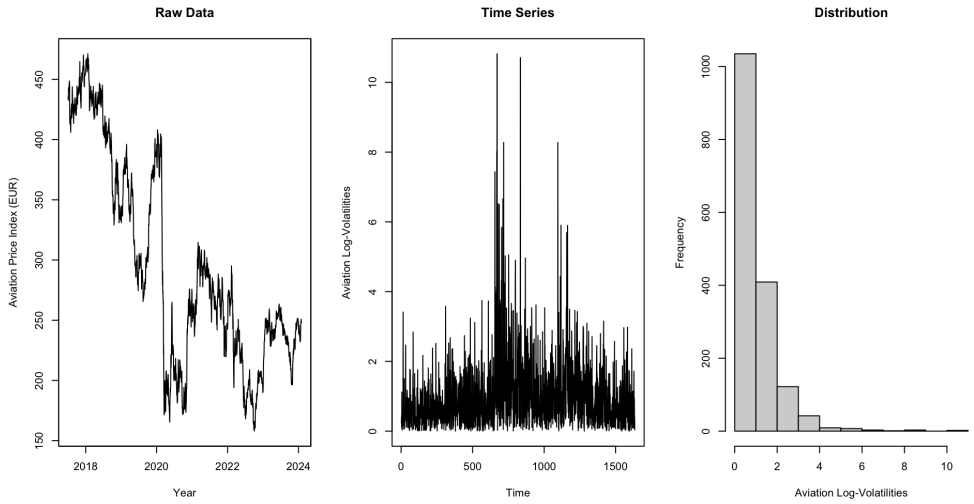

Figure 3.13: Aviation price series (left), time series plot (center), and the marginal log volatility distribution (right)

3.3.4 Natural Gas

The natural gas volatility experienced numerous spikes during the second half of 2017, with volatility measuring around 2%. In contrast, volatility decreased and stabilized to approximately 1% throughout 2018. However, it surged to 5% with large fluctuations in the winter of 2018/2019 due to higher natural gas prices resulting from cold weather conditions. During 2019, natural gas volatility decreased to 2% and remained relatively stable, except for minor variations.

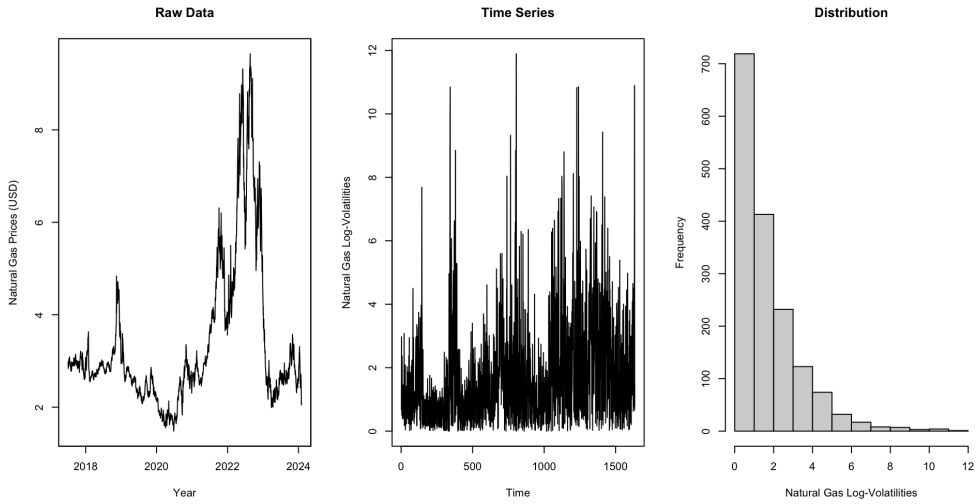

Figure 3.14: Natural Gas price series (left), time series plot (center), and the marginal log volatility distribution (right)

The breakout of COVID-19 in 2020 resulted in large natural gas volatility spikes, with volatility close to 3%. A tighter demand and supply balance, along with a cold winter, caused the natural gas volatility to approach 5% during 2021. In 2022, the Russian invasion

of Ukraine drove natural gas prices further upward, causing higher volatility characterized by significant spikes. Volatility remained at the 5% level during this period. In 2023, the level of volatility decreased from 5% to 4% and remained at this level at the start of 2024.

3.3.5 Coal

During the latter half of 2017, coal volatility remained relatively low, characterized by occasional small spikes, none of which exceeded 5%. This pattern persisted into 2018 and 2019, with minor volatility variation as coal transshipment was reduced by 44% in the period from 2015 to 2020. However, in 2020, a significant spike measuring coal volatility at 11% was observed, attributed to the COVID-19 pandemic. In 2021, coal volatility experienced a spike of approximately 12% due to rising gas prices. Coal was utilized for electricity production as an alternative to expensive gas. During 2022, the war in Ukraine drove gas prices up, leading to increased coal usage for electricity production. This resulted in significant coal volatility, with several spikes, some reaching 33% and 19%.

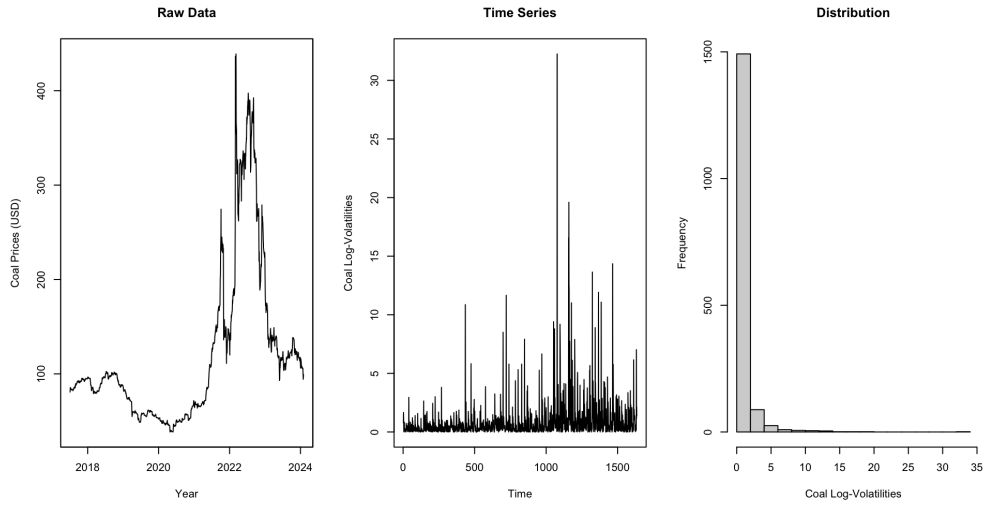

Figure 3.15: Coal series (left), time series plot (center), and the marginal log volatility distribution (right)

3.3.6 Clean Energy

The daily volatility of Clean Energy, illustrated in Figure 3.16, demonstrated stability during the latter half of the sample period, with standard deviation remaining under 2% until 2020. However, this was followed by periods of instability. Initially, there was a spike exceeding 2%, followed by the largest spike reaching up to 8%. In 2021, Clean Energy volatility was stable with minor fluctuations. Throughout 2023 and 2024, volatility remained stable, hovering

around 2%.

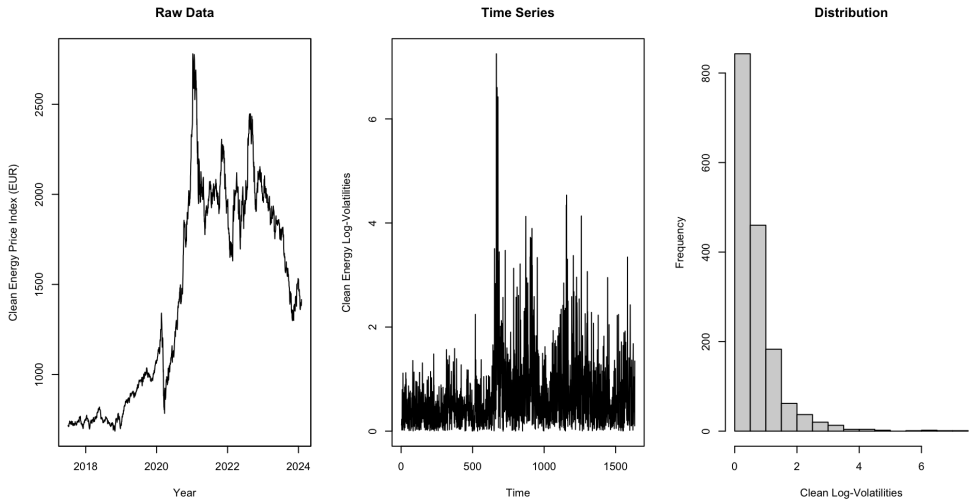

Figure 3.16: Clean Energy price series (left), time series plot (center), and the marginal log volatility distribution (right)

3.3.7 Chemicals

The daily volatility of Chemicals has been relatively stable throughout the sample period, majority of daily volatility was around 1%, occasionally reaching 2%. However, Chemicals experienced its largest spike in early 2020, coinciding with the global decline due to the COVID-19 pandemic. Following this, there was a period of relative stability until 2022, with volatility fluctuating around 3-4%. In 2023 and at the beginning of 2024, the volatility was lower, with minor fluctuations around 1%.

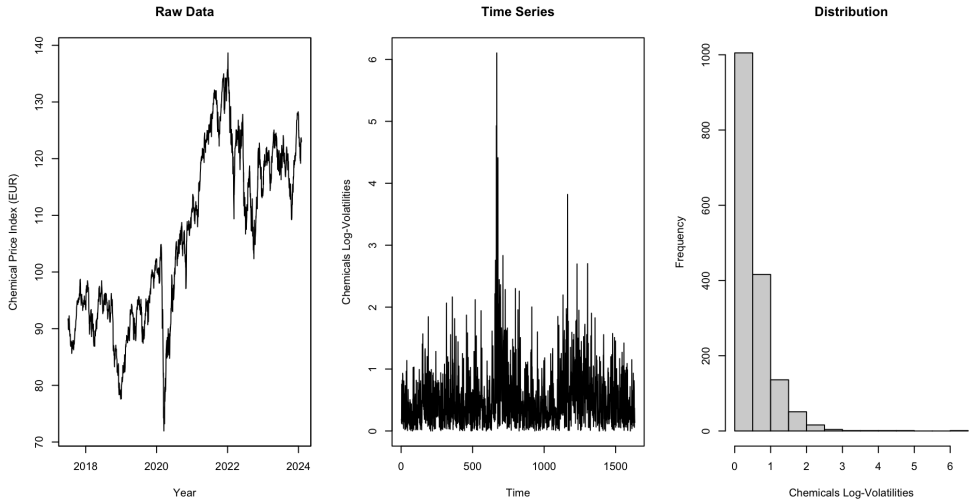

Figure 3.17: Chemicals price series (left), time series plot (center), and the marginal log volatility distribution (right)

3.3.8 Metal

Figure 3.18 illustrates the index for Metal production, indicating a range of volatility from 0.0% to 3.5%, making it one of the most stable assets in our dataset. The majority of daily volatility fluctuated between 0.5 % and 1.0 %, with occasional spikes above 2.0% throughout the sample period. Additionally, three significant spikes are observed. The first occurred in early 2020, attributed to the COVID-19 pandemic, while the other two were relatively close to each other at the end of 2023, due to factors such as war, inflation and geopolitical rivalry (Hydro, 2024).

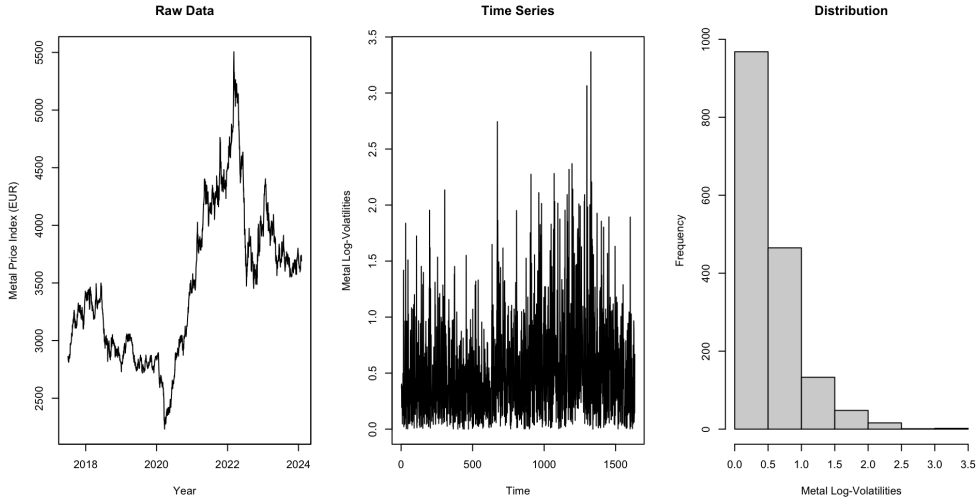

Figure 3.18: Metal price series (left), time series plot (center), and the marginal log volatility distribution (right)

3.3.9 Food

Throughout the sample period, food volatility remained stable, except for three notable periods characterized by major fluctuations. From 2017 to 2019, food volatility was relatively stable with minor fluctuations. However, in 2020, with the outbreak of COVID-19, there was a significant spike in volatility, reaching over 5%. During the period from 2021 to 2022, food volatility experienced two significant spikes, measuring 3% and 2.8%, respectively. Apart from these spikes, food volatility remained around 0.5%.

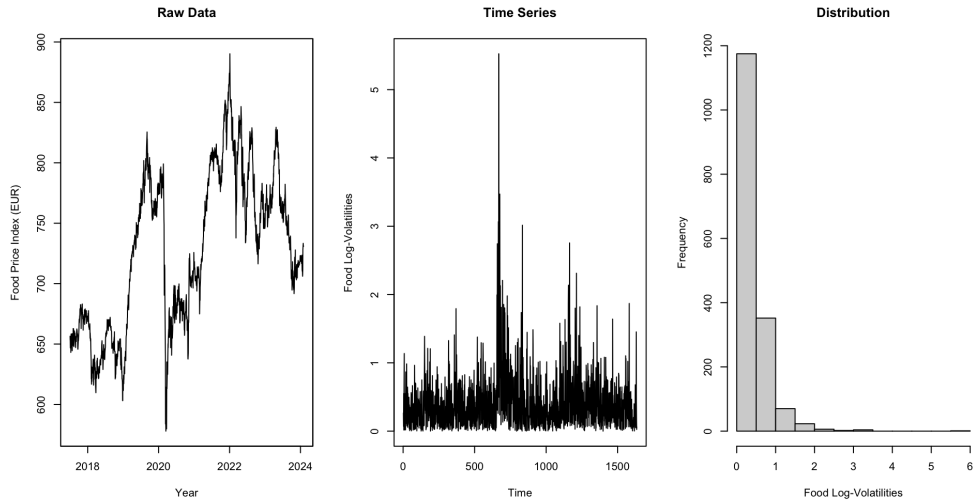

Figure 3.19: Food price series (left), time series plot (center), and the marginal log volatility distribution (right)

3.3.10 Cement

Lastly, Figure 3.20 illustrates the stock price of Cementir, an asset representing cement. Throughout the sample period, most daily volatility ranged from 0.5% to 1.0%. In the first half of the sample period, occasional spikes above 1.0% are observable, while in the latter half, spikes above 2.0% were more common. One significant spike, coinciding with others, also occurred during the COVID-19 pandemic.

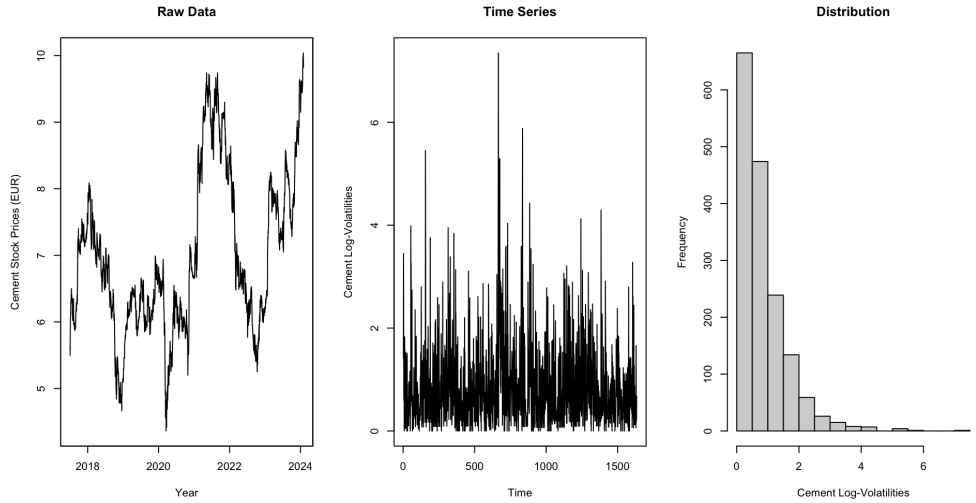

Figure 3.20: Cement price series (left), time series plot (center), and the marginal log volatility distribution (right)

3.4 Descriptive Statistics

This section reports summary statistics of both the return and volatility variables over the sample period.

3.4.1 Log Return

Table 3.2 shows the descriptive statistics of the log returns. All mean returns are positive, except for Aviation and Natural Gas; -0.034 and -0.022, respectively. Carbon has the largest mean return of 0.148. Coal and Food have the smallest mean returns of 0.011 and 0.007, respectively. In terms of variability, the standard deviation of Natural Gas and Coal returns exhibit the highest at 3.906 and 3.209, respectively. While Food and Metal returns are the most stable, at 0.949 and 1.127, respectively.

The third (skewness) and the fourth moment (kurtosis) are measures of symmetry and the heaviness of tails in the data distribution. All returns exhibit a negative skewness, indicating that most of the returns are located to the left of the mean. Coal returns are the most left-skewed (-2.556), reflecting a distribution with a longer left tail. This is also illustrated in Figure 3.5 (right). Cement returns are closest to zero, indicating that the distribution is the most symmetric (see Figure 3.10). As for the kurtosis, all assets have higher values than the standard Gaussian distribution, which is three, signifying heavier tails and a higher probability of extreme values compared to a normal distribution. Coal stands out with the highest kurtosis at 71.955, followed by Oil, indicating a leptokurtic distribution.

The minimum and maximum values report the range within which log returns fluctuated during the period. Coal displayed the broadest range with a minimum of -53.688 and a maximum of 32.622, indicative of its aforementioned higher kurtosis value.

A formal test for non-normality of distributions using the Jarque-Bera test was conducted. $H_0 : returns \sim N(\mu, \sigma)$ against the alternative hypothesis $H_a : returns \nsim N(\mu, \sigma)$. Given that H_0 is true, we reject the null hypothesis at 1% significance level for all variables, indicating that there is sufficient evidence to state that the data is not normally distributed. We employ four different stationarity tests for robustness, with the p-values reported in Table 8.1 in the appendix section. Following Elliott et al. (1996), we utilized the Augmented Dickey-Fuller (ADF) test. This test examines the null hypothesis positing the presence of a

Table 3.2: Descriptive statistics for returns

	Mean	Std	Skewness	Kurtosis	Min.	Max.	Jarque.Bera
Carbon	0.148	2.793	-0.518	7.506	-17.735	16.138	<0.01
Oil	0.028	2.648	-1.358	22.619	-27.976	19.077	<0.01
Aviation	-0.034	2.394	-0.118	10.290	-18.008	17.827	<0.01
Natural Gas	-0.022	3.906	-0.138	5.619	-18.136	19.798	<0.01
Coal	0.011	3.209	-2.556	71.955	-53.688	32.622	<0.01
Clean Energy	0.042	1.650	-0.392	10.522	-12.069	10.691	<0.01
Chemicals	0.018	1.195	-0.615	9.710	-10.161	7.344	<0.01
Metal	0.016	1.127	-0.162	4.388	-5.102	5.606	<0.01
Food	0.007	0.949	-0.862	12.092	-9.196	5.318	<0.01
Cement	0.034	1.918	-0.019	6.163	-12.230	9.787	<0.01

Note: The sample period is from July 2017 to February 2024.

unit root: $H_0 : \rho - 1 = 0$, against the alternative hypothesis suggesting the absence of a unit root: $H_A : \rho - 1 < 0$. We reject the null hypothesis at the 1% significance level, indicating all series are stationary. Phillips and Perron (1988) introduced a non-parametric version that is valid irrespective of serial correlation in the errors. The testing of null and the alternative hypotheses is the same as in the ADF test, and here we observe the exact same results: All series are stationary at 1% significance level.

The approach of Kwiatkowski et al. (1992) (KPSS), unlike the ADF test, tests for the presence of unit root; the KPSS test checks for stationarity around the deterministic trend and examines for stochastic trend component. The null hypothesis states that the series is stationary: $H_0 : \sigma_u^2 = 0$ against the alternative: $H_A : \sigma_u^2 \neq 0$, which suggests that the series has a unit root. *KPSS.level* test fails to reject the null hypothesis for all series, implying that all series have stationary attributes. Meanwhile, the *KPSS.trend* test checks for trend stationarity in the series. Here, the test fails to reject the null hypothesis for all series except for Coal, suggesting that Coal does not exhibit trend stationarity.

In summary, based on the conducted tests, we will assume that all series exhibit at least weak stationarity.

Using the Ljung-Box test proposed in Ljung and Box (1978), we examined white-noise processes in our time series to better understand the characteristics of our data. The null hypothesis states that there is no auto-correlation for lags up to i: $H_0 : \rho_1 = \rho_2 = \ldots = \rho_i = 0$, against the alternative hypothesis $H_a : \rho_i \neq 0$ for at least one. The choice of an appropriate lag length was based on a simulation study of Hassani and Yeganegi (2020). For time series

Table 3.3: Table of P-Values from the Ljung-Box Test Assessing Auto-Correlations at various lags.

	HA	SS	HY
Lag	**10**	**20**	**50**
Carbon	0.007	0.007	0.038
Oil	0.094	0.061	0.064
Aviation	0.000	0.000	0.002
Natural Gas	0.007	0.020	0.093
Coal	0.035	0.017	0.177
Clean Energy	0.000	0.000	0.000
Chemicals	0.000	0.000	0.000
Metal	0.319	0.367	0.213
Food	0.067	0.027	0.136
Cement	0.070	0.070	0.202

Note: The log returns of Carbon and its nine drivers.

with a length around 1000 and testing for a 5% significance level, Hassani and Yeganegi (2020) (HY) proposed 50 lags, while Shumway and Stoffer (2017) (SS) proposed 20, and Hyndman and Anthanasopoulos (2018) (HA) used a formula $min[10, T/5]$, where T is the length of the time series, to decide the optimal lag.

Since the optimal lag values differ according to HA, SS, and HY, we decided to use a combination of all three to better assess the existence of auto-correlations in our data. Table 3.3 reports the p-values from the Ljung-Box test at lags 10, 20, and 50. We reject the null hypothesis for Carbon, Aviation, Clean Energy and Chemicals at the given lags, indicating auto-correlation in the series and providing strong evidence against white noise. In contrast, for Oil, Metal, and Cement, we fail to reject the null hypothesis for all the given lags, suggesting a random process and indicating an efficient market. For Natural Gas and Coal, the null hypothesis is rejected at lags up to 10 and 20, but fails to be rejected at lags up to 50. This result indicates that the stationary series exhibit short-term correlations (Jungeilges, 2023a). Lastly, Food shows an alternating process: it fails to reject the null for lags up to 10, then rejects the null for lags up to 20, and then fails to reject it again for lags up to 50. This pattern indicates seasonal fluctuations (Jungeilges, 2023a).

3.4.2 Log Volatility

Table 3.4 reports the summary statistics for log volatility over the sample period. The mean volatility is positive for all assets, with Natural Gas exhibiting the highest mean at 1.687, followed by Carbon at 1.226. In contrast, Food demonstrates the lowest mean volatility at 0.399, with Metal and Chemicals showing a slightly higher values at 0.511 and 0.513, respectively. Coal and Natural Gas are the most volatile in the sample period with the highest standard deviations of 1.733 and 1.727, respectively. In contrast, Food and Metal are the most stable across all assets, with standard deviations of 0.408 and 0.443, respectively.

All variables exhibit positive skewness, suggesting a distribution heavily skewed to the right. This is also illustrated in the histograms in Section 3.3. Their high positive kurtosis indicates 'fat tails' compared to a normal distribution, meaning a higher probability of extreme deviations from the mean. The minimum values are zero since volatility cannot be negative and stem from absolute price changes, which are non-negative. While the maximum values are visible in the time series plots, observed as the biggest spikes in the figure.

Based on the Jarque-Bera test results there is a significant departure from normality for all assets. Here, $H_0 : volatility \sim N(\mu, \sigma)$ against the alternative hypothesis $H_a : volatility \nsim N(\mu, \sigma)$. Under the null hypothesis, we reject the null hypothesis at the 1% significance level for all assets, indicating that there is sufficient evidence to state that the data is not normally distributed.

Table 3.4: Descriptive statistics for volatility

	Mean	Std	Skewness	Kurtosis	Min.	Max.	Jarque.Bera
Carbon	1.226	1.149	2.508	14.872	0.000	10.656	<0.01
Oil	1.032	1.211	4.807	45.939	0.000	16.809	<0.01
Aviation	1.005	1.029	3.119	20.526	0.000	10.819	<0.01
Natural Gas	1.687	1.631	1.951	8.444	0.000	11.896	<0.01
Coal	0.844	1.733	7.530	93.923	0.000	32.258	<0.01
Clean Energy	0.674	0.727	3.094	18.834	0.000	7.252	<0.01
Chemicals	0.513	0.503	2.936	20.975	0.000	6.105	<0.01
Metal	0.511	0.443	1.611	6.597	0.000	3.368	<0.01
Food	0.399	0.408	3.381	26.370	0.000	5.525	<0.01
Cement	0.843	0.787	2.171	10.909	0.000	7.348	<0.01

Note: The sample period is from July 2017 to February 2024.

The same four stationarity tests are used as in Section 3.4.1. The results are presented in Table 8.2 (appendix). We obtained the same results for log volatilities as for log returns in

the Augmented Dickey-Fuller and Phillips-Perron tests. Given that the null hypothesis is true, we reject the null hypothesis at a 1% significance level, indicating that the volatility data is stationary. For the *KPSS.level* test, we fail to reject the null hypothesis for Carbon and Cement, suggesting that only these two out of ten series are stationary. Meanwhile, *KPSS.trend* test suggests that only Cement is stationary, while the other series exhibit the presence of unit-root.

Clearly, there is evidence of both stationarity and non-stationarity characteristics in the volatility data. Similar to the returns, we will proceed under the assumption that the data exhibit at least weak stationarity.

Table 3.5: Table of P-Values from the Ljung-Box Test Assessing Auto-Correlations at various lags.

	HA	SS	HY
Lag	**10**	**20**	**50**
Carbon	0.010	0.010	0.010
Oil	0.010	0.010	0.010
Aviation	0.010	0.010	0.010
Natural Gas	0.010	0.010	0.010
Coal	0.010	0.010	0.010
Clean Energy	0.010	0.010	0.010
Chemicals	0.010	0.010	0.010
Metal	0.010	0.010	0.010
Food	0.010	0.010	0.010
Cement	0.010	0.010	0.010

Note: The log volatilities of Carbon and its nine drivers.

Similarly, we conducted the Ljung-Box test to detect the presence of white noise. However, since this test is sensitive to the number of lags involved (Hassani & Yeganegi, 2020), we performed the test using optimal lag values, following a procedure similar to that used for the return data.

Testing for auto-correlations up to 10, 20, and 50 lags, the null hypothesis is that the auto-correlations are jointly zero: $H_0 : \rho_1 = \rho_2 = ... = \rho_{Lag=20} = 0$ against the alternative hypothesis $H_a : \rho_{Lag} \neq 0$ for at least one. Here, given that the null hypothesis is true, we reject the null hypothesis that auto-correlations up 10, 20, and 50 lags are jointly zero (Table 3.5). This indicates strong evidence against white noise in all series.

Chapter 4

Methodology

Having presented the data on return and volatility, this chapter will introduce the methodology that will enable us to analyze different measures of interdependence or *connectedness* within this data.

4.1 Methodology: Diebold and Yilmaz Framework

This thesis employs a methodology centered on constructing a network of connectedness, as proposed by Diebold and Yilmaz (2012). The generalized vector autoregressive framework is used to evaluate information spillovers, following similar methods in studies such as Ji et al. (2018) and Wen et al. (2022). This framework incorporates forecast-error variance decompositions that are invariant to the variable ordering and explicitly include directional spillovers. In this section, we first introduce the underlying model, which is the VAR model. Then, we demonstrate an enhanced method to interpret the results from a VAR model through network diagrams. Finally, we introduce the connectedness framework by Diebold and Yilmaz (2012).

4.2 Vector Autoregression

Vector autoregressive (VAR) models, popularized by Sims (1980), are a statistical framework for analyzing the dynamic linear interrelationships among multiple time series. A VAR model is an extension of the univariate autoregressive (AR) model, accommodating multiple interacting time series. Vector autoregressions are a useful tool for forecasting and studying how multiple time series evolve and interact over time. VAR models are a system of regression models. Each time series in a VAR model is treated as a function of its own previous values

and previous values of all others in the system, including an error term for each regression (Brooks, 2019).

For a system with k variables and a VAR of order p (VAR(p)), the model can be expressed in matrix form:

$$\begin{pmatrix} x_{1t} \\ x_{2t} \\ \vdots \\ x_{kt} \end{pmatrix} = \begin{pmatrix} \phi_{10} \\ \phi_{20} \\ \vdots \\ \phi_{k0} \end{pmatrix} + \phi_1 \begin{pmatrix} x_{1t-1} \\ x_{2t-1} \\ \vdots \\ x_{kt-1} \end{pmatrix} + \phi_2 \begin{pmatrix} x_{1t-2} \\ x_{2t-2} \\ \vdots \\ x_{kt-2} \end{pmatrix} + \cdots + \phi_p \begin{pmatrix} x_{1t-p} \\ x_{2t-p} \\ \vdots \\ x_{kt-p} \end{pmatrix} + \begin{pmatrix} \epsilon_{1t} \\ \epsilon_{2t} \\ \vdots \\ \epsilon_{kt} \end{pmatrix} \tag{4.1}$$

Simplified representation:

$$\mathbf{X}_t = \Phi_0 + \sum_{i=1}^{p} \Phi_i X_{t-i} + \epsilon_t \tag{4.2}$$

X_t denotes the time series vector at time t, with a dimension of $(k, 1)$, which includes carbon and the nine drivers ($k = 10$). X_{t-i} ($i = 1, 2, \ldots, p$) is the *i-th* lag of X_t. Φ_0 the constant $(k, 1)$ vector. Φ_i matrices represent the time-invariant coefficients of dimension (k, k). Lastly, ϵ_t the vector of error terms $(k, 1)$, assumed to be normally distributed with mean zero and covariance matrix, Σ, $\epsilon_t \sim N(0, \Sigma)$.

For later derivation purposes, we represent the VAR(p) in its compact form:

$$\Phi(L)^p X_t = \epsilon_t \tag{4.3}$$

Where $\Phi(L)^p = (I - \Phi_1 L - \Phi_2 L^2 - \cdots - \Phi_p L^p)$ is the matrix polynomial lag operator, with I being the identity matrix that summarizes all the past values of X_t up to p periods back on the current value of X_t.

Assumptions: Jungeilges (2023b) presented three pivotal assumptions for a VAR process:

- Assumption (1) The covariance matrix, Σ is positive definite. Implying a condition where $E(\epsilon_t \epsilon'_{t-i}) = 0$, residuals do not exhibit auto-correlations at lag i.
- Assumption (2) X_t is a weakly stationary process where $\mathbb{E}[X_t] = \mu_{(k,1)}$, $\mathbb{V}(X_t - \mu)(X_t - \mu)' = \Gamma_{k,k}$ are time-invariant. The time series variables are assumed to be weak stationary, indicating that their mean, variance, and covariance remain consistent throughout time.

- Assumption (3) Suppose the inverse matrix lag polynomial $(\Phi(L^p))^{-1}$ exists. This implies that all roots of $|\Phi(L^p)|$ are outside the unit circle, indicating X_t is weakly stationary. Any shocks to the VAR system will diminish over time, ensuring the model's stability.

4.2.1 Advantages and Limitations

There are several advantages linked to VAR models, due to their structure, which only accommodates endogenous variables. They produce estimations based on simultaneous calculations of all variables in the system, allowing the value of a variable to depend on more than just its own past values or combinations of white noise terms. VAR models are therefore able to capture more information from the data (Brooks, 2019). This results in a model with superior out-of-sample forecast accuracy relative to traditional structural models, as argued by Sims (1980).

VAR models have also drawbacks and limitations. Firstly, it is essential for all components of the VAR to be stationary, which contradicts one of the main purposes of VAR: examining relationships between endogenous variables. Inducing stationarity may discard long-term relationships. VAR models also lack a strong theoretical foundation, as they rely minimally on theoretical insights to guide model specification. Consequently, too many parameters in the system will not only lead to numerous equations but also to an increased risk of overfitting. This leads to uncertain interpretations of the coefficient estimates (Brooks, 2019). Lastly, determining the appropriate number of lags remains a challenge, although many researchers address this issue using various information criteria.

4.3 Motivation

Considering the limitations mentioned in Section 4.2.1, Diebold and Yilmaz (2012, 2014) developed a framework that capitalizes on the advantages of vector autoregressions while addressing their drawbacks. Their approach centers on the generalized variance decomposition of approximated VAR models. The goal is to derive measures of connectedness by evaluating the impact of *shocks* to variables on themselves and others over time. This framework enhances the interpretation of relationships among multiple time series in a VAR system. Additionally, by integrating their approach with network topology, they improved our understanding of spillover effects and interactions within VAR systems of higher dimensions

(Diebold & Yilmaz, 2014, 2015). This approach is exemplified in Section 4.4, illustrating how k variables in time series X_t in Equation 4.2 can be represented as a graphical network (see Figure 4.1).

4.4 Network Connectedness

A network consists of N nodes and L links connecting these nodes. It is represented by $N \times N$ adjacency matrix $\mathbf{A}$, which is filled with ones and zeros:

$$\mathbf{A} = (a_{ij}) \tag{4.4}$$

Matrix $\mathbf{A}$ reflects the network structure, where $a_{ij} = 1$ if nodes i and j are connected, and $a_{ij} = 0$ if there is no connection between i and j. Since matrix $\mathbf{A}$ is symmetric, a connection between i and j implies a connection between j and i as well. All the properties of the network are integrated into matrix $\mathbf{A}$ (Diebold & Yilmaz, 2015).

The Degree Distribution

The number of links a node has to other nodes is called *degree*, and the degree of node i is given by:

$$d_i = \sum_{j=1}^{N} A_{ij} \tag{4.5}$$

The degree of a node indicates its level of connection, and this attribute is unique for each node. By examining the degree distribution, we can understand the connectivity pattern across all nodes. The distribution consists of N distinct points and can be interpreted as a univariate distribution. A high mean degree indicates strong overall connectedness, whereas a low mean degree suggests weak overall connectedness. Thus, the degree distribution captures key elements of the connectivity across the entire network (Diebold & Yilmaz, 2015).

Network Plot

Figure 4.1 illustrates a graphical network consisting of four nodes, with varying degrees of connectivity. The size and color of the nodes vary based on their level of outgoing connectedness (Ji et al., 2018). Yellow nodes receive more connections than they give, while blue nodes give more connections than they receive. Thus, network plots visualize the relationships between connected nodes and the level of connectedness based on the thickness of the

outgoing lines. Furthermore, they can aid the interpretation of the elements presented in the *Connectedness Table* (discussed in Section 4.7), to further improve our comprehension of prevailing connectedness among the variables within the VAR system.

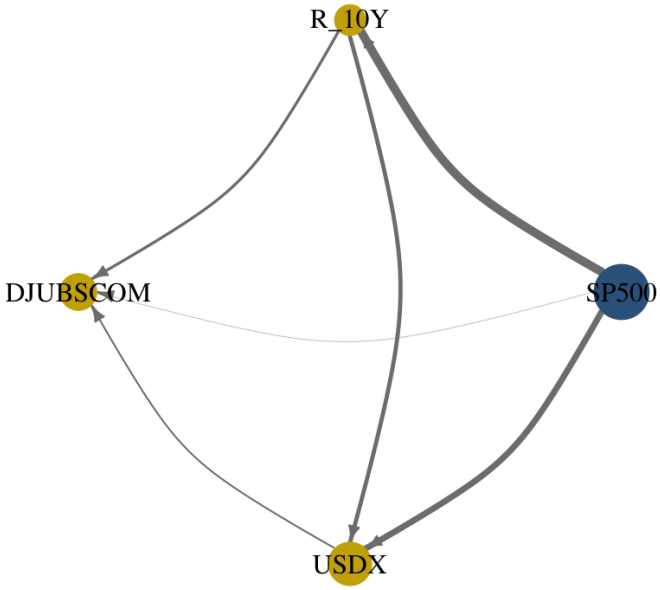

Figure 4.1: Illustration of a Network Connectedness plot, from Diebold and Yilmaz (2012)

4.5 Identifying Shocks

In a VAR environment, Brooks (2019) defines shocks using impulse responses, which trace out the responsiveness of a leading variable to unexpected changes in the variables in the equations with respect to the error term. The Diebold and Yilmaz (DY) framework is based on variance decomposition, predicting which fractions of H-step forecast error variance of variable i are due to *shocks* in other variables in the system.

4.5.1 Structural Shocks

Using the traditional variance decomposition on VARs, which assumes independent shocks and imposes an orthogonal structure, ensures that the variance of a weighted sum is the appropriate weighted sum of variances. This results in the terminology '*spillovers*' across individual assets with return characteristics, a transformation which better reveals the underlying relationship between variables (Diebold & Yilmaz, 2015). However, this method has two main drawbacks, as pointed out in Diebold and Yilmaz (2012): (1) Due to the orthogonal structure, the resulting variance decomposition is dependent on the ordering of variables. (2) The framework only addresses total spillovers in the system and does not

account for *directional* spillovers.

4.5.2 Correlated Shocks

The DY methodologically fills in the gaps through the generalized variance decomposition (GVD) of Koop et al. (1996) and Pesaran and Shin (1998). This approach solves the problem of variance decomposition's dependency on variable ordering, as the GVD framework does not require orthogonal shocks and allows for correlated shocks under normality assumptions. Consequently, all variables within the VAR system are treated as leading variables and are subject to shocks simultaneously. This facilitates the derivation of connectedness measures and the integration of network topology.

4.6 Deriving Connectedness

To present the essence behind the DY framework described in Diebold and Yilmaz (2012, 2014) and how they addressed the ordering problem identified in Diebold and Yilmaz (2009), we begin by deriving the spillover measure mentioned in Section 4.5.1. This measure assumes uncorrelated residuals from vector autoregressions (VARs) and utilizes the Cholesky factorization to impose orthogonality. By relaxing this assumption, we demonstrate how to derive network connectedness, as discussed in Section 4.4. We proceed in four main steps to establish the connectedness measures: (1) Estimation of the VAR model. (2) Conversion of the model into a moving-average representation. (3) Calculation of the variance decomposition using the orthogonalized impulse-response function. (4) Derivation of the generalized connectedness measures using the GVD matrix.

(1) The VAR(p): We first estimate a covariance stationary VAR of order p for k variables. The purpose is to estimate a model that is able to formulate lead-lag relationships in the returns and volatility systems of carbon and the nine drivers, VAR achieves this as mentioned in Section 4.2.

$$X_t = \Phi_0 + \sum_{i=1}^{p} \Phi_i X_{t-i} + \epsilon_t \tag{4.6}$$

- X_t represents the time series vector at time t, with a dimension of $(k, 1)$
- X_{t-i} is the *i-th* lag of X_t.
- Φ_0 is the constant $(k, 1)$ vector.

- Φ_i (for $i = 1, 2, \ldots, N$): represents the time-invariant coefficient matrix of dimension (k, k).
- ϵ_t the vector of error term $(k, 1)$, $\epsilon_t \sim (0, \Sigma)$.

Compact form:

$$\Phi(L)^p X_t = \epsilon_t \tag{4.7}$$

(2) From VAR(p) to MA(q): Assuming that the inverse matrix lag polynomial exists, (assumption 3 in section 4.2). We can express the VAR(p) model in an infinite moving-average (MA(q)) representation. This transformation is used to assess the magnitude of shocks from variable j to variable i. By converting the VAR(p) to an MA(q) representation, we express X_t as a function of past shocks ϵ_{t-i}, instead of past values, X_{t-i}.

Assumption 3: $\Phi(L^p)^{-1}$, then

$$X_t = \Phi(L^p)^{-1}\epsilon_t \tag{4.8}$$

We obtain the impulse-response function (IRF) of X_t

$$X_t = \mu + \sum_{i=0}^{q} \omega_i \epsilon_{t-i} \tag{4.9}$$

Compact form:

$$X_t = \omega(L)^q \epsilon_t, \tag{4.10}$$

with non-orthogonal shocks $E(\epsilon_t \epsilon_t') = \Sigma$ and $\omega(L)^q$ satisfies:

$$\begin{cases} \omega(L)^q = \Phi(L)^{-1} \\ \omega(L)^q = \omega_0 - \omega_1 L - \omega_2 L^2 - \cdots - \omega_q L^q \\ \omega_0 = I \end{cases} \tag{4.11}$$

The coefficient matrix ω_i $(i = 1, 2, .., N)$ of dimension (k, k) quantifies the influence of past innovations, ϵ_{t-i} on X_t and the impact of current innovations, ϵ_t on future realizations, X_{t+i}. However, in higher dimensions, comprehending the effect of correlated past innovations, $\epsilon_t - i$, on X_t can be complex. A transformation of the model is necessary.

(3) Variance Decomposition: Variance decomposition achieves a transformation that reveals the spillovers between variables, as discussed in Section 4.5.1. First, assuming uncorrelated error terms, we induce orthogonality through Cholesky's variance decomposition (Jungeilges, 2023b). Thus, obtaining the orthogonalized IRF of X_{it}, where the shocks are made uncorrelated.

$$X_{it} = \sum_{l=0}^{q} (\epsilon_i' \omega_l \mathbf{P} \epsilon_j)^2 \tag{4.12}$$

- e_i and e_j are basis vectors with unity at i and j.
- ω_l is the matrix containing the impact of ϵ_{t-i} on future x_t.
- $\mathbf{P}$ is the lower triangular matrix of the Cholesky factor of Σ; $PP' = \Sigma$.

Equation 4.12 describes the cumulative error of the forecast horizon q from a shock to variable i from variable j at time t_{t-i}. Thereafter, using the orthogonalized IRF on the entire set of variables and divide it by the total forecast error for a given variable. This results in the variance decomposition in Equation 4.13, where the sum of each rows are equal 1.

$$\theta_{ij}^{H} = \frac{\sum_{l=0}^{H} (\epsilon_i' \omega_l \mathbf{P} \epsilon_j)^2}{\sum_{l=0}^{H} (\epsilon_i' \omega_l \Sigma \omega_l' \epsilon_i)} \tag{4.13}$$

The numerator is simply Equation 4.12 - the orthogonalized IRF. The denominator is the *total* forecast error variance for variable i. This way, one can easily interpret the contribution of each shocks from variable j to the shocks for variable i. However, considering the limitations in Section 4.5.1, the dependency on the ordering of variables and the lack of consideration for directional spillovers, an alternative approach is necessary.

(4) Generalized Variance Decomposition DY addresses the ordering problem through the Generalized Variance Decomposition, as pointed out in Section 4.5.2. Since GVD does not require orthogonality, DY relaxed the assumption of uncorrelated error terms and approached the matter with unorthogonalized shocks under a normality assumption. Connectedness requires similar calculations as spillovers, except that the shocks in the IRF are no longer assumed orthogonal. Instead of using $\mathbf{P}$, which is the lower triangular matrix of Cholesky factor in Equation 4.12, the covariance matrix of the residuals, Σ, is used.

$$d_{ij}^{H} = \frac{\sigma_{jj}^{-1} \sum_{l=0}^{H} (\epsilon_i' \omega_l \Sigma \epsilon_j)^2}{\sum_{l=0}^{H} (\epsilon_i' \omega_l \Sigma \omega_l' \epsilon_i)} \tag{4.14}$$

Equation 4.14 expresses the directed connectedness from j to i. σ_{jj} being the standard deviation of the j-th component of X_t. Due to the correlated shocks, the sum of rows in the GVD matrices is not necessarily unity: $\sum_{j=1}^{H} C_{ij}^{H} \neq 1$. Therefore, to be able to use the information provided by the GVD matrix, DY normalized[1] each entry of the GVD matrix by the row sum, resulting in:

$$\hat{d}_{ij}^{H} = \frac{d_{ij}^{H}}{\sum_{j=1}^{N} d_{ij}^{H}} \tag{4.15}$$

Through the construction of $\sum_{j=1}^{N} \hat{d}_{ij}^{H} = 1$ and $\sum_{ij=1}^{N} \hat{d}_{ij}^{H} = N$.

4.7 Connectedness Measures

Diebold and Yilmaz (2012)'s approach to connectedness is based on investigating shares of forecast error variation in different locations subject to shocks arising elsewhere (Diebold & Yilmaz, 2014, 2015). This relates to the classical econometric notion variance decomposition. The forecast error variance of variable i is decomposed into fractions attributed to the various variables in the system. The *ij-th H-step* variance decomposition component, denoted by d_{ij}^{H}, represents the fraction of variable i's H-step forecast error variance due to shocks in variable j. Table 4.1 shows the full set of variance decompositions. All connectedness measures that we will present later - from simple pairwise to system-wide are based on the 'cross' variance decompositions, d_{ij}^{H}, $i, j = 1, 2..., N, i \neq j$. Here, we underline the importance of $i \neq j$ (Diebold & Yilmaz, 2014, 2015).

Table 4.1: Connectedness Table Schematic

	x_1	x_2	$\cdots$	x_N	From others
x_1	d_{11}^{H}	d_{12}^{H}	$\cdots$	d_{1N}^{H}	$\sum_{j=1}^{N} d_{1}^{H}, j \neq 1$
x_2	d_{21}^{H}	d_{22}^{H}	$\cdots$	d_{2N}^{H}	$\sum_{j=1}^{N} d_{2}^{H}, j \neq 1$
$\vdots$	$\vdots$	$\vdots$	$\ddots$	$\vdots$	$\vdots$
x_N	d_{N1}^{H}	d_{N2}^{H}	$\cdots$	d_{NN}^{H}	$\sum_{j=1}^{N} d_{Nj}^{H}, j \neq N$
To others	$\sum_{i=1}^{N} d_{i1}^{H}$ $i \neq 1$	$\sum_{i=1}^{N} d_{i2}^{H}$ $i \neq 2$	$\cdots$	$\sum_{i=1}^{N} d_{iN}^{H}$ $i \neq N$	$\frac{1}{N} \sum_{i,j=1}^{N} d_{ij}^{H}$ $i \neq j$

[1] Caloia et al. (2019) and Lastrapes and Wiesen (2021) criticized this 'arbitrary' normalization scheme, as detailed in Chapter 2.

4.7.1 The Population Connectedness Matrix

Table 4.1 shows a simple connectedness table. The main upper-left $N \times N$ block contains the variance decomposition matrix, which we denote as $D^H = [d_{ij}^H]$. The connectedness table expands D^H with the bottom-most row containing column sums, rightmost column containing row sums, and the bottom-right element containing the grand-mean, in all cases for $i \neq j$. Instantly, we are interested in the off-diagonal elements of D^H, which are parts of the N forecast error variance decompositions. From a connectedness perspective, they measure pairwise directional connectedness (Diebold & Yilmaz, 2014). Hence, the *pairwise directional connectedness* from j to i is defined as:

$$C_{i \leftarrow j}^H = d_{ij}^H \tag{4.16}$$

Diebold and Yilmaz (2014) pointed out that in general $C_{i \leftarrow j}^H \neq C_{j \leftarrow i}^H$. Hence, there are $N^2 - N$ separate pairwise directional connectedness measure. This is analogous to bilateral imports and exports for each of a set of N countries (Diebold & Yilmaz, 2015). This resembles the familiar territory of a bilateral trade balance between two countries, in which we are sometimes interested in 'net', as opposed to 'gross', pairwise directional connectedness (Diebold & Yilmaz, 2014). Instantly, we can define a *net pairwise* directional connectedness between variable i and j, as:

$$C_{ij}^H = C_{j \leftarrow i}^H - C_{i \leftarrow j}^H \tag{4.17}$$

There are $\frac{N^2-N}{2}$ net pairwise directional connectedness measures. Now, suppose we are interested in the total connectedness from other variables to variable i, or the total connectedness from variable i to other variables in the system. We then consider all the off-diagonal entries in Table 4.1, as each of these elements represents the share of the H-step forecast error variance. For instance, consider the first row. The sum of its off-diagonal elements yields the share of the H-step forecast error variance of variable 1 originating from influences in other variables. Thus, the sum of all off-diagonal row and column elements, labeled 'FROM others' and 'TO others' in the connectedness table, constitutes the total directional connectedness measure. Defining total directional connectedness from others to i as:

$$C_{i \leftarrow \bullet}^H = \sum_{\substack{j=1 \\ j \neq i}}^{N} d_{ij}^H, \tag{4.18}$$

and evidently, the total directional connectedness to others from j as:

$$C^H_{\bullet \leftarrow j} = \sum_{\substack{i=1 \\ i \neq j}}^{N} d^H_{ij}. \tag{4.19}$$

There are $2N$ total directional connectedness measures, N 'TO others' and 'FROM others' analogous to 'total exports' and 'total imports' for each of a set of N countries (Diebold & Yilmaz, 2015). Similar to pairwise directional connectedness, we are sometimes interested in net total effects. Hence, the *net total directional connectedness* is defined as $C^H_i = C^H_{\bullet \leftarrow i} - C^H_{i \leftarrow \bullet}$. There are N net total directional connectedness measures, also analogous to the total trade balances of each of a set of N countries (Diebold & Yilmaz, 2015). Lastly, the grand total of the off-diagonal elements in D^H measures *total system-wide connectedness*, which is equivalent to the sum of 'FROM others' column or 'TO others' row (Diebold & Yilmaz, 2014, 2015). We define it as:

$$C^H = \frac{1}{N} \sum_{\substack{i,j=1 \\ i \neq j}}^{N} d_{ij}. \tag{4.20}$$

There exists only one total connectedness measure, as total connectedness maps a system into a single number. Through the connectedness table, it is clear how Diebold and Yilmaz (2014) approached connectedness measures at all levels - from the most disaggregated connectedness measures, such as firm-level pairwise directional, and aggregated them in several ways to obtain macroeconomic economy-wide total directional and total connectedness (Diebold & Yilmaz, 2015).

4.8 Rolling Window Estimation

One of the limitations concerning VAR models - the requirement for time series to be stationary and the potential loss of long-term characteristics, as discussed in Subsection 4.2.1. We incorporated a rolling window approach to capture the dynamic relationships in the data. The purpose is to monitor time-varying connectedness with chosen window size w throughout the sample period. The width of the rolling window depends on the sample size. Specifically, the window width w represents the number of consecutive observation per rolling window. In each time period, the model is estimated and the connectedness measures are calculated using only data from the most recent w periods. The benefit of the rolling window approach is that it offers a straightforward way to detect underlying parameter mechanisms that change over time. The disadvantage is that the window length needs to be interpreted

with caution, as large windows can produce 'oversmoothing', while too short windows can produce 'undersmoothing', in a way that is directly comparable to selecting the bandwidth in density estimation (Diebold & Yilmaz, 2015).

4.9 Computations in R

All data handling, statistical analyses, and visualizations in this study used *RStudio* version 2023.12.1+402. The following packages, such as *MTS*, *zoo* and *ConnectedApproach*, were used to implement our chosen methodology on ten different variables.

As mentioned, our dataset contained 508 missing values distributed across different dates in the whole sample period, rendering it an irregular time series. The *zoo* function unified our data matrix under a shared index, aligning all variables to a consistent time frame.

The *MTS* package by Tsay (2013) provides the *VARorder()* function for performing lag length selection. The function calculates several information criteria and the sequential Chi-square statistics for a vector autoregressive process (Tsay, 2013).

We determined the appropriate lag order using the Akaike Information Criterion (AIC), as proposed by Akaike (1974). Utilizing the *VARorder()* function, lag 1 and lag 5 minimize the AIC for the returns and volatility, yielding values of 11.614 and -5.0836, respectively. This resulted in obtaining VAR(1) for the returns and VAR(5) for the volatility.

For the connectedness horizon, we chose $H = 10$ following the majority of the literature. This choice also aligns with the 10-day value at risk required under the Basel Accord (Diebold & Yilmaz, 2015).

To carry out connectedness measures by Diebold and Yilmaz (2012), we utilized the *ConnectednessApproach* package by Gabauer (2022). This package can be used to perform several statistical analyses to estimate both static and dynamic connectedness measures. Table 4.2 illustrates the plot functions used in our method to display our results.

Table 4.2: Plot Functions in R

Function	Description
PlotNetwork	Visualize net pairwise or pairwise connectedness measures between nodes.
PlotTCI	Visualize dynamic total connectedness.
PlotNET	Visualize dynamic net total directional connectedness.

Note: Overview of plot functions from the *ConnectednessApproach* package.

4.9.1 Artificial Intelligence

This thesis utilized an artificial intelligence (AI) software called ChatGPT, provided by OpenAI (2024), to enhance the academic quality of the paper in terms of grammar, spelling, clarity and flow. Additionally, we used the AI software to assist with LaTeX codes for tables, figures, and other specific matters that require experience, such as the front page. We disclaim that while we used the AI as a primary resource for these improvements, all text was initially written by us and then refined with the AI's assistance in the aforementioned aspects.

Chapter 5

Results

5.1 Empirical Results

This section presents the empirical results derived from our analysis using the Diebold and Yilmaz framework. We proceed as follows: First, we show the connectedness measures for Carbon (CARB), Oil, Aviation (AVN), Natural Gas (NG), Coal, Clean Energy (CE), Chemicals (CHM), Metal (MTL), Food, and Cement (CMT), using a generalized VAR model for analyzing returns and volatility. Next, we illustrate key findings through network plots. Lastly, we extend this by employing rolling window estimations to analyze dynamic connectedness and highlight temporal variations in the sample period.

5.2 Return and Volatility Connectedness

Tables 5.1 and 5.2 feature the connectedness tables for the returns and volatility over the full sample period, respectively. The tables are obtained through the generalized variance decomposition, as discussed in Section 4.6.

The total system-wide connectedness in the returns and volatility system distills to 32.10% ($\hat{C}^H_{returns}$) and 25.40% ($\hat{C}^H_{volatility}$), respectively. Implying that connectedness, or variations in the returns system, are due to market interactions, with the remaining 67.90% is attributed to market specific factors. Similarly, in the volatility system, the expected variation of 25.40% due to interactions in the market, with the largest contributors being distributed among market-specific factors of 74.60%.

The diagonal elements in the connectedness tables indicate the extent to which each asset can be explained by its own market shocks. In general, the self-contribution is relatively high in

Table 5.1: Return Connectedness Table, Carbon and nine drivers

	CARB	OIL	AVN	NG	COAL	CE	CHM	MTL	FOOD	CMT	FROM
CARB	80.26	2.73	4.36	0.26	1.32	1.35	4.05	1.72	2.78	1.17	19.74
OIL	2.51	73.05	1.51	0.74	1.70	4.02	4.21	7.49	2.06	2.70	26.95
AVN	3.01	1.13	53.68	0.13	0.17	5.80	15.29	2.27	10.20	8.33	**46.32**
NG	0.34	0.81	0.25	95.23	0.71	0.78	1.01	0.41	0.37	0.08	4.77
COAL	0.72	2.26	0.16	0.60	95.32	0.14	0.16	0.44	0.01	0.18	4.68
CE	0.97	3.24	6.48	0.75	0.09	59.31	14.02	2.44	8.17	4.53	**40.69**
CHM	2.07	2.37	11.65	0.44	0.16	9.79	41.03	4.11	18.72	9.67	**58.97**
MTL	1.49	7.41	3.09	0.52	0.26	3.49	7.27	72.48	1.21	2.79	27.52
FOOD	1.71	1.39	9.41	0.23	0.08	7.28	22.56	0.91	49.50	6.93	**50.50**
CMT	0.86	2.20	9.08	0.06	0.13	4.31	13.82	2.25	8.16	59.11	**40.89**
TO	13.68	23.54	**45.99**	3.73	4.63	**36.96**	**82.41**	22.04	**51.69**	**36.38**	32.10
NET	-6.07	-3.41	-0.33	-1.04	-0.05	-3.73	23.44	-5.48	1.19	-4.52	

Note: Derived from ten-variable VAR(1) and generalized variance decompositions of 10-day-ahead return forecast errors.

each market, but it still varies. Table 5.1 presents the connectedness table for returns, where the returns on Carbon (CARB) have an 80.26% connectedness to its own returns, indicating that on average throughout the sample period, Carbon returns is due to its own variations. Notably, both Natural Gas (NG) and Coal have over 95% connectedness with themselves, representing the highest connectedness in the system. In contrast, Chemicals (CHM) show only 41.03% connectedness to their own returns. In terms of volatility, as shown in Table 5.2, the connectedness for Carbon's volatility is explained by its own volatility share at 86.96%, which is also notably higher than that for returns. Here, the highest self-connectedness is also for Natural Gas and Coal at 92.41% and 92.05% respectively, which is a slight decrease compared to the returns system. The lowest self-connectedness for volatility is also observed for Chemicals at 53.96%, yet higher than in the returns system.

In Table 5.1, values highlighted in bold in the 'TO' column and 'FROM' row indicate that Aviation, Clean Energy, Chemicals, Food, and Cement are ranked as the top five relative to both contributors (givers: $C^H_{\bullet\leftarrow j}$) and inheritors (receivers: $C^H_{i\leftarrow\bullet}$) of connectedness within the system. Chemicals give and receive the most with 82.41% ($\hat{C}^H_{\bullet\leftarrow CHM}$) and 58.97% ($\hat{C}^H_{CHM\leftarrow\bullet}$), respectively. In contrast, Natural Gas and Coal contribute the least, with 4.77% ($\hat{C}^H_{\bullet\leftarrow NG}$) and 4.68% ($\hat{C}^H_{\bullet\leftarrow Coal}$), respectively, and receive only 3.73% ($\hat{C}^H_{NG\leftarrow\bullet}$) and 4.63% ($\hat{C}^H_{Coal\leftarrow\bullet}$), respectively.

For volatility connectedness, featured in Table 5.2, similar patterns emerge, except for fewer major contributors and receivers compared to the returns system. Chemicals ($\hat{C}^H_{\bullet\leftarrow CHM} = 46.04\%$) and Food ($\hat{C}^H_{\bullet\leftarrow Food} = 42.48\%$) contribute the most and they also receive the most,

$\hat{C}^H_{CHM\leftarrow\bullet} = 57.63\%$, $\hat{C}^H_{Food\leftarrow\bullet} = 43.76\%$, respectively. Similarly, Natural Gas ($\hat{C}^H_{\bullet\leftarrow NG} = 7.59\%$) and Coal ($\hat{C}^H_{\bullet\leftarrow Coal} = 7.95\%$) contribute the least to system connectedness. While, Carbon ($\hat{C}^H_{CARB\leftarrow\bullet} = 7.00\%$), Natural Gas ($\hat{C}^H_{NG\leftarrow\bullet} = 7.61\%$), and Coal ($\hat{C}^H_{Coal\leftarrow\bullet} = 8.12\%$) receive the least.

Table 5.2: Volatility Connectedness Table, Carbon and nine drivers

	CARB	OIL	AVN	NG	COAL	CE	CHM	MTL	FOOD	CMT	FROM
CARB	86.96	0.93	3.09	0.31	1.20	1.44	2.48	0.76	1.93	0.91	13.04
OIL	0.52	68.75	4.44	0.53	1.57	5.51	7.86	2.07	6.28	2.48	31.25
AVN	1.52	4.01	65.80	0.69	0.46	6.83	9.82	1.06	7.05	2.76	34.20
NG	0.74	1.48	1.08	92.41	2.11	0.33	0.26	0.85	0.57	0.16	7.59
COAL	0.87	0.97	0.78	2.85	92.05	0.82	0.14	1.00	0.41	0.11	7.95
CE	0.39	4.96	6.06	0.85	0.25	68.37	9.93	1.25	5.80	2.14	31.63
CHM	0.75	6.54	7.67	0.53	0.57	7.15	53.96	1.73	15.74	5.36	**46.04**
MTL	0.77	2.80	2.14	1.06	1.43	2.85	2.67	84.46	1.07	0.75	15.54
FOOD	0.79	5.06	7.77	0.23	0.38	6.27	16.79	0.58	57.52	4.62	**42.48**
CMT	0.65	2.37	3.36	0.58	0.14	4.11	7.67	0.51	4.91	75.70	24.30
TO	7.00	29.12	36.38	7.61	8.12	35.30	**57.63**	9.80	**43.76**	19.29	25.40
NET	-6.04	-2.13	2.18	0.02	0.17	3.67	11.60	-5.74	1.28	-5.02	

Note: Derived from the ten-variable VAR(5) and generalized variance decompositions of 10-day-ahead (volatility) forecast errors

The highest measures of pairwise connectedness in the returns system are underscored in Table 5.1, originating from Chemicals to Aviation, Clean Energy, and Food. The foremost being between Chemicals to Food ($\hat{C}^H_{FOOD\leftarrow CHM} = 22.56\%$), and from Food to Chemicals ($\hat{C}^H_{CHM\leftarrow FOOD} = 18.72\%$). Followed by connections from Chemicals to Aviation ($\hat{C}^H_{AVN\leftarrow CHM} = 15.29\%$) and from Chemicals to Clean Energy ($\hat{C}^H_{CE\leftarrow CHM} = 14.02\%$).

In the volatility system in Table 5.2, the overall pairwise connectedness is lower, yet Chemicals still demonstrate the most influence. The connection with Food shows a slight decrease compared to the return connectedness ($\hat{C}^H_{FOOD\leftarrow CHM} = 15.29\%$) and from Food to Chemicals ($\hat{C}^H_{CHM\leftarrow FOOD} = 15.74\%$). Followed by Chemicals to Clean Energy ($\hat{C}^H_{CE\leftarrow CHM} = 9.93\%$) and Aviation ($\hat{C}^H_{AVN\leftarrow CHM} = 9.82\%$).

5.2.1 Network Connectedness

In the last section, the net total directional connectedness values are specified in the final row, labeled 'NET'. A positive value in this row indicates that the majority of the asset's total connectedness contribution to the system originated from that particular asset, implying that it exported more connectedness than it received within the system. In the returns system (Table 5.1), only Chemicals and Food exported more than they received, at 23.44% and

1.19%, respectively. Carbon shows the highest level of connectedness received, at -6.07%, followed by Metal and Cement, -5.48% and -4.52%, respectively.

The net pairwise directional connectedness (C_{ij}^{H}) is visualized in Figure 5.1, the nodes resemble the ten assets - Carbon and the nine drivers. In the figure all nodes are yellow, except for the nodes representing Chemicals and Food, which are blue, mirroring the total net connectedness measures. Chemicals exert the most net influence on Clean Energy ($\hat{C}_{CHM,CE}^{H}$ = 4.23%), Aviation ($\hat{C}_{CHM,AVN}^{H}$ = 3.64%), Cement ($\hat{C}_{CHM,CMT}^{H}$ = 4.15%), Food ($\hat{C}_{CHM,FOOD}^{H}$ = 3.84%), and Metal ($\hat{C}_{CHM,MTL}^{H}$ = 0.94%). While Carbon is the most influenced in terms of net connectedness, receiving all arrows in its node, aside from Natural Gas.

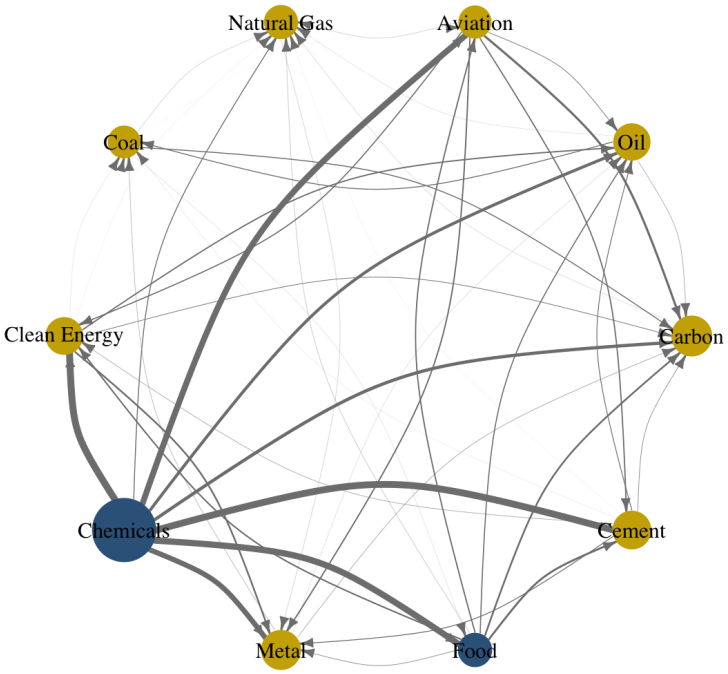

Figure 5.1: Net Pairwise Directional Connectedness for returns

Figure 5.2 illustrates the net pairwise directional connectedness network for the volatility system. In contrast to the returns system, the majority of nodes are blue. Carbon, Oil, Metal and Cement remain net receivers. Chemicals continue to be the largest net giver but a decrease in exported connectedness, now 11.60%. Clean Energy and Aviation shifted roles from net receivers to net givers, 3.67% and 2.18%, respectively. Carbon remains the most net influenced, maintaining the same levels as in the returns system, at now 6.04%.

In terms of net pairwise directional connectedness, Chemicals exhibit a lower overall net influence, with three major links: to Clean Energy ($\hat{C}_{CHM,CE}^{H}$ = 2.78%), Aviation ($\hat{C}_{CHM,AVN}^{H}$ = 2.15%), and Cement ($\hat{C}_{CHM,CMT}^{H}$ = 2.31%). There is a notable decrease on its net influence on Food ($\hat{C}_{CHM,FOOD}^{H}$ = 1.05%), while it remained the same for Metal ($\hat{C}_{CHM,MTL}^{H}$ = 0.94%)

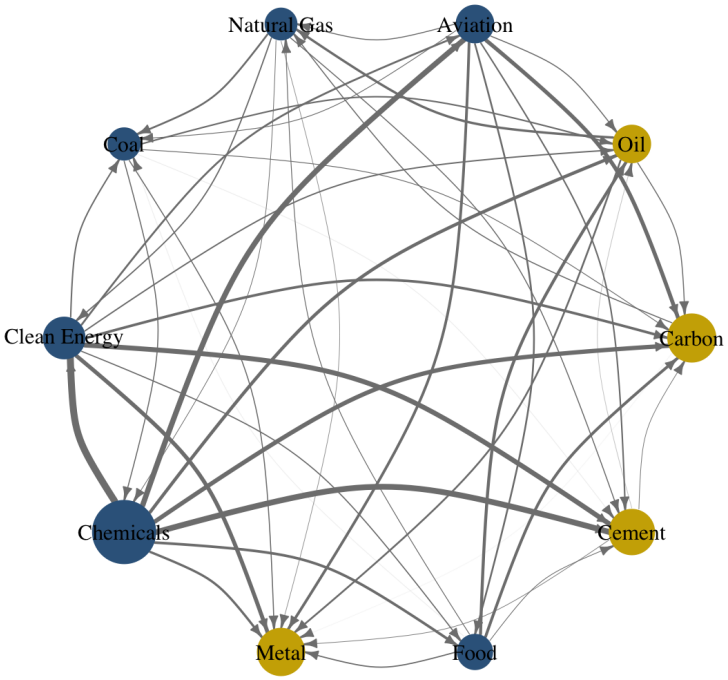

Figure 5.2: Net Pairwise Directional Connectedness for volatility

compared with the returns system. Cement has joined Carbon as one of the most net influenced in the system, importing six and seven arrow respectively.

5.3 Dynamic Connectedness

The results in Section 5.2 provide the expected (or 'average') connectedness in both the return and volatility systems over the sample period. In Sections 3.2 and 3.3, we discussed events that potentially disrupted both systems. To further analyze these effects, this section introduces a time-varying parameter to explore significant secular and cyclical movements in connectedness, addressing the concerns in Subsection 4.2.1. We used a 100-day rolling samples to capture 16 ($\frac{1634 days}{100 days} = 16.34$) sub-periods within the sample period, allowing us to investigate the nature of variation across different time intervals and the non-linear[1] characteristics of the carbon price data.

5.3.1 Total Dynamic Connectedness

Figure 5.3 presents the total dynamic connectedness for the returns from 3, July 2017, to 1, February 2024. The connectedness ranges from 25% to around 78%. This index started at

[1] Alberola et al. (2008), D. Liu et al. (2024), and Wang et al. (2023) pointed out that carbon data exhibits non-linear characteristics

just around 30%, which then diminished to the lowest point in the period at around 25%. Followed by an increase to approximately 38%. Overall, total connectedness shows variability but stays mostly above 20%. The plot also reveals a significant peak in the index around early 2020, reaching the highest connectedness near 80%. After this peak, connectedness gradually declined to the second lowest point in the index, and stabilized. Throughout 2024, connectedness primarily fluctuated between 20% and 40%.

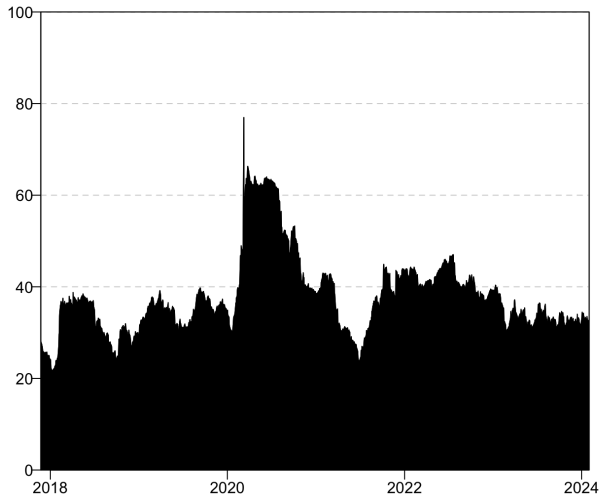

Figure 5.3: Total Dynamic Directional Returns Connectedness Index

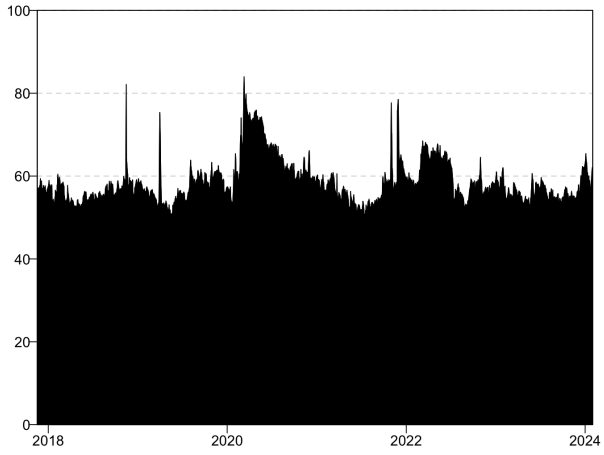

Figure 5.4: Total Dynamic Volatility Connectedness Index

Figure 5.4, covering the similar timeframe, presents the total dynamic connectedness for volatility. This plot displays similar pattern, but significant peaks are more frequent. We observe five significant spikes; one in early 2019, just above 80%, followed by another around 75%. A similar with the returns is noted in the highest spike in early 2020. Finally, there are two consecutive spikes at the beginning of 2022. Despite more frequent spikes, connectedness remains just below 60%. Additionally, the plot indicates that volatility demonstrates

smoother fluctuations compared to the returns.

5.3.2 The Dynamic Net Total Directional Connectedness

Figure 5.5 illustrates the dynamic net total directional connectedness for the returns, representing the difference between total directional 'TO' and 'FROM' others in the system. Each panel details the net total directional connectedness between an asset and the system over the sample period. The zero line indicates whether connectedness originates from the asset or from the system, in net terms. Hence, a negative connectedness value -

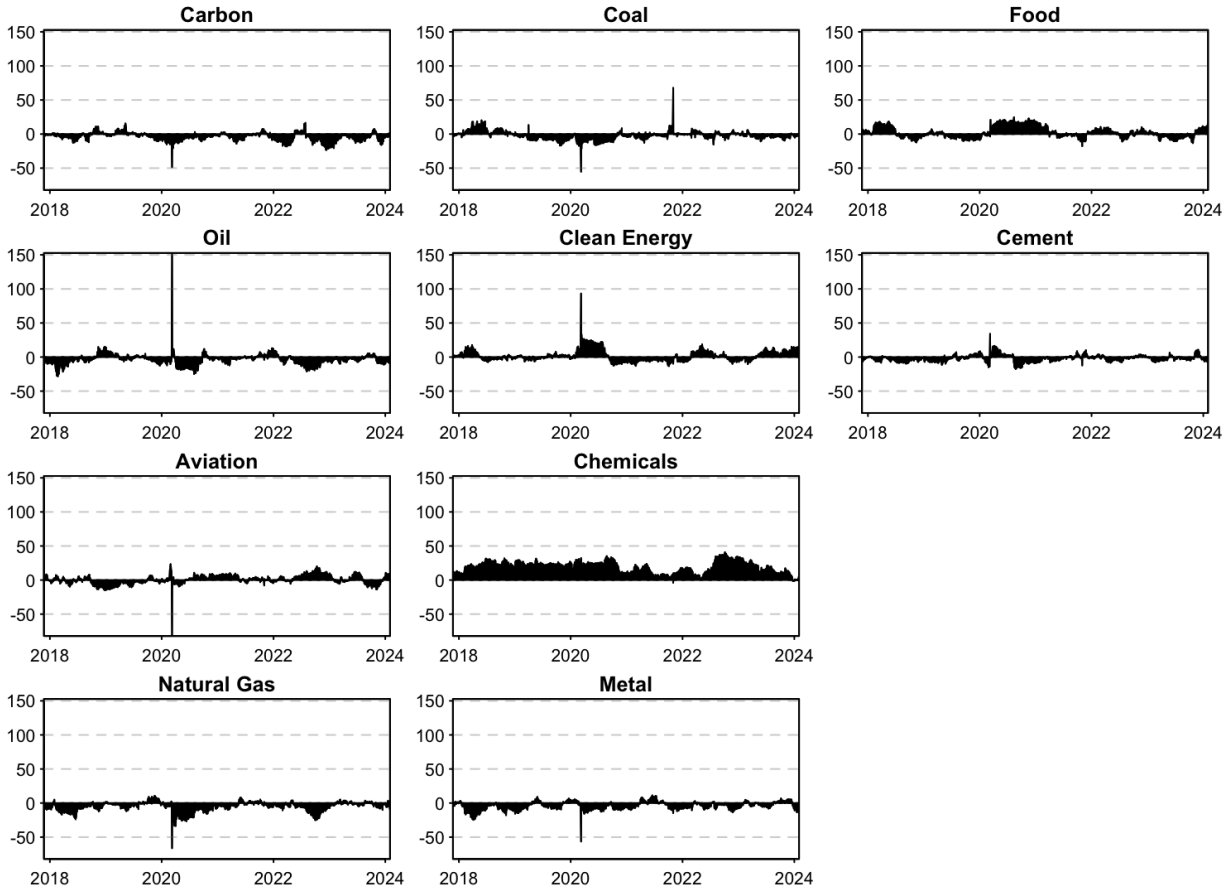

Figure 5.5: Net Dynamic Return Connectedness Plot

indicates that shocks from the system are larger than the connectedness originating from the asset. We will explain this in further detail in Section 6.1. Similarly, for volatility, Figure 5.6 shows the dynamic net total directional connectedness for the volatility system, over the same period. To facilitate comparison with the returns plot, the volatility plot was scaled; the original plot can be found in the appendix (Figure 8.1), where the connectedness for Natural Gas approached 400%. The plots shows that the overall net connectedness is higher. All assets exhibited more fluctuations compared to those in the returns system. Additionally, spikes are more frequent and occur across various sub-periods. We observe

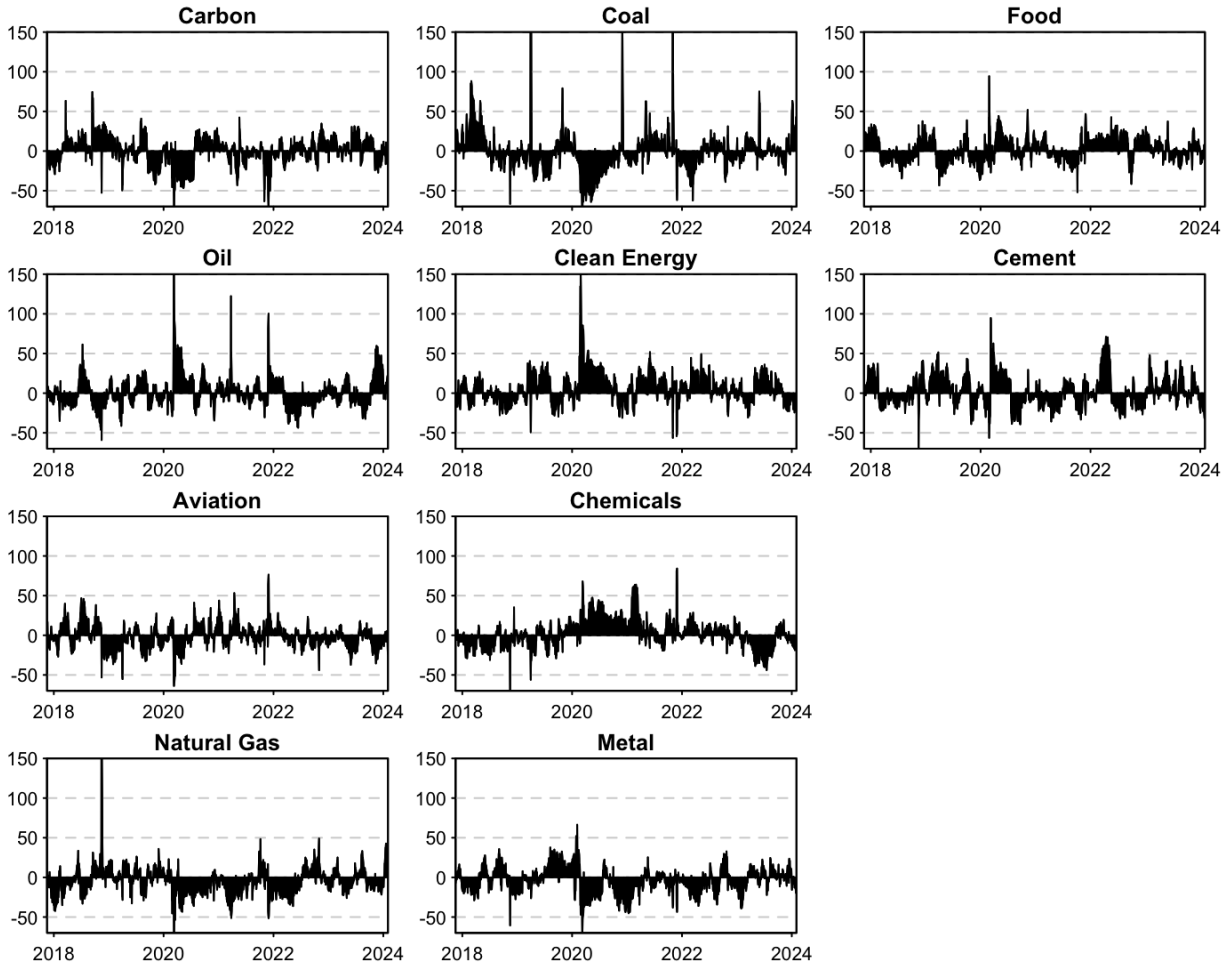

Figure 5.6: Net Dynamic Volatility Connectedness Plot

common spikes for all assets in 2019, early 2020, and some in 2021. Spikes exceeding 100% net connectedness, which is always positive, can be found in Coal in early 2019 and 2021, and at the end of 2021; for Oil in early 2019, early 2020, and at the end of 2019; in Clean Energy throughout 2020; and in Natural Gas in 2019.

5.4 Model Diagnostics & Robustness

This section reviews the underlying model used in this study to produce the connectedness results. A generalized vector autoregressive (VAR) model was applied to daily returns and volatility of the variables, as detailed in Chapter 4. The purpose is to determine whether the residuals generated by the generalized VAR align with the model's assumptions. All tests will be applied to VAR(1) and VAR(5) models, corresponding to returns and volatility datasets, respectively. We begin by conducting the Ljung-Box test to check for serial correlation, then check for normality using Quantile-Quantile plots and a multivariate Jarque-Bera test. Furthermore, we will vary the horizon and in the VAR and examine different windows

in the rolling sample, to assess if the model yields varying results. For convenience, tables and figures are located in the appendix.

Residuals should behave like white noise, signifying that the model has successfully captured the underlying structure of the data (Tsay, 2014). Using the multivariate Portmanteau test to asses whether residuals up to lag m are not serially correlated, where: $H_0 : R_1 = R_2 = ... = R_m = 0$, against the alternative hypothesis $H_a : R_j \neq 0$ for some $1 \leq j \leq m$, there is evidence under H_0 that residuals are serially correlated. Based on the results in Table 8.5, given that the the null hypothesis, we fail to reject the null hypothesis for the returns system, indicating that the residuals resemble a white noise process up until the fourth lag. Similiarly, for the volatility system modeled with a VAR(5), we fail to reject the null hypothesis, suggesting that there is no strong evidence that the residuals do not exhibit a white noise process (see Table 8.6).

A generalized VAR model facilitates and presumes correlated error terms in the system. Figures 8.2 and 8.3 illustrate the cross-correlation matrices up to m lags, for the returns and volatility VAR models, respectively. Points that lie above the Bartlett line indicate p-values above 0.05, suggesting cross-correlated residuals. We observe that residuals of the VAR(1) model are cross-correlated at lag 1, while residuals of the VAR(5) model are cross-correlated at lags 1 to 5. This implies that our estimated generalized VAR models are adequately aligned with the underlying assumption up to certain lags.

In Section 4.6, we briefly discussed how the GVD approach accounts for correlated shocks and relies on the historically observed error distribution, assuming normality (Diebold & Yilmaz, 2015). Figures 8.4 and 8.5 validate this assumption through the Quantile-Quantile (Q-Q) plots of the residuals for both the returns and volatility VAR models. Observations diverging from the red line indicate deviations from normality, and alignment with the line supports normality. The points closely align with the red line across quantiles ranging from $[-2, 2]$ for returns and $[-2.5, 1.5]$ for volatility, indicating that the assumption of normality generally holds. However, deviations observed in the outer quantiles suggest the presence of special observations across all assets. To further verify, we conducted a multivariate Jarque-Bera test on the residuals. The null hypothesis states that the vectors in a multivariate time series are normally distributed, against the alternative hypothesis that the time series do not follow a normal distribution. Given that the null hypothesis is true, we reject the null

hypothesis for all residuals in the time series, indicating that the residuals do not follow a normal distribution.

Having analyzed the 'workhorse' approximating model - VAR model. We examined a menu of horizon, H, and window width, w, in the dynamic analysis. The objective was to examine the model's sensitivity to its parameters using the total dynamic connectedness plot as an indicator. We assess for horizons, $H = [6, 10, 18]$, and window width, $w = [70, 100, 200]$, illustrated in Figures 8.7 and 8.6. The returns system, in general, did not exhibited any significant deviation in pattern across the different parameters, except for when the COVID-19 pandemic started. For $w = 70$ total connectedness were slightly higher and spikes are more revealing. While for $w = 200$ the plots are smoother and lower in total connectedness. The volatility system exhibited more variations, for $w = 70$ total connectedness exceeded 80% across the three horizons, while for $H = 18$ and $w = 200$, total connectedness were as low as 30%, but revealed a spike in 2019, around 70%.

Chapter 6

Discussion

This chapter examines the empirical results presented in Chapter 5. First, we discuss the findings from the application of the Diebold and Yilmaz (2014) connectedness framework. Second, we compare the results with other related studies. Lastly, we discuss the adequacy of the underlying approximating model.

6.1 Interpretations

6.1.1 Static Results

The static results may represent the 'average' information spillovers between assets from July 3, 2017, through February 1, 2024. We found that the total (system-wide) connectedness in both the returns (32.10%) and volatility (25.40%) plays a relatively important role, indicating a significant share of the forecast error variance comes from connectedness across sectors for both the returns and volatility. This reflects the interdependence between sectors in Europe and global energy commodity markets. As globalization increases, it allows firms and countries worldwide to trade, ensuring any resources they may require. The difference in total connectedness between the returns and volatility shows the behavior of the assets in the full sample; the higher total connectedness in returns implies that shocks, whether positive or negative, in one index tend to spread to others. In terms of volatility, connectedness is usually low during periods of tranquility, as markets tend to be diversified against potential risks in their corresponding sectors. However, during crisis periods, volatility connectedness tends to be high. The two major crisis in our sample are the COVID-19 pandemic and the Ukraine-Russia conflict; the reason for the low volatility connectedness may be that crisis periods represent only a small fraction of the sample period.

Considering the total directional return connectedness, the Chemicals and Food sectors differentiate themselves from others by having high 'TO' connectedness at 82.41% and 51.69%, respectively. Additionally, these sectors also demonstrate the highest 'FROM' connectedness, 58.97% and 50.50%, respectively. Consequently, their net connectedness measures are the only positive values across all assets, suggesting that shocks originating from these indexes have an indirect impact on the return shocks of the others over the full sample. In contrast, Natural Gas and Coal exhibit the lowest levels of 'TO' connectedness at 4.77% and 4.68%, respectively, and 'FROM' connectedness at 3.73% and 4.63%, respectively. Therefore, their net connectedness measures (difference between 'TO' and 'FROM') are negative and are among the lowest in terms of absolute value, along with Aviation (-0.33%). These negative net values imply that, despite being global energy commodities, Natural Gas and Coal, similar to the Aviation sector, are predominantly recipients of shocks originating from other assets. Moreover, a net connectedness value close to zero indicates that shocks from other assets have little or no impact on their own shocks.

Turning to volatility, the overall total directional connectedness is lower, except for the energy commodities (Oil, Natural Gas, and Coal), which exhibit higher 'TO' and 'FROM' connectedness measures. This pattern aligns with the observation that volatility connectedness tends be higher during crisis periods and decreases in tranquility periods. Our sample period covered several minor crisis that significantly influenced the prices of these commodities. For instance, sanctions imposed by former US President Donald Trump on Iran in 2018 led to a drop in Oil prices, the irregularly cold winter in 2018/2019 increased the demand for Natural Gas, and the switch from Natural Gas to Coal spiked the demand for Coal. These events, along with the COVID-19 pandemic, which saw a decline in all price series, and the ongoing Ukraine-Russia conflict, were all captured in the full sample period. Chemicals and Food indexes still demonstrate the highest total directional connectedness, but lower 'TO' connectedness at 46.04% and 42.48%, respectively. Additionally, their 'FROM' connectedness also remains the highest, 57.63% for Chemicals and 43.76% for Food. In terms of net connectedness, there are now more assets with positive net values compared to returns, indicating that shocks are originating from a broader range of assets, not limited to just Chemicals and Food. Carbon (-6.04%), Metal (-5.74%), and Cement (-5.02%) are the assets most affected by shocks originating from others in terms of net connectedness.

Focusing on the distribution of total net connectedness, the network plots in Figures 5.1 and 5.2 reveal these relationships clearly. In the returns, net connectedness from Chemicals is primarily distributed to Clean Energy, Aviation, Cement, Food, and Metal, with lesser extents to Oil and Carbon. This suggests that shocks originating from the Chemical index influence the return shocks in these assets. A possible reason could be that the Chemical index includes firms that supply several types of chemicals essential for the production processes associated with these industries. This suggests that a disruption in the supply chain of these firms could indirectly impact the returns of these assets. Similarly, this reasoning can be applied to Carbon futures. A higher demand for chemical products may lead to increased production, which in turn could lead to higher CO_2 emissions, thereby increasing the need for more carbon allowances and potentially driving up the prices of Carbon futures. Considering the energy commodities - Coal, Natural Gas, and Oil. They did not contribute any significant connectedness either to others or among themselves. This observation mirrors the low total net connectedness values in Table 5.1. This finding indicates that the returns of the energy commodities had little influence on the returns of other assets in the sample period.

In terms of volatility (Figure 5.2), more assets are now acting as exporters rather than importers of net connectedness compared to the returns. Additionally, a wider distribution of total net connectedness is also observed. Clean Energy, Coal, Natural Gas, and Aviation have joined Chemicals and Food as net importers of connectedness, while Metal, Cement, Carbon, and Oil continue as net importers. The Chemical index remains the biggest net exporter, but at reduced levels of total connectedness. Carbon futures continue to be the most influenced by shocks originating from others, including the volatility in Cement stocks. This shift may indicate how crisis can alter the nature of connectedness, revealing a pattern of more minor connectedness between assets. This could be evidence of volatility connectedness between assets that are not being thoroughly captured by the full sample analysis.

6.1.2 Total Dynamic Connectedness

The dynamic analysis provides new information that the static analysis did not capture. As mentioned, the analysis over the full sample only provides a characteristic of the expected connectedness across assets. Using 100-day rolling samples, the connectedness analysis allows us to capture new information in 16 different sub-periods. The purpose is to magnify the connectedness in those periods that would otherwise be flattened out by the 'average' connectedness in the full sample. Starting with the total dynamic connectedness (Figures

5.3 and 5.4)

The total dynamic connectedness for the returns, represented in Figure 5.3, ranges from 25% to 78%. The first window experienced strong economic growth in Europe at the end of 2017, where all price series, except for Coal, either increased or stabilized. This period started at just below 30% total connectedness, which gradually diminished to the lowest point in the graph at around 25%. An increase to around 38% followed, coinciding with the China-US trade war, during which all prices fluctuated significantly. Subsequently, the total connectedness decreased and fluctuated at similar levels in 2018 and 2019. The all-time high total connectedness was in early 2020, reaching nearly 80%, triggered by the COVID-19 pandemic. The index then declined but remained stable just above 60% until the beginning of 2021. At this point, the total connectedness dipped to the second lowest point in the graph, possibly due to the introduction of COVID-19 vaccinations and the starting point of economic recovery. Then, an escalation due to the Russia-Ukraine war disrupting the energy market, stabilizing again with minor fluctuations above 40% until 2023. The index settled at around 35% toward the end of the sample period.

Figure 5.4 shows the total dynamic connectedness for the volatility system. The index has similar patterns to the returns system, illustrated in Figure 5.3, but with a higher degree of connectedness, ranging from 55% to 85%. The total connectedness started just below 60%, then diminished to around 55% in mid-2018. This marks a divergence compared to the returns system, which saw an increase in total connectedness during the same period. Attributed to the China-US trade war in 2019, the total volatility connectedness surpassed 80%, while the returns system experienced a decrease. Thereafter, the index decreased to a range between 55% and 58%. While in mid-2019 another spike is observed to approximately 70%, a pattern similar in the returns system but less pronounced, before declining to the sample period's lowest point of around 50%. During 2020, the COVID-19 pandemic drove the total connectedness up to around 83% before a reduction to 60% in 2021, mirroring the returns system. The index returned to 55% during mid-2021, before experiencing two significant spikes nearing 80% towards the year's end. In the latter half of 2022, total connectedness approached 65%, before fluctuating under 60%, influenced by the conflict between Russia and Ukraine. Throughout 2023, total connectedness remained stable around 55%, aside from minor variations. Finally, throughout the sample period, the index did not drop below 50%.

Overall, the total connectedness for both returns and volatility appears to be higher when analyzed over shorter time intervals within the sample period.

6.1.3 The Dynamic Net Total Directional Connectedness

Figures 5.5 and 5.6 in Subsection 5.3.2 illustrate the behavior of the net total directional connectedness discussed in Section 5.2, with the addition of its dynamic nature. The purpose of these plots is to identify how shocks from each asset contribute to others in the returns and volatility systems during different phases of the sample period.
Starting with the returns, all assets exhibited seasonal fluctuations in directional net connectedness, using the zero line as the baseline. A net connectedness value on the zero line suggests that the asset is decoupled from the rest. The Chemical index is the only variable that consistently exhibits positive net connectedness in each window, except for one period in late 2021, implying that return shocks from the Chemical index drive the shock returns of the return system in all sub-periods. In contrast, Carbon, Natural Gas, and Metal consistently exhibit negative net connectedness aside from a few positive spikes in some periods. This indicates that their returns are indirectly impacted by the returns from the other assets in the system.

We also observe that all assets except Chemicals and Food experienced spikes during the COVID-19 pandemic in 2020. Carbon (-50%), Coal (-60%), Aviation (-80%), Natural Gas (-70%), and Metal (-50%) demonstrated negative spikes, while Oil and Clean Energy had positive spikes, approaching 150% and 100%, respectively. This observation suggests that the return connectedness between assets is heightened during turbulent periods. Specifically, assets that experienced negative spikes were highly vulnerable to impacts originating from other assets, while those with positive spikes influenced the returns of other assets.

In terms of volatility (Figure 5.6), net connectedness appears to fluctuate between positive and negative values for each asset per window. During the COVID-19 pandemic (2020-2021), volatility net connectedness remained relatively stable at higher levels for Carbon, Coal, Clean Energy, Chemicals, Natural Gas and Metal. Specifically, Carbon, Coal, Natural Gas, and Metal experienced negative net connectedness, while it was positive for Clean Energy and Chemicals. This observation coincides with the earlier finding that volatility connectedness is higher during distressing periods.
The energy commodities and the Clean Energy index exhibited spikes in net connectedness

exceeding 100%. This indicates that the corresponding asset's sum of rows (total 'TO' connectedness) surpasses 100%, suggesting that shocks originating from these assets contribute high levels of shocks to others during these periods. The common factor in each period where volatility connectedness exceeded 100% is linked to disruptions in the energy market or broader crises. For instance, the US-China trade war in 2019 led to abnormally high Oil prices, the COVID-19 pandemic in 2020, and the energy crisis in 2021 that saw soaring Natural Gas prices and increased demand for Oil. This finding casts new light on the static results discussed in Subsection 5.2.

6.2 Limitations

This section provides limitations concerning the chosen methodology, and addresses limitations highlighted by other papers.

The residuals in each equation of both VAR models do not exhibit serial correlation, indicating that the models have captured the data's dynamics to a certain degree. However, the residuals violates the normality assumption in both models. We also investigated the models' sensitivity to variable ordering, tested the effect of withdrawing different variables, and examined the influence of forecast horizons, lag lengths, and window widths. Generally, the models do not show significant variations in the results using connectedness measures as indicators, suggesting that the models are relatively robust.

Caloia et al. (2019) argued that the 'TO' directional connectedness measures are sensitive to the normalization scheme used to enforce the row sums to 1. This approach may inaccurately identify the system's most (least) affected asset by others, leading to misrepresentation of the exact degree of the other connectedness measures. This is also evident in Subsection 5.3.2, where the directional connectedness for natural gas exceeded over 400% (see Figure 8.1), which can also cause misinterpretation.

Lastrapes and Wiesen (2021) have raised concerns that cross-correlation between variables might result in inappropriate weighting in determining their joint contribution, causing an overestimation of directional connectedness between variables. The study proposed a method to control these cross-correlations and improve the normalization method used by Diebold and Yilmaz (2012), ensuring that contributions of connectedness in the rows ('TO' connect-

edness) do not exceed 100%. We compared our results using Lastrapes and Wiesen (2021) proposed method. All connectedness values were similar except for the directional connectedness measures, which demonstrated lower connectedness values. This coincides with the study's conclusion.

We underscore that the results of this study are not robust across all contexts but are specific to the reference universe. The variables in the dataset may not be the best representation of the sectors within the scope of the EU ETS as defined by EuropeanCommission (2024c). For instance, due to data access issues, the data used to represent cement production, as mentioned in Section 3, is based on only one company that produces white cement. This may not be the best representation of the cement sector in the EU ETS.

6.3 Comparison with other studies

This section compares our findings with other studies that utilized the same method in the literature review in Chapter 2.

Ji et al. (2018) examined the information linkages and dynamic spillover effects between the Carbon and energy markets over the period July 17, 2006, to October 31, 2017. Their findings indicate that Oil, Clean Energy, and Coal play pivotal roles in both the returns and volatility systems, with Oil prices having the most influence on Carbon prices. In contrast, our analysis indicates that the Aviation index prices contribute the most to Carbon in both the returns (4.36%) and volatility (3.09%). To facilitate the same baseline, we compared common measures. In their static analysis, Ji et al. (2018) reported that Oil contributes 2.88% in the returns and 8.69% in the volatility system. In contrast, our findings show that Oil contributes 2.73% (returns) and 0.93% (volatility). The differences between these results are attributed to the different sample periods analyzed. Regarding dynamic connectedness, although different approaches to presenting results pose challenges for direct comparison, their conclusion aligns with the results in our analysis: that information linkages and spillovers are much stronger in the volatility system than in the returns system. Additionally, both return and volatility connectedness have time-varying characteristics.

Wen et al. (2022) explored the driving factors of carbon prices in three different carbon markets from August 8, 2013, to March 10, 2020. The static analysis suggests that Carbon

prices in these markets are only affected by their previous prices. This finding aligns with our empirical results, which also indicate that the main contributors to carbon returns and volatility are the carbon prices themselves. However, our analysis diverges slightly, revealing that 19.74% of its shock returns originate from the shock returns of other assets, compared to their findings, where connectedness from other to Carbon ranges between 0.37% and 4.57%. The directional dynamic connectedness analysis reveals that the driving factors of carbon prices are heterogeneous and vary over time. However, their sample period missed out on global significant events such as COVID-19 and the Russia-Ukraine war. The omission of these events could affect the results, as they had significant impact on global markets. In contrast, our study investigates information spillovers between the Carbon market and its key drivers, while Wen et al. (2022) focused on identifying factors that drive carbon prices. The focus areas diverge in our studies.

Jiang et al. (2024) employed the DY framework alongside the Bahruník and Krehlik (2018) method to assess time-frequency connectedness concerning volatility among carbon markets, energy markets, and geopolitical risks. The analysis of total dynamic directional net connectedness revealed patterns similar to our findings; during the COVID-19 pandemic, Carbon received net directional volatility connectedness, while Coal and Oil contributed in terms of net directional volatility connectedness to the system. However, the levels of connectedness reported in their study were lower than those we observed. This parallel in findings underscores the robustness of the DY framework in capturing the dynamics of market connectedness under different significant events.

Chapter 7

Conclusions

This thesis explored the dynamics of carbon credits within the European Union Emissions Trading System, focusing on how these dynamics interact with energy-intensive industries and global energy commodities. Applying the Diebold and Yilmaz (2012) Connectedness framework, we examined price data on EUA ETS carbon futures, Brent crude oil, the Airlines index, natural gas, coal, the global clean energy index, the chemical commodities index, the metal production index, the food production index, and cement production. The chosen sample period, from July 3, 2017, to February 1, 2024, captures the financial market disruptions caused by the COVID-19 pandemic and the ongoing Ukraine-Russia conflict. All prices were transformed into logarithmic growth rates and daily volatility, providing insights into the interrelationships among assets.

Starting with the analysis over the full sample, our findings suggest that total system-wide connectedness plays a pivotal role in both returns (32.10%) and volatility (25.40%). This underscores the significant influence of shocks across various industries, reflecting the integrated nature of European and global energy markets. The difference in total connectedness between returns and volatility suggests that while markets are more interconnected in terms of returns, volatility connectedness spikes during crisis periods, indicating the markets' sensitivity during unstable times.

We identified that the Chemical and Food production indexes exhibit the highest levels of directional connectedness, indicating that these sectors are responsible for the transmission of shocks across the system. In contrast, Natural Gas and Coal, despite being among the biggest participants in the energy market, demonstrated low levels of 'TO' connectedness, acting more as recipients of shocks rather than contributors. This finding may be crucial for

policymakers and economic agents in understanding the roles of different sectors within the EU ETS.

The dynamic analysis revealed varying connectedness over different phases in the sample period, with peaks corresponding to major economic and geopolitical events. Volatility connectedness was notable among energy commodities, especially during crisis periods. These findings align with historical events that significantly affected commodity prices, such as the 2018 sanctions on Iran, the irregular winter of 2018/2019, the COVID-19 pandemic, and Russia's invasion of Ukraine. The analysis also reveals that chemical index is the main driver of shock returns, while Carbon, Natural Gas, and Metal are the main recipients.

Hypothesis 1: Carbon allowances contribute to connecting energy-intensive sectors through carbon trading, in terms of returns and volatility.
Our results do not support this hypothesis, showing that carbon was mainly a recipient of shocks originating from others. The connectedness measures suggest that the Chemical index is the main contributor in integrating various sectors. Shocks originating from carbon credit prices have little influence on energy-intensive sectors participating in the EU ETS.

Hypothesis 2: Brent crude oil plays a pivotal role in driving carbon credit dynamics.
This hypothesis is also not supported by our findings. Brent crude oil has little impact on the returns (2.73%) and volatility (0.93%) of carbon credits. The results suggest that Aviation is the main driver of carbon credits in both returns (4.36%) and volatility (3.09%), relative to other assets. This suggests that monitoring the aviation sector is quite relevant for predicting carbon credit movements.

Hypothesis 3: Connectedness in volatility exceeds that in returns.
Our analysis consists of two parts: static and dynamic, leading to a twofold conclusion. The static analysis does not support this hypothesis, while the dynamic analysis does. We believe the main reason is the selected sample period, where crises comprised only a small fraction of the entire sample period and volatility is more sensitive to crises. This is evident in the dynamic analysis, where we observed a clear gap between return and volatility connectedness, with volatility exceeding returns and capturing more of the smaller crises in the sub-periods.

In terms of limitations, the normality assumption is violated in the VAR models and the sensitivity of directional connectedness measures to the arbitrary normalization schemes suggest areas for methodological improvements. Future research could refine these models by using methods proposed by Caloia et al. (2019) and Lastrapes and Wiesen (2021), potentially offering even more accurate insights into market dynamics. Further studies should also consider expanding our work to include variables to represent electricity and maritime transport to achieve a more comprehensive representation of the industries covered by the EU ETS.

In conclusion, this thesis contributes to the exploration of the influence of carbon credits on industries participating in the EU ETS using the connectedness approach of Diebold and Yilmaz (2012). The findings suggest that carbon credits have little influence on the variables representing these industries. This study also identified that the chemical market plays a pivotal role in driving prices in the EU ETS and energy markets. Therefore, policymakers and economic agents should thoroughly consider their level of exposure in their future investments and portfolios in the chemical market, especially during unstable periods.

Bibliography

Aatola, P., Ollikainen, M., & Toppinen, A. (2013). Price determination in the eu ets market: Theory and econometric analysis with market fundamentals. *Energy Economics*, *36*, 380–395. https://doi.org/https://doi.org/10.1016/j.eneco.2012.09.009

Adekoya, O. B. (2021). Predicting carbon allowance prices with energy prices: A new approach. *Journal of Cleaner Production*, *282*, 124519. https://doi.org/https://doi.org/10.1016/j.jclepro.2020.124519

Agency, U. S. E. P. (2024). *Sources of greenhouse gas emissions*. Retrieved May 20, 2024, from https://www.epa.gov/ghgemissions/sources-greenhouse-gas-emissions

Akaike, H. (1974). *A new look at the statistical model identification*. IEEE Transactions on Automatic Control AC-19(6), 716-23.

Alberola, E., Chevallier, J., & Chèze, B. (2008). Price drivers and structural breaks in european carbon prices 2005–2007. *Energy Policy*, *36*, 787–797. https://doi.org/https://doi.org/10.1016/j.enpol.2007.10.029

Bahruník, J., & Krehlik, T. (2018). Measuring the Frequency Dynamics of Financial Connectedness and Systemic Risk*. *Journal of Financial Econometrics*, *16*(2), 271–296. https://doi.org/10.1093/jjfinec/nby001

Batten, J. A., Maddox, G. E., & Young, M. R. (2021). Does weather, or energy prices, affect carbon prices? *Energy Economics*, *96*, 105016. https://doi.org/https://doi.org/10.1016/j.eneco.2020.105016

Benton, T. G., Froggatt, A., with Owen Grafham, L. W., King, R., Morisetti, N., Nixey, J., & Schröder, P. (2023). The ukraine war and threats to food and energy security. *Economy of Ukraine*, 46. https://doi.org/10.15407/economyukr.2023.08.028

Britannica. (2024). *Petroleum*. Retrieved May 20, 2024, from https://www.britannica.com/science/petroleum

Brooks, C. (2019). *Introductory econometrics for finance*. Cambridge University Press.

Caloia, F. G., Cipollini, A., & Muzzioli, S. (2019). How do normalization schemes affect net spillovers? a replication of the diebold and yilmaz (2012) study. *Energy Economics*, *84*, 104536. https://doi.org/https://doi.org/10.1016/j.eneco.2019.104536

CarbonCredits. (2024a). *Carbon pricing explained: How carbon credits, carbon offsets and taxes are priced*. Retrieved May 11, 2024, from https://carboncredits.com/carbon-pricing-explained-credits-offsets-taxes/

CarbonCredits. (2024b). *The ultimate guide to understanding carbon credits*. Retrieved March 22, 2024, from https://carboncredits.com/the-ultimate-guide-to-understanding-carbon-credits/

Cefic. (2018). *The eu chemicals sector faring better and closer to its pre-crisis level*. Retrieved April 5, 2024, from https://cefic.org/app/uploads/2018/12/2018-01-07-Cefic-Chemical-Trends-Report-The_EU_Chemicals_Sector_faring_better_and_closer_to_its_pre-crisis_level.pdf

Cefic. (2020). *Eu chemical production slightly declined in 2019*. Retrieved April 5, 2024, from https://cefic.org/app/uploads/2020/01/2020-01-28-Cefic-Chemicals-Quarterly-Report.pdf

Cefic. (2021). *Latest data reveals the recovery of the eu chemical output is slowing down*. Retrieved April 8, 2024, from https://cefic.org/app/uploads/2020/11/Cefic-Chemicals-Quarterly-Report-2020-11-26.pdf

Cefic. (2022). *High energy prices and economic uncertainty continue to drive down the chemicals output in the eu27 area*. Retrieved April 8, 2024, from https://cefic.org/app/uploads/2022/12/EU27-Chemicals-Business-Monthly-Briefings-Nov-2022.pdf

Cefic. (2024). *2023 ends on a weak note for the chemicals industry in europe*. Retrieved April 8, 2024, from https://cefic.org/app/uploads/2024/02/EU27-Chemicals-Business-Monthly-Briefings-Feb-2024-002.pdf

CementirHolding. (2018). *Annual report 2017*. Retrieved April 4, 2024, from https://www.cementirholding.com/sites/default/files/general-meetings/2019-11/18801.pdf

CementirHolding. (2019). *Annual report 2018*. Retrieved April 4, 2024, from https://www.cementirholding.com/sites/default/files/documenti/2019-11/20112.pdf

CementirHolding. (2020). *Annual report 2019*. Retrieved April 4, 2024, from https://www.cementirholding.com/sites/default/files/documenti/2021-04/CH_AnnualReport2019%20singole.pdf

CementirHolding. (2022). *Annual report 2021*. Retrieved April 4, 2024, from https://www.cementirholding.com/sites/default/files/general-meetings/2022-03/CH_2021%20Annual%20Report_20220310.pdf

CementirHolding. (2023). *Annual report 2022*. Retrieved April 4, 2024, from https://www.cementirholding.com/sites/default/files/general-meetings/2023-03/CH_2022%20Annual%20Report.pdf

CementirHolding. (2024). *Annual report 2023*. Retrieved April 4, 2024, from https://www.cementirholding.com/sites/default/files/documenti/2024-03/CH_2023%20Annual%20Report.pdf

Chen, Z.-H., Ren, F., Yang, M.-Y., Lu, F.-Z., & Li, S.-P. (2023). Dynamic lead,äìlag relationship between chinese carbon emission trading and stock markets under exogenous shocks. *International Review of Economics & Finance*, *85*, 295–305. https://doi.org/https://doi.org/10.1016/j.iref.2023.01.028

Chou, R. Y., Chou, H., & Liu, N. (2015). Range volatility: A review of models and empirical studies. In C.-F. Lee & J. C. Lee (Eds.), *Handbook of financial econometrics and statistics* (pp. 2029–2050). Springer New York. https://doi.org/10.1007/978-1-4614-7750-1_74

DiChristopher, T. (2019). *Oil prices just had their worst year since 2015 — here's what went wrong*. Retrieved March 22, 2024, from https://www.cnbc.com/2018/12/31/oil-prices-are-set-for-their-worst-year-since-2015.html

Diebold, F. X., & Yilmaz, K. (2009). Measuring financial asset return and volatility spillovers, with application to global equity markets. *Journal of Econometrics*, *119*(1), 158–171. http://www.jstor.org/stable/20485298

Diebold, F. X., & Yilmaz, K. (2012). Better to give than to receive: Predictive directional measurement of volatility spillovers [Special Section 1: The Predictability of Financial Markets Special Section 2: Credit Risk Modelling and Forecasting]. *International Journal of Forecasting*, *28*(1), 57–66. https://doi.org/https://doi.org/10.1016/j.ijforecast.2011.02.006

Diebold, F. X., & Yilmaz, K. (2014). On the network topology of variance decompositions: Measuring the connectedness of financial firms [Causality, Prediction, and Specification Analysis: Recent Advances and Future Directions]. *Journal of Econometrics*, *182*(1), 119–134. https://doi.org/https://doi.org/10.1016/j.jeconom.2014.04.012

Diebold, F. X., & Yilmaz, K. (2015). *Financial and macroeconomics connectedness: A network approach to measurement and monitoring*. Oxford University Press.

Eia. (2020). *Natural gas prices in 2019 were the lowest in the past three years*. Retrieved March 21, 2024, from https://www.eia.gov/todayinenergy/detail.php?id=42455

Eia. (2022a). *Crude oil prices increased in 2021 as global crude oil demand outpaced supply*. Retrieved March 22, 2024, from https://www.eia.gov/todayinenergy/detail.php?id=50738

Eia. (2022b). *U.s. natural gas prices spiked in february 2021, then generally increased through october*. Retrieved March 21, 2024, from https://www.hydrocarbonengineering.com/gas-processing/07012022/the-eia-reports-on-2021-natural-gas-prices/

Eia. (2023). *Crude oil prices increased in first-half 2022 and declined in second-half 2022*. Retrieved March 22, 2024, from https://www.eia.gov/todayinenergy/detail.php?id=55079

Eia. (2024a). *Brent crude oil prices averaged $19 per barrel less in 2023 than 2022*. Retrieved March 22, 2024, from https://www.eia.gov/todayinenergy/detail.php?id=61142

Eia. (2024b). *U.s. henry hub natural gas prices in 2023 were the lowest since mid-2020*. Retrieved March 21, 2024, from https://www.hydrocarbonengineering.com/gas-processing/07012022/the-eia-reports-on-2021-natural-gas-prices/

Elliott, G., Rothenberg, T. J., & Stock, J. H. (1996). Efficient tests for an autoregressive unit root. *Econometrica*, *64*(4), 813–836. Retrieved March 15, 2024, from http://www.jstor.org/stable/2171846

EuropeanCommission. (2024a). *Development of eu ets (2005-2020)*. Retrieved May 14, 2024, from https://climate.ec.europa.eu/eu-action/eu-emissions-trading-system-eu-ets/development-eu-ets-2005-2020_en#evolution-of-the-european-carbon-market

EuropeanCommission. (2024b). *Emissions cap and allowances*. Retrieved May 14, 2024, from https://climate.ec.europa.eu/eu-action/eu-emissions-trading-system-eu-ets/emissions-cap-and-allowances_en

EuropeanCommission. (2024c). *Scope of the eu emissions trading system*. Retrieved March 14, 2024, from https://climate.ec.europa.eu/eu-action/eu-emissions-trading-system-eu-ets/scope-eu-emissions-trading-system_en

EuropeanCouncil. (2024a). *Energy price rise since 2021*. Retrieved April 5, 2024, from https://www.consilium.europa.eu/en/infographics/energy-prices-2021/

EuropeanCouncil. (2024b). *Energy prices and security of supply*. Retrieved April 5, 2024, from https://www.consilium.europa.eu/en/policies/energy-prices-and-security-of-supply/

EuropeanParliament. (2023). *What is carbon neutrality and how can it be achieved by 2050?* Retrieved March 22, 2024, from https://www.europarl.europa.eu/topics/en/article/20190926STO62270/what-is-carbon-neutrality-and-how-can-it-be-achieved-by-2050

Gabauer, D. (2022). *Connectedness approach*. CRAN.

Hassani, H., & Yeganegi, M. R. (2020). Selecting optimal lag order in ljung-box test. *Physica A: Statistical Mechanics and its Applications*, *541*, 123700. https://doi.org/https://doi.org/10.1016/j.physa.2019.123700

Hydro. (2018). *Annual report 2017*. Retrieved April 8, 2024, from https://www.hydro.com/Document/Doc/Hydro%20Annual%20Report%202017?docId=3097

Hydro. (2019). *Annual report 2018*. Retrieved April 8, 2024, from https://www.hydro.com/Document/Doc/2018%20Annual%20report.pdf?docId=8525

Hydro. (2020). *Annual report 2019*. Retrieved April 8, 2024, from https://www.hydro.com/en/investors/reports-and-presentations/annual-reports/annual-report-2019/

Hydro. (2021). *Annual report 2020*. Retrieved April 8, 2024, from https://www.hydro.com/en/investors/reports-and-presentations/annual-reports/annual-report-2020/

Hydro. (2022). *Annual report 2021*. Retrieved April 8, 2024, from https://www.hydro.com/globalassets/06-investors/reports-and-presentations/annual-report/rdmar21/annual-report-2021-eng.pdf

Hydro. (2023). *Annual report 2022*. Retrieved April 8, 2024, from https://www.hydro.com/globalassets/06-investors/reports-and-presentations/annual-report/jenincharge22/annual-report-2022eng2.pdf

Hydro. (2024). *Annual report 2023*. Retrieved April 8, 2024, from https://www.hydro.com/globalassets/06-investors/reports-and-presentations/annual-report/nhar23/integrated-annual-report-2023_eng.pdf

Hyndman, R. J., & Anthanasopoulos, G. (2018). *Forecasting: Principles and practice* (Second Edition). OText.

IEA. (2021). *Coal 2021 executive summary*. Retrieved March 22, 2024, from https://www.iea.org/reports/coal-2021/executive-summary

IEA. (2023). *Coal 2023 executive summary*. Retrieved March 22, 2024, from https://www.iea.org/reports/coal-2023/executive-summary

Ji, Q., Zhang, D., & Geng, J.-b. (2018). Information linkage, dynamic spillovers in prices and volatility between the carbon and energy markets. *Journal of Cleaner Production*, *198*, 972–978. https://doi.org/https://doi.org/10.1016/j.jclepro.2018.07.126

Jiang, W., Zhang, Y., & Wang, K.-H. (2024). Analyzing the connectedness among geopolitical risk, traditional energy and carbon markets. *Energy*, *298*, 131411. https://doi.org/https://doi.org/10.1016/j.energy.2024.131411

Jungeilges, J. (2023a). *Unit 6: Inference concerning auto-covariance/correlation*. University of Agder.

Jungeilges, J. (2023b). *Vector autoregressive models (unit9)*. University of Agder.

Koop, G., Pesaran, M., & Potter, S. M. (1996). Impulse response analysis in nonlinear multivariate models. *Journal of Econometrics*, *74*(1), 119–147. https://doi.org/https://doi.org/10.1016/0304-4076(95)01753-4

Kwiatkowski, D., Phillips, P. C., Schmidt, P., & Shin, Y. (1992). Testing the null hypothesis of stationarity against the alternative of a unit root: How sure are we that economic time series have a unit root? *Journal of Econometrics*, *54*(1), 159–178. https://doi.org/https://doi.org/10.1016/0304-4076(92)90104-Y

Lastrapes, W. D., & Wiesen, T. F. (2021). The joint spillover index. *Economic Modelling*, *94*, 681–691. https://doi.org/https://doi.org/10.1016/j.econmod.2020.02.010

Liu, D., Chen, K., Cai, Y., & Tang, Z. (2024). Interpretable eu ets phase 4 prices forecasting based on deep generative data augmentation approach. *Finance Research Letters*, *61*, 105038. https://doi.org/https://doi.org/10.1016/j.frl.2024.105038

Liu, Y., Yang, A., Pei, H., & Han, X. (2024). Forecasting risk of european carbon emissions trading market with dysco-skst model. *Journal of Cleaner Production*, *434*, 139933. https://doi.org/https://doi.org/10.1016/j.jclepro.2023.139933

Ljung, G. M., & Box, G. E. P. (1978). On a measure of lack of fit in time series models. *Biometrika*, *65*(2), 297–303. https://doi.org/10.1093/biomet/65.2.297

LufthansaGroup. (2018). *Annual report 2017*. Retrieved April 9, 2024, from https://investor-relations.lufthansagroup.com/fileadmin/downloads/en/financial-reports/annual-reports/LH-AR-2017-e.pdf

LufthansaGroup. (2019). *Annual report 2018*. Retrieved April 9, 2024, from https://investor-relations.lufthansagroup.com/fileadmin/downloads/en/financial-reports/annual-reports/LH-AR-2018-e.pdf

LufthansaGroup. (2020). *Annual report 2019*. Retrieved April 9, 2024, from https://investor-relations.lufthansagroup.com/fileadmin/downloads/en/financial-reports/annual-reports/LH-AR-2019-e.pdf

LufthansaGroup. (2021). *Annual report 2020*. Retrieved April 9, 2024, from https://investor-relations.lufthansagroup.com/fileadmin/downloads/en/financial-reports/annual-reports/LH-AR-2020-e.pdf

LufthansaGroup. (2022). *Annual report 2021*. Retrieved April 9, 2024, from https://investor-relations.lufthansagroup.com/fileadmin/downloads/en/financial-reports/annual-reports/LH-AR-2021-e.pdf

LufthansaGroup. (2023). *Annual report 2022*. Retrieved April 9, 2024, from https://investor-relations.lufthansagroup.com/fileadmin/downloads/en/financial-reports/annual-reports/LH-AR-2022-e.pdf

LufthansaGroup. (2024). *Annual report 2023*. Retrieved April 9, 2024, from https://investor-relations.lufthansagroup.com/fileadmin/downloads/en/financial-reports/annual-reports/LH-AR-2023-e.pdf

Meng, W., Sun, H., & Yang, Z. (2024). Can carbon emission trading markets reduce the risks in traditional energy markets? *Journal of Cleaner Production*, *454*, 142239. https://doi.org/https://doi.org/10.1016/j.jclepro.2024.142239

Mills, T. C. (2019). *Applied time series analysis: A practical guide to modeling and forecasting*. Elsevier Inc.

Nestle. (2020). *Annual review 2019*. Retrieved April 5, 2024, from https://www.nestle.com/sites/default/files/2020-03/2019-annual-review-en.pdf

Newell, R. G., Pizer, W. A., & Raimi, D. (2013). Carbon markets 15 years after kyoto: Lessons learned, new challenges. *Journal of Economic Perspectives*. https://www.aeaweb.org/articles?id=10.1257/jep.27.1.123

OpenAI. (2024). *Chatgpt* (GPT-4o). Retrieved May 22, 2024, from https://openai.com/about/

Parkinson, M. (1980). The extreme value method for estimating the variance of the rate of return. *The Journal of Business*, *53*(1), 61–65. Retrieved March 7, 2024, from http://www.jstor.org/stable/2352357

Pesaran, H., & Shin, Y. (1998). Generalized impulse response analysis in linear multivariate models. *Economics Letters*, *58*(1), 17–29. https://doi.org/https://doi.org/10.1016/S0165-1765(97)00214-0

Phillips, P. C. B., & Perron, P. (1988). Testing for a unit root in time series regression. *Biometrika*, *75*(2), 335–346. Retrieved March 15, 2024, from http://www.jstor.org/stable/2336182

PortofRotterdam. (2024). *Coal*. Retrieved March 22, 2024, from https://www.portofrotterdam.com/en/logistics/cargo/dry-bulk/coal

Shumway, R. H., & Stoffer, D. S. (2017). *Time series analysis and its applications* (Fourth Edition). Springer International Publishing.

Sims, C. A. (1980). Macroeconomics and reality. *Econometrica*, *48*(01), 1–48. https://doi.org/https://doi.org/10.2307/1912017

Sousa, R., Aguiar-Conraria, L., & Soares, M. J. (2014). Carbon financial markets: A time-frequency analysis of co2 prices. *Physica A: Statistical Mechanics and its Applications*, *414*, 118–127. https://doi.org/https://doi.org/10.1016/j.physa.2014.06.058

Su, C. W., Qin, M., Chang, H.-L., & Țăran, A.-M. (2023). Which risks drive european natural gas bubbles? novel evidence from geopolitics and climate. *Resources Policy*, *81*, 103381. https://doi.org/https://doi.org/10.1016/j.resourpol.2023.103381

Tiwari, A. K., Trabelsi, N., Abakah, E. J. A., Nasreen, S., & Lee, C.-C. (2023). An empirical analysis of the dynamic relationship between clean and dirty energy markets. *Physica A: Statistical Mechanics and its Applications*, *124*, 106766. https://doi.org/https://doi.org/10.1016/j.eneco.2023.106766

Tsay, R. S. (2013). *Multivariate time series analysis*. John Wiley & Sons, Inc.

Tsay, R. S. (2014). *Multivariate time series analysis with r and financial applications*. John Wiley & Sons, Inc.

UNFCC. (2024). *The paris agreement*. Retrieved April 2, 2024, from https://unfccc.int/process-and-meetings/the-paris-agreement

UnitedNations. (2024). What is the kyoto protocol. *United Nations Framework Convention on Climate Change*. https://unfccc.int/kyoto_protocol

Wang, J., Guo, X., Tan, X., Chevallier, J., & Ma, F. (2023). Which exogenous driver is informative in forecasting european carbon volatility: Bond, commodity, stock or uncertainty? *Energy Economics*, *117*, 106419. https://doi.org/https://doi.org/10.1016/j.eneco.2022.106419

Wen, F., Zhao, H., Zhao, L., & Yin, H. (2022). What drive carbon price dynamics in china? *International Review of Financial Analysis*, *79*, 101999. https://doi.org/https://doi.org/10.1016/j.irfa.2021.101999

Chapter 8

appendix

Table 8.1: This table presents the p-values from four different stationarity tests applied on the return series.

	DickeyFuller	PhillipsPerron	KPSS.level	KPSS.trend
Carbon	< 0.010	< 0.01	0.082	0.100
Oil	< 0.010	< 0.01	0.100	0.100
Aviation	< 0.010	< 0.01	0.100	0.100
Natural Gas	< 0.010	< 0.01	0.100	0.100
Coal	< 0.010	< 0.01	0.100	0.039
Clean Energy	< 0.010	< 0.01	0.100	0.100
Chemicals	< 0.010	< 0.01	0.100	0.100
Metal	< 0.010	< 0.01	0.100	0.100
Food	< 0.010	< 0.01	0.100	0.100
Cement	< 0.010	< 0.01	0.100	0.100

Note: '< 0.010' means less than the 1% significant level.

Table 8.2: This table presents the p-values from four different stationarity tests applied on the volatility series.

	DickeyFuller	PhillipsPerron	KPSS.level	KPSS.trend
Carbon	0.010	0.010	0.100	0.010
Oil	0.010	0.010	0.010	0.010
Aviation	0.010	0.010	0.010	0.010
Natural Gas	0.010	0.010	0.010	0.021
Coal	0.010	0.010	0.010	0.010
Clean Energy	0.010	0.010	0.010	0.010
Chemicals	0.010	0.010	0.024	0.010
Metal	0.010	0.010	0.010	0.010
Food	0.010	0.010	0.045	0.010
Cement	0.010	0.010	< 0.100	0.010

Note: Outputs are calculated from Rstudio.

Table 8.3: List of Missing Observation Dates

Na.dates	**Na.dates**	**Na.dates**
2017-08-15	2018-05-28	2019-12-31
2017-08-28	2018-08-15	2020-01-01
2017-09-03	2018-08-27	2020-01-19
2017-10-03	2018-09-02	2020-02-16
2017-10-31	2018-10-03	2020-04-13
2017-12-25	2018-12-24	2020-05-01
2017-12-26	2018-12-25	2020-05-08
2018-01-01	2018-12-26	2020-05-24
2018-01-14	2018-12-31	2020-05-25
2018-02-18	2019-01-01	2020-06-01
2018-03-30	2019-01-20	2020-08-31
2018-04-02	2019-02-17	2020-09-06
2018-05-01	2019-04-22	2020-12-24
2018-05-07	2019-05-01	2020-12-25
2018-05-21	2019-05-06	2020-12-26
2018-05-28	2019-05-26	2020-12-28
2018-08-15	2019-06-10	2020-12-31
2018-08-27	2019-08-15	2021-01-17
2018-09-02	2019-08-26	2021-02-14
2018-10-03	2019-09-01	2021-04-02
2018-12-24	2019-10-03	2021-04-05
2018-12-25	2019-12-24	2021-05-03
2018-12-26	2019-12-25	2021-05-24
2018-12-31	2019-12-26	2021-05-30

Table 8.4: List of Missing Observation Dates (continued)

Na.dates	Na.dates	Na.dates
2021-07-04	2022-06-19	2023-05-08
2021-08-30	2022-07-03	2023-05-28
2021-09-05	2022-08-29	2023-05-29
2021-09-15	2022-09-04	2023-06-18
2021-12-24	2022-09-23	2023-08-15
2021-12-27	2022-10-03	2023-08-28
2021-12-28	2022-12-26	2023-09-03
2021-12-31	2022-12-27	2023-11-14
2022-01-03	2023-01-02	2023-11-15
2022-01-16	2023-01-15	2023-11-16
2022-02-20	2023-02-19	2023-12-25
2022-04-15	2023-12-20	2023-12-26
2022-04-18	2023-04-07	2024-01-01
2022-05-02	2023-04-10	2024-01-14
2022-05-29	2023-05-01	
2022-06-02	2023-05-28	
2022-06-03	2023-05-29	
2022-06-19	2023-06-18	
2022-07-03	2023-08-15	
2022-08-29	2023-08-28	
2022-09-04	2023-09-03	
2022-09-23	2023-11-14	
2022-10-03	2023-11-15	

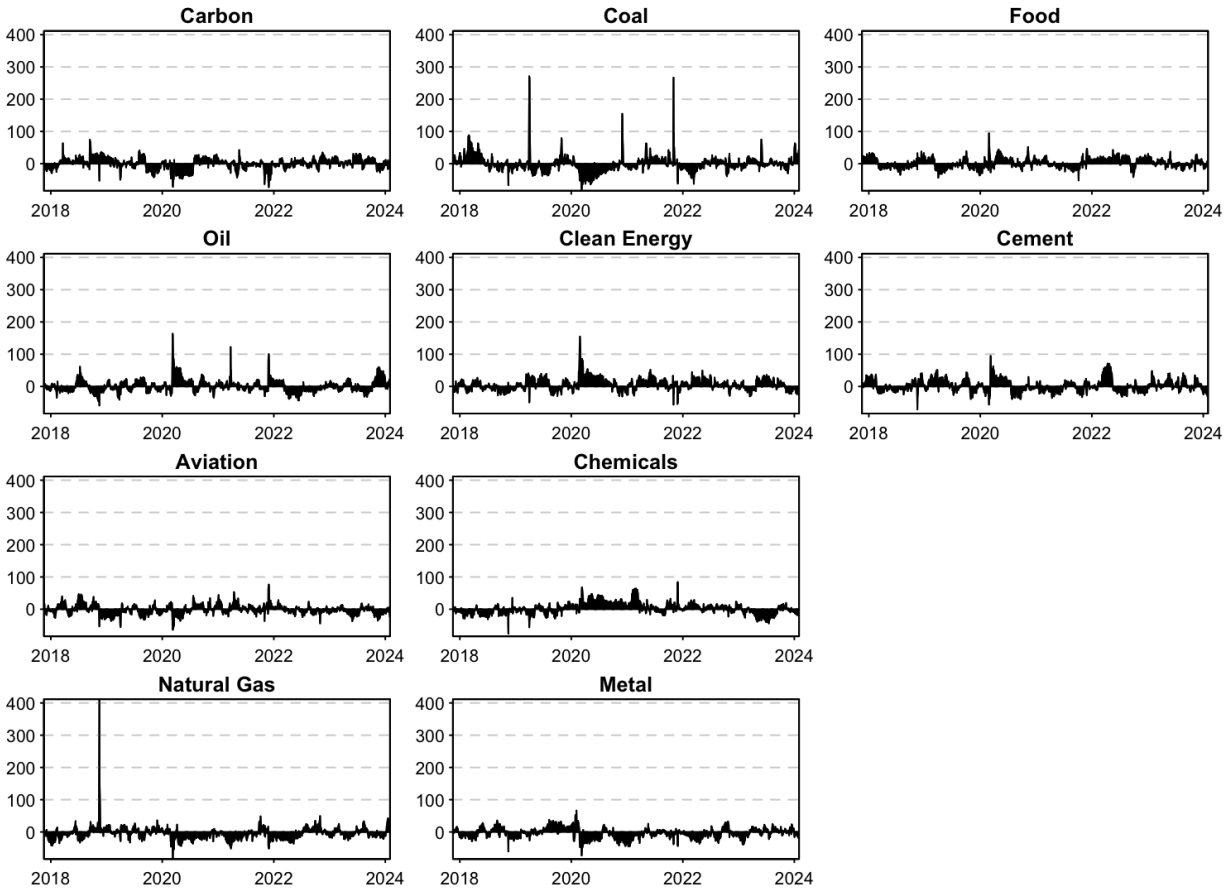

Figure 8.1: The 'Original' Net Dynamic Volatility Connectedness Plot

Table 8.5: Multivariate Portmanteau test of a VAR(1)

m	Q(m)	df	p-value
1	1.92	100.00	1.00
2	132.74	200.00	1.00
3	309.09	300.00	0.35
4	482.38	400.00	0.00

Note: Replication of the results from the Multivariate Portmanteau test produced in R

Table 8.6: Multivariate Portmanteau test of a VAR(5)

m	Q(m)	df	p-value
1	3.98	100.00	1.00
2	10.79	200.00	1.00
3	22.07	300.00	1.00
4	45.28	400.00	1.00

Note: Replication of the results from the Multivariate Portmanteau test produced in R

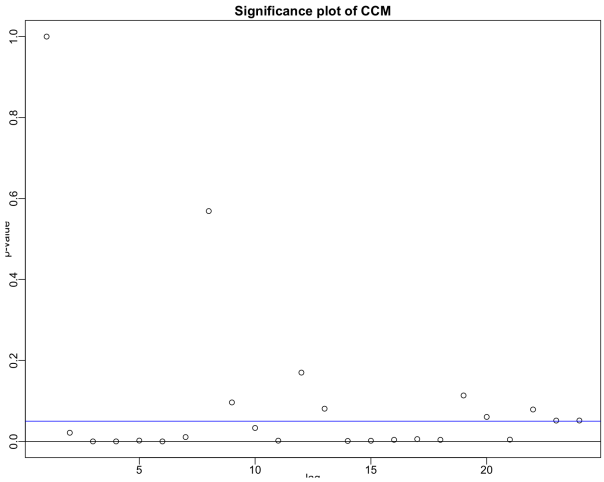

Figure 8.2: Cross-Correlation Matrix VAR(1) returns system

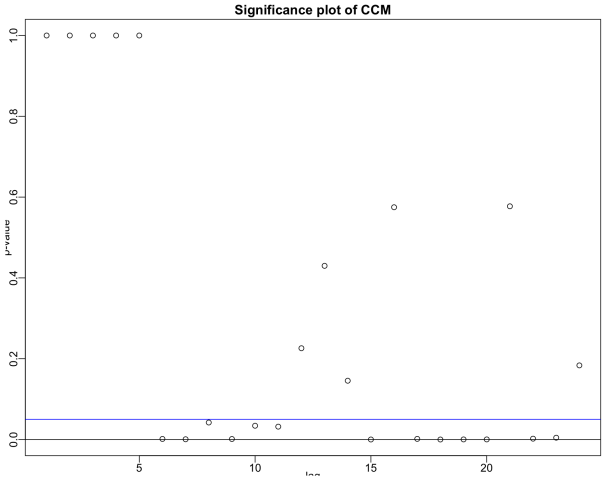

Figure 8.3: Cross-Correlation Matrix VAR(5) volatility system

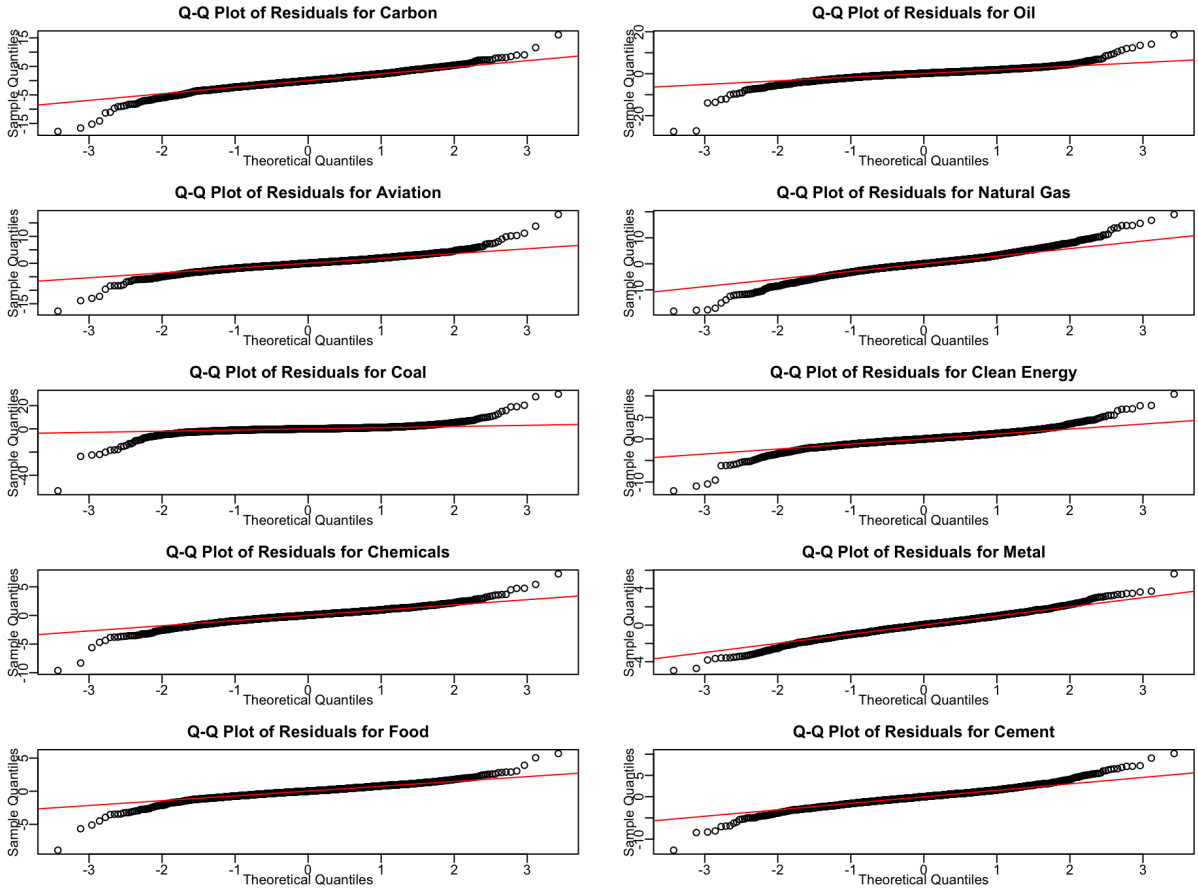

Figure 8.4: QQplot for the returns

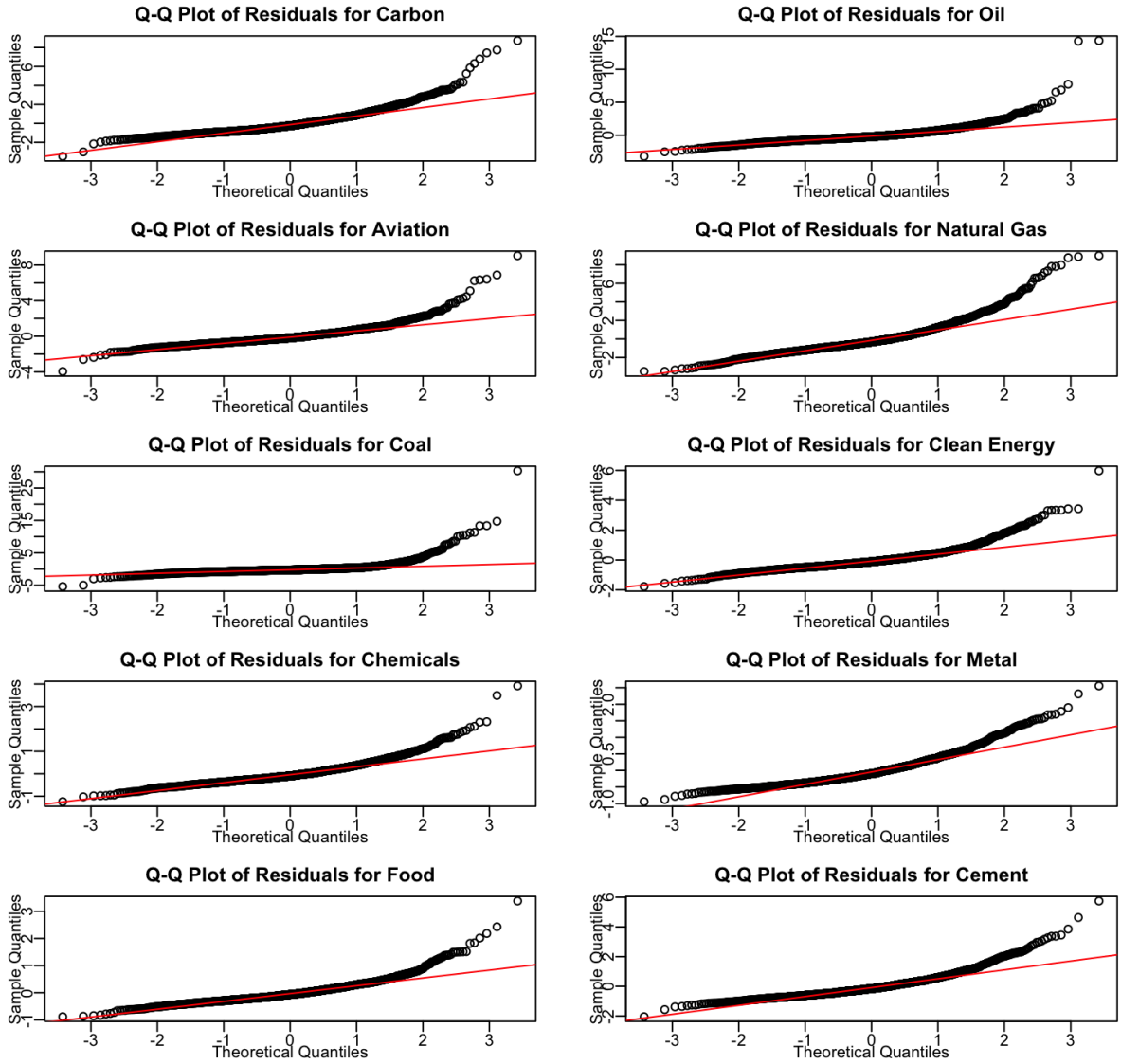

Figure 8.5: Q-Q Plot for the Volatility

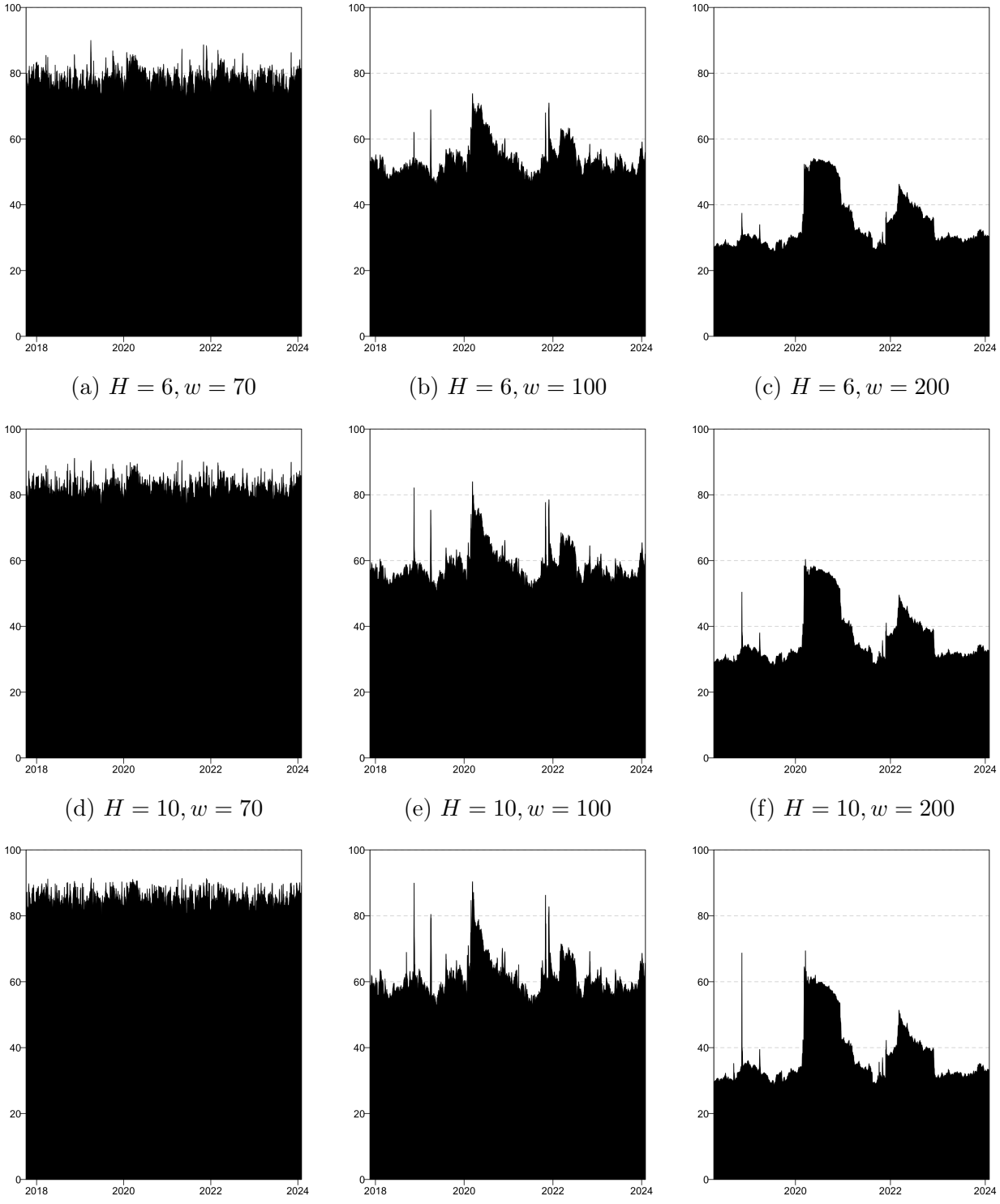

(a) $H = 6, w = 70$ (b) $H = 6, w = 100$ (c) $H = 6, w = 200$

(d) $H = 10, w = 70$ (e) $H = 10, w = 100$ (f) $H = 10, w = 200$

(g) $H = 18, w = 70$ (h) $H = 18, w = 100$ (i) $H = 18, w = 200$

Figure 8.6: Total Dynamic Connectedness: Volatility System

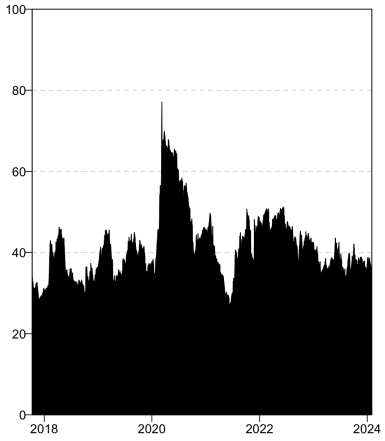

(a) $H = 6, w = 70$

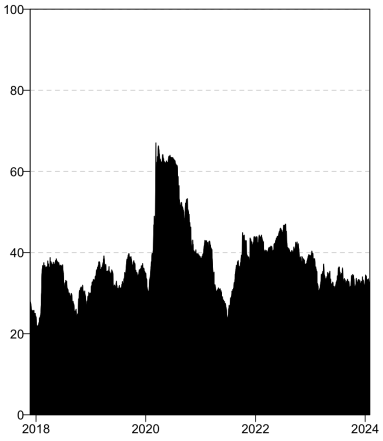

(b) $H = 6, w = 100$

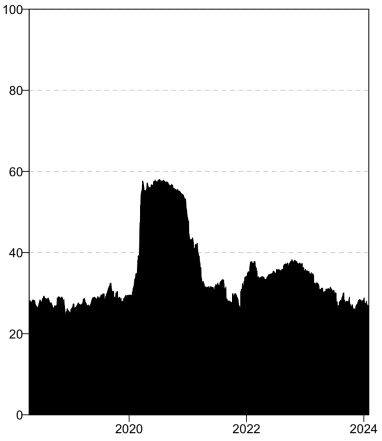

(c) $H = 6, w = 200$

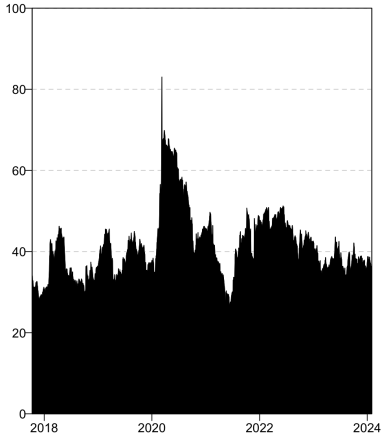

(d) $H = 10, w = 70$

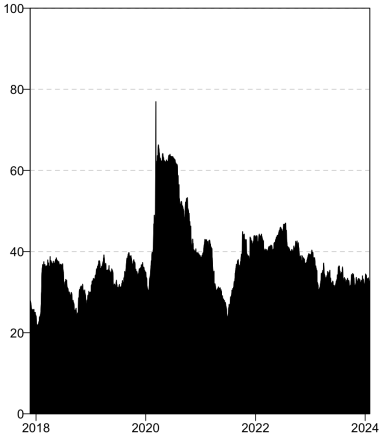

(e) $H = 10, w = 100$

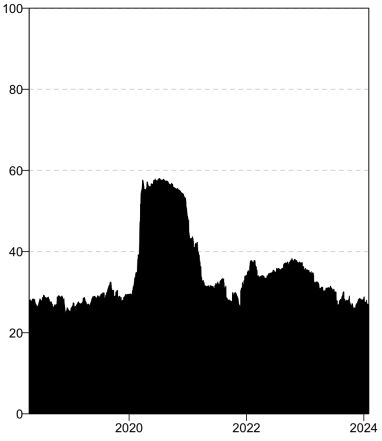

(f) $H = 10, w = 200$

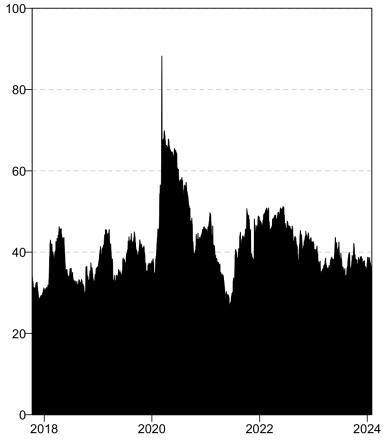

(g) $H = 18, w = 70$

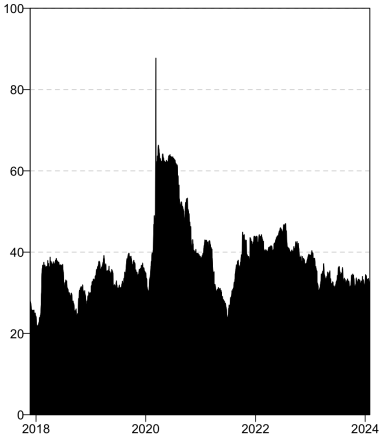

(h) $H = 18, w = 100$

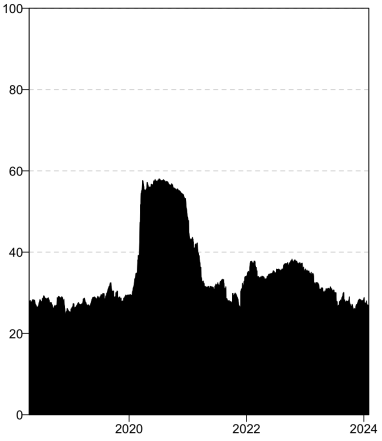

(i) $H = 18, w = 200$

Figure 8.7: Total Dynamic Connectedness: Returns System

Chapter 9

R Script

```
rm(list=ls(all=TRUE))
setwd("~/OneDrive - Universitetet i Agder/R/Master")

library(tseries)
library(zoo)
library(Quandl)
library(moments)
library(MTS)
library(quantmod)
library(pastecs)
library(readr)
library(tidyverse)
library(xtable)
library(ConnectednessApproach)
library(readxl)
library(dplyr)

#Upload dataset

aviation <-read.csv("~/OneDrive - Universitetet i ...
   Agder/R/Master/data/Aviation.charlie.csv"
                    ,header = TRUE)
carbon <- read.csv("~/OneDrive - Universitetet i ...
   Agder/R/Master/data/Carbon.charlie.csv"
                   , header = TRUE)
coal <- read.csv("~/OneDrive - Universitetet i ...
   Agder/R/Master/data/Coal.charlie.csv"
                 ,header = TRUE)
```

```
ng <- read.csv("~/OneDrive - Universitetet i ...
   Agder/R/Master/data/NaturalGas.charlie.csv"
               ,header = TRUE)
ce <- read.csv("~/OneDrive - Universitetet i ...
   Agder/R/Master/data/CleanEnergy.charlie.csv"
               ,header = TRUE)
oil <- read.csv("~/OneDrive - Universitetet i ...
   Agder/R/Master/data/Oil.charlie.csv"
                ,header = TRUE)
chm <- read.csv("~/OneDrive - Universitetet i ...
   Agder/R/Master/data/Chemicals.charlie.csv"
                , header=TRUE)
food <- read.csv("~/OneDrive - Universitetet i ...
   Agder/R/Master/data/FoodandBeverage.charlie.csv"
                 , header = TRUE)
metal <- read.csv("~/OneDrive - Universitetet i ...
   Agder/R/Master/data/Metal.charlie.csv"
                  ,header=TRUE)
cement <- read.csv("~/OneDrive - Universitetet i ...
   Agder/R/Master/data/Cement.charlie.csv"
                   , header=TRUE)
# Extracting Prices

carbon.price<-carbon$Price
oil.price<-oil$Price
aviation.price<-aviation$Price
ng.price<-ng$Price
coal.price<-coal$Price
ce.price<-ce$Price
chm.price<-chm$Price
food.price<-food$Price
metal.price<-metal$Price
cement.price<-cement$Price

# Deleting commas
ce.price=as.numeric(gsub(",","",ce.price))
metal.price=as.numeric(gsub(",","",metal.price))



# Transforming to zoo

```

```
carbon.price<-zoo(carbon.price, order.by =as.Date(carbon$Date, format = ...
    "%m/%d/%Y") )

oil.price<-zoo(oil.price, order.by = as.Date(oil$Date, format = "%m/%d/%Y"))
aviation.price<-zoo(aviation.price, order.by = as.Date(aviation$Date, ...
    format = "%m/%d/%Y"))

ng.price<-zoo(ng.price, order.by = as.Date(ng$Date, format = "%m/%d/%Y"))

coal.price<-zoo(coal.price, order.by = as.Date(coal$Date, format = ...
    "%m/%d/%Y"))

ce.price<-zoo(ce.price, order.by = as.Date(ce$Date, format = "%m/%d/%Y"))

chm.price<-zoo(chm.price, order.by = as.Date(chm$Date, format = "%m/%d/%Y"))

food.price<-zoo(food.price, order.by = as.Date(food$Date, format = ...
    "%m/%d/%Y"))

metal.price<-zoo(metal.price, order.by = as.Date(metal$Date, format = ...
    "%m/%d/%Y"))

cement.price<-zoo(cement.price, order.by = as.Date(cement$Date, format = ...
    "%m/%d/%Y"))



# Inspection of lengths

length(carbon.price)
length(oil.price)
length(aviation.price)
length(ng.price)
length(coal.price)
length(ce.price)
length(chm.price)
length(food.price)
length(metal.price)
length(cement.price)
```

```
# Data matrix

data.alpha<-data.frame(cbind(carbon.price, oil.price,aviation.price,ng.price,
                             coal.price,ce.price, chm.price,
                             metal.price, food.price, cement.price))


colnames(data.alpha)<-c("Carbon", "Oil", "Aviation","Natural Gas","Coal",
                        "Clean Energy", "Chemicals", "Metal", "Food"
                        ,"Cement")


# Checking for NAs

sum(is.na(data.alpha))
data.alpha<-na.omit(data.alpha);  # Omiting the na's
sum(is.na(data.alpha))
#NA_data <- read_excel("~/OneDrive - Universitetet i ...
   Agder/R/Master/NA-Omega.xlsx")

#NA_data<-data.frame(NA_data)
#xtable(NA_data)
                  # Transforming to time series

                     dat.ts<-ts(data.alpha)

                  # Daily log-returns

                    datret<-diff(log(dat.ts))*100 # Log returns


    # Date Vector

datret.df <- data.frame(datret)
rownames(datret.df)<- rownames(data.frame(data.alpha))[-1]
date <- as.Date(rownames(datret.df))

### ===== Plotting Returns ===== ###

    # Carbon
#par(mfrow=c(1,3))
```

```
#plot(carbon.price,type="l", ylab="Carbon Prices (EUR)", xlab="Year", ...
   main="Raw Data")
#plot(datret[,"Carbon"],ylab="Carbon Log-Returns", main="Time Series")
#hist(datret[,"Carbon"], main="Distribution", xlab= "Carbon Log-Returns")


    # Oil
#plot(oil.price,type="l" ,ylab="Oil Prices (USD)",xlab="Year", main="Raw ...
   Data")
#plot(datret[,"Oil"], main="Time Series",ylab="Oil Log-Returns")
#hist(datret[,"Oil"], main="Distribution", xlab= "Oil Log-Returns")

    # Aviation
#plot(aviation.price,type="l" ,ylab="Aviation Price Index ...
   (EUR)",xlab="Year", main="Raw Data")
#plot(datret[,"Aviation"], main="Time Series",ylab="Aviation Log-Returns")
#hist(datret[,"Aviation"],main="Distribution", xlab= "Aviation Log-Returns")

    # NG
#plot(ng.price,type="l" ,ylab="Natural Gas Prices (USD)",xlab="Year", ...
   main="Raw Data")
#plot(datret[,"Natural Gas"], main="Time Series",ylab="Natural Gas ...
   Log-Returns")
#hist(datret[,"Natural Gas"], main="Distribution", xlab= "Natural Gas ...
   Log-Returns")

    # Coal
#plot(coal.price,type="l" ,ylab="Coal Prices (USD)",xlab="Year", main="Raw ...
   Data")
#plot(datret[,"Coal"], main="Time Series",ylab="Coal Log-Returns")
#hist(datret[,"Coal"], main="Distribution", xlab= "Coal Log-Returns")

    # CE
#plot(ce.price, type="l", ylab="Clean Energy Price Index ...
   (EUR)",xlab="Year", main="Raw Data")
#plot(datret[,"Clean Energy"],main="Time Series",ylab="Clean Energy ...
   Log-Returns")
#hist(datret[,"Clean Energy"],main="Distribution", xlab= "Clean ...
   Log-Returns" )

    # CHM
```

```
#plot(chm.price, type="l", ylab="Chemical Price Index (EUR)",xlab="Year", ...
   main="Raw Data")
#plot(datret[,"Chemicals"], main="Time Series",ylab="Chemicals Log-Returns")
#hist(datret[,"Chemicals"], main="Distribution", xlab= "Chemicals ...
   Log-Returns")

    # Food
#plot(food.price, type="l",ylab="Food Price Index (EUR)",xlab="Year", ...
   main="Raw Data")
#plot(datret[,"Food"], main="Time Series",ylab="Food Log-Returns")
#hist(datret[,"Food"], main="Distribution", xlab= "Food Log-Returns")

    # Cement
#plot(cement.price, type="l", ylab="Cement Stock Prices ...
   (EUR)",xlab="Year", main="Raw Data")
#plot(datret[,"Cement"], main="Time Series",ylab="Cement Log-Returns")
#hist(datret[,"Cement"],main="Distribution", xlab= "Cement Log-Returns" )

    # Metal
#plot(metal.price, type="l",ylab="Metal Price Index (EUR)",xlab="Year", ...
   main="Raw Data")
#plot(datret[,"Metal"], main="Time Series",ylab="Metal Log-Returns")
#hist(datret[,"Metal"], main="Distribution", xlab= "Metal Log-Returns")


                # Daily log-volatilities

                datvoll<- 0.361 * diff((log(dat.ts)))^2
                datvol<-(sqrt(datvoll))*100


### ===== Plotting Volatilities ===== ###


# Carbon
#par(mfrow=c(1,3))
#plot(carbon.price,type="l", ylab="Carbon Prices (EUR)", xlab="Year", ...
   main="Raw Data")
#plot(datvol[,"Carbon"],ylab="Carbon Log-Volatilities", main="Time Series")
#hist(datvol[,"Carbon"], main="Distribution", xlab= "Carbon Log-Volatilities")
```

```
# Oil
#plot(oil.price,type="l" ,ylab="Oil Prices (USD)",xlab="Year", main="Raw ...
   Data")
#plot(datvol[,"Oil"], main="Time Series",ylab="Oil Log-Volatilities")
#hist(datvol[,"Oil"], main="Distribution", xlab= "Oil Log-Volatilities")

# Aviation
#plot(aviation.price,type="l" ,ylab="Aviation Price Index ...
   (EUR)",xlab="Year", main="Raw Data")
#plot(datvol[,"Aviation"], main="Time Series",ylab="Aviation ...
   Log-Volatilities")
#hist(datvol[,"Aviation"],main="Distribution", xlab= "Aviation ...
   Log-Volatilities")

# NG
#plot(ng.price,type="l" ,ylab="Natural Gas Prices (USD)",xlab="Year", ...
   main="Raw Data")
#plot(datvol[,"Natural Gas"], main="Time Series",ylab="Natural Gas ...
   Log-Volatilities")
#hist(datvol[,"Natural Gas"], main="Distribution", xlab= "Natural Gas ...
   Log-Volatilities")

# Coal
#plot(coal.price,type="l" ,ylab="Coal Prices (USD)",xlab="Year", main="Raw ...
   Data")
#plot(datvol[,"Coal"], main="Time Series",ylab="Coal Log-Volatilities")
#hist(datvol[,"Coal"], main="Distribution", xlab= "Coal Log-Volatilities")

# CE
#plot(ce.price, type="l", ylab="Clean Energy Price Index ...
   (EUR)",xlab="Year", main="Raw Data")
#plot(datvol[,"Clean Energy"],main="Time Series",ylab="Clean Energy ...
   Log-Volatilities")
#hist(datvol[,"Clean Energy"],main="Distribution", xlab= "Clean ...
   Log-Volatilities" )

# CHM
#plot(chm.price, type="l", ylab="Chemical Price Index (EUR)",xlab="Year", ...
   main="Raw Data")
```

```
#plot(datvol[,"Chemicals"], main="Time Series",ylab="Chemicals ...
   Log-Volatilities")
#hist(datvol[,"Chemicals"], main="Distribution", xlab= "Chemicals ...
   Log-Volatilities")

# Food
#plot(food.price, type="l",ylab="Food Price Index (EUR)",xlab="Year", ...
   main="Raw Data")
#plot(datvol[,"Food"], main="Time Series",ylab="Food Log-Volatilities")
#hist(datvol[,"Food"], main="Distribution", xlab= "Food Log-Volatilities")

# Cement
#plot(cement.price, type="l", ylab="Cement Stock Prices ...
    (EUR)",xlab="Year", main="Raw Data")
#plot(datvol[,"Cement"], main="Time Series",ylab="Cement Log-Volatilities")
#hist(datvol[,"Cement"],main="Distribution", xlab= "Cement ...
   Log-Volatilities" )

# Metal
#plot(metal.price, type="l",ylab="Metal Price Index (EUR)",xlab="Year", ...
   main="Raw Data")
#plot(datvol[,"Metal"], main="Time Series",ylab="Metal Log-Volatilities")
#hist(datvol[,"Metal"], main="Distribution", xlab= "Metal Log-Volatilities")



# ===== descriptive data of returns ===== #

# mean, quantiles, interquantile range, skewness, kurtosis

mu<-apply(datret, 2, mean); mu
sigma<-apply(datret, 2, sd); sigma
skew<-skewness(datret); skew
kurt<-kurtosis(datret); kurt


stat.desc(datret)

summary(datret)

# vector for mim & max & iqr
```

```
min<-c(-17.7347,-27.9762, -18.00751,-18.13582,-53.68803, -12.06941,
       -10.16089, -5.10154, -9.196018, -12.23043)

max<-c(16.1378,19.0774,17.82715,19.79844,32.62157,10.69128, 7.34444,
       5.6055, 5.3182, 9.78698)




# Interquantile range

#iqr.Carbon<-IQR(datret[,"Carbon"])
#iqr.Oil<-IQR(datret[,"Oil"])
#iqr.Aviation<-IQR(datret[,"Aviation"])
#iqr.NG<-IQR(datret[,"Natural Gas"])
#iqr.Coal<-IQR(datret[,"Coal"])
#iqr.CE<-IQR(datret[,"Clean Energy"])


#iqr.datret<-c(iqr.Carbon,iqr.Oil,iqr.Aviation,iqr.NG,iqr.Coal,iqr.El,iqr.CE)


# Normality test Jarque-bera test

#jarque.bera.test(datret[,"Carbon"])
#jarque.bera.test(datret[,"Oil"])
#jarque.bera.test(datret[,"Aviation"])
#jarque.bera.test(datret[,"Natural Gas"])
#jarque.bera.test(datret[,"Coal"])
#jarque.bera.test(datret[,"Clean Energy"])
#jarque.bera.test(datret[,"Chemicals"])
#jarque.bera.test(datret[,"Metal"])
#jarque.bera.test(datret[,"Food"])
#jarque.bera.test(datret[,"Cement"])

#jb<- c(rep(0.01,10));


#d.stat<- data.frame(Mean=mu, Std = sigma,
```

```
    # Skewness = skew, Kurtosis=kurt, Min.=min, Max.=max,Jarque.Bera=jb)

#xtable(d.stat, digits=3)

# ===== autocorrelation log-returns ===== #

#par(mfrow=c(1,1))
#acf(datret[, "Carbon"], lag=20)

#acf(datret[, "Oil"], lag=30)

#acf(datret[, "Aviation"], lag=20)

#acf(datret[, "Natural Gas"], lag=20)

#acf(datret[, "Coal"], lag=20)

#acf(datret[, "Clean Energy"], lag=20)

#acf(datret[, "Chemicals"], lag=20)

#acf(datret[, "Metal"], lag=40)

#acf(datret[, "Food"], lag=30)

#acf(datret[, "Cement"], lag=40)



# ===== Ljung-Box ===== #

#Box.test(datret[,"Carbon"], lag= lagHA, type="Ljung-Box") # Reject H0

#Box.test(datret[,"Oil"],lag=lagHA, type="Ljung-Box") # reject H0

#Box.test(datret[, "Aviation"], lag=lagHA, type="Ljung-Box") # Reject H0

#Box.test(datret[,"Natural Gas"], lag= lagHA, type="Ljung-Box") # reject H0

#Box.test(datret[,"Coal"], lag=lagHA, type="Ljung-Box") # fail to reject H0
```

```
#Box.test(datret[, "Clean Energy"], lag=lagHA, type="Ljung-Box") # reject H0

#Box.test(datret[, "Chemicals"], lag=lagHA, type="Ljung-Box") #reject H0

#Box.test(datret[, "Metal"], lag=lagHA, type="Ljung-Box") # fail to reject H0

#Box.test(datret[, "Food"], lag=lagHA, type="Ljung-Box") # fail to reject H0

#Box.test(datret[, "Cement"], lag=lagHA, type="Ljung-Box") # fail to ...
   reject H0


#lag50<-c(0.03806, 0.06372, 0.001576, 0.0928,0.1767, 0.000,0.000, 0.2134, ...
   0.1359,0.2017)

#lag20<-c(0.00675,0.06075, 0.000,0.02032,0.01695 ...
   ,0.000,0.000,0.3672,0.02703,0.07001 )


#lagHA<-min(10,1634/5); lagHA

#lagHA1<-c(0.007214,0.09445,0.00,0.007313,0.0352,
 #         0.000,0.00,0.3189,0.06704,0.07037)


#lagz<-data.frame(HA=lagHA1,SS=lag20,lag50 )

#xtable(lagz, digits = 3)


for (lag in 1:20) {
  result <- Box.test(datret[, "Carbon"], lag = lag, type = "Ljung-Box", ...
     fitdf = 0)
  print(result)
  }

for (lag in 1:10) {
  result <- Box.test(datret[, "Oil"], lag = lag, type = "Ljung-Box", fitdf ...
     = 0)
  print(result)
  }
```

```
for (lag in 1:10) {
  result <- Box.test(datret[, "Aviation"], lag = lag, type = "Ljung-Box", ...
      fitdf = 0)
  print(result)
}

for (lag in 1:10) {
  result <- Box.test(datret[, "Natural Gas"], lag = lag, type = ...
      "Ljung-Box", fitdf = 0)
  print(result)
}

for (lag in 1:10) {
  result <- Box.test(datret[, "Coal"], lag = lag, type = "Ljung-Box", ...
      fitdf = 0)
  print(result)
}

for (lag in 1:10) {
  result <- Box.test(datret[, "Clean Energy"], lag = lag, type = ...
      "Ljung-Box", fitdf = 0)
  print(result)
}

for (lag in 1:10) {
  result <- Box.test(datret[, "Chemicals"], lag = lag, type = "Ljung-Box", ...
      fitdf = 0)
  print(result)
}

for (lag in 1:50) {
  result <- Box.test(datret[, "Metal"], lag = lag, type = "Ljung-Box", ...
      fitdf = 0)
  print(result)
}

for (lag in 1:20) {
  result <- Box.test(datret[, "Food"], lag = lag, type = "Ljung-Box", ...
      fitdf = 0)
  print(result)
```

```
}

for (lag in 1:20) {
  result <- Box.test(datret[, "Cement"], lag = lag, type = "Ljung-Box", ...
     fitdf = 0)
  print(result)
}



# ===== partial-correlation ===== #

#pacf(datret[, "Carbon"])
#pacf(datret[, "Oil"])
#pacf(datret[, "Aviation"])
#pacf(datret[, "Natural Gas"])
#pacf(datret[, "Coal"])
#pacf(datret[, "Clean Energy"])
#pacf(datret[, "Chemicals"])
#pacf(datret[, "Metal"])
#pacf(datret[, "Food"])
#pacf(datret[, "Cement"])


# Making table for descriptive statistics
#tabx<-(data.frame(Mean=mu, St.d=sigma, Min.=min, Max.=max, IQR=c(iqr.C, ...
    iqr.F, iqr.O)
# ,Kurt=kurt, Skew. = skew, J.B.=rep(c("p-value <0.01"),3 )))
#xtable(tabx,digits=4)

# ===== ===== ===== Stationarity tests ===== ===== ===== #


# ===== Augmented Dickey-Fuller ===== #

#carbDF<-adf.test(datret[,"Carbon"],alternative="stationary"); carbDF

#oilDF<-adf.test(datret[,"Oil"],alternative="stationary"); oilDF

#aviationDF<-adf.test(datret[,"Aviation"],alternative="stationary"); ...
    aviationDF
```

```
#ngDF<-adf.test(datret[,"Natural Gas"],alternative="stationary"); ngDF

#coalDF<-adf.test(datret[,"Coal"],alternative="stationary"); coalDF

#ceDF<-adf.test(datret[,"Clean Energy"],alternative="stationary"); ceDF

#chmDF<-adf.test(datret[,"Chemicals"],alternative="stationary"); chmDF

#metalDF<-adf.test(datret[,"Metal"],alternative="stationary"); metalDF

#foodDF<-adf.test(datret[,"Food"],alternative="stationary");foodDF

#cementDF<-adf.test(datret[,"Cement"],alternative="stationary");cementDF

#ADF<-c(rep(0.01, 10))

# ===== PHILLIPS-PERRON ===== #

carbPP<-pp.test(datret[,"Carbon"], alternative ="stationary",
                type ="Z(alpha)", lshort =TRUE); carbPP

oilPP<-pp.test(datret[,"Oil"], alternative ="stationary",
               type ="Z(alpha)", lshort =TRUE); oilPP

aviationPP<-pp.test(datret[,"Aviation"], alternative ="stationary",
                    type ="Z(alpha)", lshort =TRUE); aviationPP

ngPP<-pp.test(datret[,"Natural Gas"], alternative ="stationary",
              type ="Z(alpha)", lshort =TRUE); ngPP

coalPP<-pp.test(datret[,"Coal"], alternative ="stationary",
                type ="Z(alpha)", lshort =TRUE); coalPP

cePP<-pp.test(datret[,"Clean Energy"], alternative ="stationary",
              type ="Z(alpha)", lshort =TRUE); cePP

chmPP<-pp.test(datret[,"Chemicals"], alternative ="stationary",
              type ="Z(alpha)", lshort =TRUE); chmPP

metalPP<-pp.test(datret[,"Metal"], alternative ="stationary",
```

```
              type ="Z(alpha)", lshort =TRUE); metalPP

foodPP<-pp.test(datret[,"Food"], alternative ="stationary",
              type ="Z(alpha)", lshort =TRUE); foodPP

cementPP<-pp.test(datret[,"Cement"], alternative ="stationary",
              type ="Z(alpha)", lshort =TRUE); cementPP

PP<-c(rep(0.01, 10))
# ===== KPSS ===== #


# For stationarity

carbKPSS<-kpss.test(datret[,"Carbon"],null="Level", lshort=TRUE); carbKPSS

oilKPSS<-kpss.test(datret[,"Oil"],null="Level", lshort=TRUE); oilKPSS

aviationKPSS<-kpss.test(datret[,"Aviation"],null="Level", lshort=TRUE); ...
   aviationKPSS

ngKPSS<-kpss.test(datret[,"Natural Gas"],null="Level", lshort=TRUE); ngKPSS

coalKPSS<-kpss.test(datret[,"Coal"],null="Level", lshort=TRUE); coalKPSS

ceKPSS<-kpss.test(datret[,"Clean Energy"],null="Level", lshort=TRUE); ceKPSS

chmKPSS<-kpss.test(datret[,"Chemicals"],null="Level", lshort=TRUE); chmKPSS

metalKPSS<-kpss.test(datret[,"Metal"],null="Level", lshort=TRUE); metalKPSS

foodKPSS<-kpss.test(datret[,"Food"],null="Level", lshort=TRUE); foodKPSS

cementKPSS<-kpss.test(datret[,"Cement"],null="Level", lshort=TRUE); cementKPSS

KPSS.level<-c(rep(0.1, 10))
# Trend stationarity

carbKPSS<-kpss.test(datret[,"Carbon"],null="Trend", lshort=TRUE); carbKPSS

oilKPSS<-kpss.test(datret[,"Oil"],null="Trend", lshort=TRUE); oilKPSS
```

```
aviationKPSS<-kpss.test(datret[,"Aviation"],null="Trend", lshort=TRUE); ...
   aviationKPSS

ngKPSS<-kpss.test(datret[,"Natural Gas"],null="Trend", lshort=TRUE); ngKPSS

coalKPSS<-kpss.test(datret[,"Coal"],null="Trend", lshort=TRUE); coalKPSS

ceKPSS<-kpss.test(datret[,"Clean Energy"],null="Trend", lshort=TRUE); ceKPSS

chmKPSS<-kpss.test(datret[,"Chemicals"],null="Trend", lshort=TRUE); chmKPSS

metalKPSS<-kpss.test(datret[,"Metal"],null="Trend", lshort=TRUE); metalKPSS

foodKPSS<-kpss.test(datret[,"Food"],null="Trend", lshort=TRUE); foodKPSS

cementKPSS<-kpss.test(datret[,"Cement"],null="Trend", lshort=TRUE); cementKPSS

KPSS.trend<-c(rep(0.1,4), 0.03912, rep(0.1,5))

#station.t<-data.frame(DickeyFuller=ADF, PhillipsPerron=PP,
 #                     KPSS.level=KPSS.level,KPSS.trend=KPSS.trend)

#xtable(station.t, digits=3)

# Making table for stationarity tests

#tab.station<-data.frame(DF=DF, PP=PP, KPSS=kpss, KPSS=Kpss , L.B=autocorr)
#xtable(tab.station)









# ===== descriptive data of volatility returns ===== #

#mu<-apply(datvol, 2, mean); mu
#sigma<-apply(datvol, 2, sd); sigma
#skew<-skewness(datvol); skew
#kurt<-kurtosis(datvol); kurt
```

```
#stat.desc(datvol)

#summary(datvol)

# vector for mim & max & iqr

#min<-c(rep(0,10))

#max<-c(10.6556,16.8090,10.8195,11.8956,32.2575,
 #      7.2517,6.1050,3.3680,5.5253,7.3484)

# Interquantile range

#iqr.Carbon<-IQR(datvol[,"Carbon"])
#iqr.Oil<-IQR(datvol[,"Oil"])
#iqr.Aviation<-IQR(datvol[,"Aviation"])
#iqr.NG<-IQR(datvol[,"Natural Gas"])
#iqr.Coal<-IQR(datvol[,"Coal"])
#iqr.CE<-IQR(datvol[,"Clean Energy"])
#iqr.chm<-IQR(datvol[,"Chemicals"])
#iqr.metal<-IQR(datvol[,"Metal"])
#iqr.food<-IQR(datvol[,"Food"])
#iqr.cement<-IQR(datvol[,"Cement"])



#iqr.datvol<-c(iqr.Carbon,iqr.Oil,iqr.Aviation,iqr.NG,iqr.Coal,iqr.El,iqr.CE)



# Normality test Jarque-bera test

jarque.bera.test(datvol[,"Carbon"])
jarque.bera.test(datvol[,"Oil"])
jarque.bera.test(datvol[,"Aviation"])
jarque.bera.test(datvol[,"Natural Gas"])
jarque.bera.test(datvol[,"Coal"])
jarque.bera.test(datvol[,"Clean Energy"])
jarque.bera.test(datvol[,"Chemicals"])
```

```
jarque.bera.test(datvol[,"Metal"])
jarque.bera.test(datvol[,"Food"])
jarque.bera.test(datvol[,"Cement"])



jb<- c(rep(0,10))


#d.stat<- data.frame(Mean=mu, Std = sigma,
 #                   Skewness = skew, Kurtosis=kurt, Min.=min, ...
    Max.=max,Jarque.Bera=jb)

#xtable(d.stat, digits=3)

# ===== autocorrelation log-volatility ===== #

acf(datvol[, "Carbon"], lag=20)

acf(datvol[, "Oil"], lag=20)

acf(datvol[, "Aviation"], lag=20)

acf(datvol[, "Natural Gas"], lag=20)

acf(datvol[, "Coal"], lag=20)

acf(datvol[, "Clean Energy"], lag=20)

acf(datvol[, "Chemicals"], lag=20)

acf(datvol[, "Metal"], lag=20)

acf(datvol[, "Food"], lag=20)

acf(datvol[, "Cement"], lag=20)



# ===== Ljung-Box ===== #
```

```
Box.test(datvol[,"Carbon"], lag= 50, type="Ljung-Box") # Reject

Box.test(datvol[,"Oil"], lag=50, type="Ljung-Box") # reject

Box.test(datvol[, "Aviation"], lag=50, type="Ljung-Box") # reject

Box.test(datvol[,"Natural Gas"], lag= 50, type="Ljung-Box") # reject

Box.test(datvol[,"Coal"], lag=50, type="Ljung-Box") # reject

Box.test(datvol[, "Clean Energy"], lag=50, type="Ljung-Box") # reject

Box.test(datvol[, "Chemicals"], lag=50, type="Ljung-Box") #reject

Box.test(datvol[, "Metal"], lag=50, type="Ljung-Box") #reject

Box.test(datvol[, "Food"], lag=50, type="Ljung-Box") #reject

Box.test(datvol[, "Cement"], lag=50, type="Ljung-Box") #reject


LB<-c(rep(2.2e-1,7),0.0003226, 2.2e-16,3.605e-10 )




for (lag in 1:10) {
  result <- Box.test(datret[, "Carbon"], lag = lag, type = "Ljung-Box", ...
      fitdf = 0)
  print(result)
}   # 5 lags

for (lag in 1:10) {
  result <- Box.test(datret[, "Oil"], lag = lag, type = "Ljung-Box", fitdf ...
      = 0)
  print(result)
} # 6

for (lag in 1:10) {
  result <- Box.test(datret[, "Aviation"], lag = lag, type = "Ljung-Box", ...
      fitdf = 0)
```

```
  print(result)
} # 5 lags

for (lag in 1:10) {
  result <- Box.test(datret[, "Natural Gas"], lag = lag, type = ...
      "Ljung-Box", fitdf = 0)
  print(result)
}

for (lag in 1:10) {
  result <- Box.test(datret[, "Coal"], lag = lag, type = "Ljung-Box", ...
      fitdf = 0)
  print(result)
}

for (lag in 1:10) {
  result <- Box.test(datret[, "Clean Energy"], lag = lag, type = ...
      "Ljung-Box", fitdf = 0)
  print(result)
}

for (lag in 1:10) {
  result <- Box.test(datret[, "Chemicals"], lag = lag, type = "Ljung-Box", ...
      fitdf = 0)
  print(result)
}

for (lag in 1:50) {
  result <- Box.test(datret[, "Metal"], lag = lag, type = "Ljung-Box", ...
      fitdf = 0)
  print(result)
}

for (lag in 1:20) {
  result <- Box.test(datret[, "Food"], lag = lag, type = "Ljung-Box", ...
      fitdf = 0)
  print(result)
}

for (lag in 1:20) {
```

```
  result <- Box.test(datret[, "Cement"], lag = lag, type = "Ljung-Box", ...
      fitdf = 0)
  print(result)
}



# ===== partial-correlation ===== #

pacf(datvol[, "Carbon"])
pacf(datvol[, "Oil"])
pacf(datvol[, "Aviation"])
pacf(datvol[, "Natural Gas"])
pacf(datvol[, "Coal"])
pacf(datvol[, "Clean Energy"])
pacf(datvol[, "Chemicals"])
pacf(datvol[, "Metal"])
pacf(datvol[, "Food"])
pacf(datvol[, "Cement"])


# Making table for descriptive statistics
#tabx<-(data.frame(Mean=mu, St.d=sigma, Min.=min, Max.=max, IQR=c(iqr.C, ...
    iqr.F, iqr.O)
# ,Kurt=kurt, Skew. = skew, J.B.=rep(c("p-value <0.01"),3 )))
#xtable(tabx,digits=4)

# ===== ===== ===== Stationarity tests ===== ===== ===== #


# ===== Augmented Dickey-Fuller ===== #

#carbDF<-adf.test(datvol[,"Carbon"],alternative="stationary"); carbDF

#oilDF<-adf.test(datvol[,"Oil"],alternative="stationary"); oilDF

#aviationDF<-adf.test(datvol[,"Aviation"],alternative="stationary"); ...
    aviationDF

#ngDF<-adf.test(datvol[,"Natural Gas"],alternative="stationary"); ngDF
```

```
#coalDF<-adf.test(datvol[,"Coal"],alternative="stationary"); coalDF

#ceDF<-adf.test(datvol[,"Clean Energy"],alternative="stationary"); ceDF

#chmDF<-adf.test(datvol[,"Chemicals"],alternative="stationary"); chmDF

#metalDF<-adf.test(datvol[,"Metal"],alternative="stationary"); metalDF

#foodDF<-adf.test(datvol[,"Food"],alternative="stationary");foodDF

#cementDF<-adf.test(datvol[,"Cement"],alternative="stationary");cementDF

#ADF<-c(rep(0.01,10))
# ===== PHILLIPS-PERRON ===== #

#carbPP<-pp.test(datvol[,"Carbon"], alternative ="stationary",
           #     type ="Z(alpha)", lshort =TRUE); carbPP

#oilPP<-pp.test(datvol[,"Oil"], alternative ="stationary",
            #   type ="Z(alpha)", lshort =TRUE); oilPP

#aviationPP<-pp.test(datvol[,"Aviation"], alternative ="stationary",
 #                  type ="Z(alpha)", lshort =TRUE); aviationPP

#ngPP<-pp.test(datvol[,"Natural Gas"], alternative ="stationary",
 #             type ="Z(alpha)", lshort =TRUE); ngPP

#coalPP<-pp.test(datvol[,"Coal"], alternative ="stationary",
             #   type ="Z(alpha)", lshort =TRUE); coalPP

#cePP<-pp.test(datvol[,"Clean Energy"], alternative ="stationary",
 #             type ="Z(alpha)", lshort =TRUE); cePP


#chmPP<-pp.test(datvol[,"Chemicals"], alternative ="stationary",
 #              type ="Z(alpha)", lshort =TRUE); chmPP

#metalPP<-pp.test(datvol[,"Metal"], alternative ="stationary",
 #                type ="Z(alpha)", lshort =TRUE); metalPP

#foodPP<-pp.test(datvol[,"Food"], alternative ="stationary",
```

```
 #               type ="Z(alpha)", lshort =TRUE); foodPP

#cementPP<-pp.test(datvol[,"Cement"], alternative ="stationary",
 #                 type ="Z(alpha)", lshort =TRUE); cementPP

#PP<-c(rep(0.01,10))

# ===== KPSS ===== #

# For stationarity

carbKPSS<-kpss.test(datvol[,"Carbon"],null="Level", lshort=TRUE); carbKPSS

oilKPSS<-kpss.test(datvol[,"Oil"],null="Level", lshort=TRUE); oilKPSS

aviationKPSS<-kpss.test(datvol[,"Aviation"],null="Level", lshort=TRUE); ...
   aviationKPSS

ngKPSS<-kpss.test(datvol[,"Natural Gas"],null="Level", lshort=TRUE); ngKPSS

coalKPSS<-kpss.test(datvol[,"Coal"],null="Level", lshort=TRUE); coalKPSS

ceKPSS<-kpss.test(datvol[,"Clean Energy"],null="Level", lshort=TRUE); ceKPSS

chmKPSS<-kpss.test(datvol[,"Chemicals"],null="Level", lshort=TRUE); chmKPSS

metalKPSS<-kpss.test(datvol[,"Metal"],null="Level", lshort=TRUE); metalKPSS

foodKPSS<-kpss.test(datvol[,"Food"],null="Level", lshort=TRUE); foodKPSS

cementKPSS<-kpss.test(datvol[,"Cement"],null="Level", lshort=TRUE); cementKPSS

KPSS.level<-c(0.1, rep(0.01, 5), 0.023452,0.01, 0.09143, 0.1 ); KPSS.level


# Trend stationarity

carbKPSS<-kpss.test(datvol[,"Carbon"],null="Trend", lshort=TRUE); carbKPSS

oilKPSS<-kpss.test(datvol[,"Oil"],null="Trend", lshort=TRUE); oilKPSS
```

```
aviationKPSS<-kpss.test(datvol[,"Aviation"],null="Trend", lshort=TRUE); ...
    aviationKPSS

ngKPSS<-kpss.test(datvol[,"Natural Gas"],null="Trend", lshort=TRUE); ngKPSS

coalKPSS<-kpss.test(datvol[,"Coal"],null="Trend", lshort=TRUE); coalKPSS

ceKPSS<-kpss.test(datvol[,"Clean Energy"],null="Trend", lshort=TRUE); ceKPSS

chmKPSS<-kpss.test(datvol[,"Chemicals"],null="Trend", lshort=TRUE); chmKPSS

metalKPSS<-kpss.test(datvol[,"Metal"],null="Trend", lshort=TRUE); metalKPSS

foodKPSS<-kpss.test(datvol[,"Food"],null="Trend", lshort=TRUE); foodKPSS

cementKPSS<-kpss.test(datvol[,"Cement"],null="Trend", lshort=TRUE); cementKPSS

KPSS.trend<-c(rep(0.01,3), 0.01999, rep(0.01,6) ); KPSS.trend

#station.b<-data.frame(DickeyFuller=ADF, PhillipsPerron=PP,
 #                      KPSS.level=KPSS.level, KPSS.trend=KPSS.trend)

#xtable(station.b, digits=3)

# ===== Cross-Correlation ===== #

#ccm(datret)
#ccm(datvol)


      # ===== ===== ===== Methodology ===== ===== ===== #
# date vector: date

          # Transforming to zoo

# For Returns


       zoodatret<-zoo(datret, order.by = date)
```

```
      orderdatret<-VARorder(zoodatret, maxp=10, output="TRUE")     # AIC ...
         = 1


# Volatility

      zoodatvol<-zoo(datvol, order.by = date)


  orderdatvol<-VARorder(zoodatvol, maxp=10, output="TRUE")    # AIC = 5

# ===== DY Connectedness ===== #

#install.packages("ConnectednessApproach")
#library('ConnectednessApproach')

# Log-returns: Static Connectedness of the full sample


  fitret = VAR(zoodatret, configuration = list(nlag = 1))



 # fitret = VAR(dy2012, configuration = list(nlag = 4))


  dyc.ret<- TimeConnectedness(Phi=fitret$B, Sigma=fitret$Q, nfore=10, ...
     generalized = TRUE)


  # Comparison with Lastrapes & Wien: Join connectedness

# lwc.ret<- JointConnectedness(Phi=fitret$B, Sigma=fitret$Q, nfore=10)

#View(lwc.ret$TABLE)

  # Comparison using Cholesky decomposition

#  Cholesky.ret<- TimeConnectedness(Phi=fitret$B, Sigma=fitret$Q, ...
   nfore=10, generalized = FALSE)
```

```
            # Return Connectedness Table


#View(dyc.ret$TABLE)

#View(Cholesky.ret$TABLE)
       # dyc.ret$NPDC

#xtable(dyc.ret$TABLE, digits = 3) # Making Latex table


  # Network Plot

#PlotNetwork(dyc.ret, "NPDC", threshold = 0)


# Log-volatilities: Static connectedness of the full sample

  fitvol = VAR(zoodatvol, configuration=list(nlag=5))

dyc.vol<- TimeConnectedness(Phi=fitvol$B, Sigma=fitvol$Q,
                            nfore=10, generalized = TRUE)


            # Volatility Connectedness Table

      # dyc.tablel <-dyc.vol$TABLE

        #dyc.vol$NPDC

#xtable(dyc.vol$TABLE, digits = 3) # Making Latex table
#PlotNetwork(dyc.vol, "NPDC", threshold = 0)



# Log-return: Dynamic connectedness

#CHOLESKY.ret<-ConnectednessApproach(zoodatret, nlag=1, nfore=10, window=100,
 #                                  model="VAR" ,connectedness="Time",
```

```
  #                               Connectedness_config = list(generalized = ...
     FALSE))


DYC.ret<-ConnectednessApproach(zoodatret, nlag=1, nfore=10, window=100,
                               model="VAR" ,connectedness="Time")

#DYC.ret6<-ConnectednessApproach(zoodatret, nlag=1, nfore=6, window=100,
                           #      model="VAR" ,connectedness="Time")

#DYC.ret18<-ConnectednessApproach(zoodatret, nlag=1, nfore=18, window=100,
                            #     model="VAR" ,connectedness="Time")

# Log-return: Dynamic connectedness of the full sample

#DYC.ret.70<-ConnectednessApproach(zoodatret, nlag=1, nfore=10, window=70,
                             #    model="VAR" ,connectedness="Time")

#DYC.ret6.70<-ConnectednessApproach(zoodatret, nlag=1, nfore=6, window=70,
                               #   model="VAR" ,connectedness="Time")

#DYC.ret18.70<-ConnectednessApproach(zoodatret, nlag=1, nfore=18, window=70,
                       #           model="VAR" ,connectedness="Time")

# Log-return: Dynamic connectedness of the full sample

#DYC.ret.200<-ConnectednessApproach(zoodatret, nlag=1, nfore=10, window=200,
                           #          model="VAR" ,connectedness="Time")

#DYC.ret6.200<-ConnectednessApproach(zoodatret, nlag=1, nfore=6, window=200,
                            #          model="VAR" ,connectedness="Time")

#DYC.ret18.200<-ConnectednessApproach(zoodatret, nlag=1, nfore=18, window=200,
                             #          model="VAR" ,connectedness="Time")

# W = 70
#PlotTCI(DYC.ret.70) # Lik H=18, men mindre tydelig på covid
#PlotTCI(DYC.ret6.70) # Mindre tydelig på COVID
#PlotTCI(DYC.ret18.70) # Lik H=10, men mer tydelig

# W = 100
```

```
#PlotTCI(DYC.ret) # Lik som H=18
#PlotTCI(DYC.ret6) # Mindre tydelig på COVID.
#PlotTCI(DYC.ret18) # Lik som H=10

# W = 200
#PlotTCI(DYC.ret.200)
#PlotTCI(DYC.ret6.200)
#PlotTCI(DYC.ret18.200)


# Log-volatilities: Dynamic Connectedness X windows

#DYC.vol10.70<-ConnectednessApproach(zoodatvol, nlag=5, nfore=10, window=70,
          #                  model="VAR",connectedness="Time")

#DYC.vol6.70<-ConnectednessApproach(zoodatvol, nlag=5, nfore=6, window=70,
        #                         model="VAR" ,connectedness="Time")

#DYC.vol18.70<-ConnectednessApproach(zoodatvol, nlag=5, nfore=18, window=70,
 #                               model="VAR" ,connectedness="Time")
#
DYC.vol<-ConnectednessApproach(zoodatvol, nlag=5, nfore=10, window=100,
                               model="VAR" ,connectedness="Time")

#DYC.vol.6<-ConnectednessApproach(zoodatvol, nlag=5, nfore=6, window=100,
   #                               model="VAR" ,connectedness="Time")

#DYC.vol.18<-ConnectednessApproach(zoodatvol, nlag=5, nfore=18, window=100,
  #                               model="VAR" ,connectedness="Time")
#
#DYC.vol10.200<-ConnectednessApproach(zoodatvol, nlag=5, nfore=10, window=200,
 #                               model="VAR" ,connectedness="Time")

#DYC.vol6.200<-ConnectednessApproach(zoodatvol, nlag=5, nfore=6, window=200,
   #                               model="VAR" ,connectedness="Time")

#DYC.vol18.200<-ConnectednessApproach(zoodatvol, nlag=5, nfore=18, window=200,
 #                               model="VAR" ,connectedness="Time")


# Plotting total connectedness - dynamic
```

```
#PlotTCI(DYC.vol10.70)
#PlotTCI(DYC.vol6.70)
#PlotTCI(DYC.vol18.70)

#PlotTCI(DYC.vol)
#PlotTCI(DYC.vol.6)
#PlotTCI(DYC.vol.18)

#PlotTCI(DYC.vol10.200)
#PlotTCI(DYC.vol6.200)
#PlotTCI(DYC.vol18.200)

#       Returns  ==========

#

# Connectedness NET

PlotNET(DYC.ret)


#       Volatility  ==========


# Connectedness TO the system
#PlotTO(DYC.vol, ylim = c(0,500))

# Connectedness FROM the system
#PlotFROM(DYC.vol, ylim = c(0,100))

# Connectedness NET

PlotNET(DYC.vol)


#Diagnostics


#var1<-MTS::VAR(as.matrix(zoodatret), p=1, output=FALSE) # Returns system
#MTSdiag(var1)
```

```
#var2<-MTS::VAR(as.matrix(zoodatvol), p=5, output=FALSE) # Volatility system
#MTSdiag(var2)

#rezz<-resid(var1)


# Q-Q plot for the first variable's residuals

par(mfrow=c(5,2))
qqnorm(rezz[,1], main = "Q-Q Plot of Residuals for Carbon")
qqline(rezz[,1], col = "red")

qqnorm(rezz[,2], main = "Q-Q Plot of Residuals for Oil")
qqline(rezz[,2], col = "red")

qqnorm(rezz[,3], main = "Q-Q Plot of Residuals for Aviation")
qqline(rezz[,3], col = "red")

qqnorm(rezz[,4], main = "Q-Q Plot of Residuals for Natural Gas")
qqline(rezz[,4], col = "red")

qqnorm(rezz[,5], main = "Q-Q Plot of Residuals for Coal")
qqline(rezz[,5], col = "red")

qqnorm(rezz[,6], main = "Q-Q Plot of Residuals for Clean Energy")
qqline(rezz[,6], col = "red")

qqnorm(rezz[,7], main = "Q-Q Plot of Residuals for Chemicals")
qqline(rezz[,7], col = "red")

qqnorm(rezz[,8], main = "Q-Q Plot of Residuals for Metal")
qqline(rezz[,8], col = "red")


qqnorm(rezz[,9], main = "Q-Q Plot of Residuals for Food")
qqline(rezz[,9], col = "red")

qqnorm(rezz[,10], main = "Q-Q Plot of Residuals for Cement")
qqline(rezz[,10], col = "red")
```

```
# Volatility

#rezz<-resid(var2)


par(mfrow=c(5,2))
qqnorm(rezz[,1], main = "Q-Q Plot of Residuals for Carbon")
qqline(rezz[,1], col = "red")

qqnorm(rezz[,2], main = "Q-Q Plot of Residuals for Oil")
qqline(rezz[,2], col = "red")

qqnorm(rezz[,3], main = "Q-Q Plot of Residuals for Aviation")
qqline(rezz[,3], col = "red")

qqnorm(rezz[,4], main = "Q-Q Plot of Residuals for Natural Gas")
qqline(rezz[,4], col = "red")

qqnorm(rezz[,5], main = "Q-Q Plot of Residuals for Coal")
qqline(rezz[,5], col = "red")

qqnorm(rezz[,6], main = "Q-Q Plot of Residuals for Clean Energy")
qqline(rezz[,6], col = "red")

qqnorm(rezz[,7], main = "Q-Q Plot of Residuals for Chemicals")
qqline(rezz[,7], col = "red")

qqnorm(rezz[,8], main = "Q-Q Plot of Residuals for Metal")
qqline(rezz[,8], col = "red")


qqnorm(rezz[,9], main = "Q-Q Plot of Residuals for Food")
qqline(rezz[,9], col = "red")

qqnorm(rezz[,10], main = "Q-Q Plot of Residuals for Cement")
qqline(rezz[,10], col = "red")
```

```
#library(vars)

#normality.test(VARz,multivariate.only = TRUE)
#VARz<-VAR(zoodatret, p=1)
#VARz
#var1

####====================####


# Forecasting h= 10
var1.forq<-VARpred(var1,h=10,orig=0,Out.level=FALSE,output=TRUE)
var2.forq<-VARpred(var2,h=10,orig=0,Out.level=FALSE,output=TRUE)

ret.for<-var1.forq$pred
ret.se<-var1.forq$se.err


plot(futdata.ret, type="l", col="red")
lines(ret.for[,"Carbon"],col="Blue")


vol.for<-var2.forq$pred
vol.se<-var2.forq$se.err


plot(futdata.vol, type="l", col="red")
lines(vol.for[,"Carbon"],col="Blue")


# 'Future data' Carbon: 01.02.2024 -
library(readr)
carb.fut <- read_csv("~/OneDrive - Universitetet i Agder/R/Master/Future ...
    Data/Carbon Emissions Futures Historical Data.csv")

#futdata<-c(62.32, 63.5, 62.59,63.49,62.32, 60.71,58.80,57.20, 56.65, 56.44)

carb.fut<-rev(carb.fut$Price)

carb.fut<-ts(as.matrix(carb.fut))
```

```
futdata.ret<-diff(log(carb.fut))*100 ; futdata.ret



futdata.vol<- 0.361 * diff((log(carb.fut)))^2
futdata.vol<-(sqrt(futdata.vol))*100
```

Chapter 10

Discussion Paper

10.1 International by Sander Østby Nordbotten

This discussion paper serves as the final part of the Master's degree in Business and Administration with a specialization in Analytical Finance at the University of Agder. Throughout this journey as a student, I have gained extensive knowledge and valuable experiences, all of which are reflected in the work of our master's thesis. I found it very interesting to collaborate with Rex in writing the thesis, and we have supported each other throughout the whole process. The discussion paper is the last requirement from the school as part of the AACSB accreditation for the School of Business and Law at UiA. In this paper, I will explore how our thesis relates to the topic of 'international' in light of research findings. First, a presentation of the thesis will be given. Second, the discussion will focus on how our thesis relates to international trends and forces. Lastly, the paper will provide a summary and conclusion.

Our thesis investigates the dynamic interactions between carbon credits, various high-energy demanding sectors within the EU Emissions Trading System, and global energy markets. We utilized the connectedness approach by Diebold and Yilmaz on data spanning from July 3, 2017, to February 1, 2024. We examined price data from carbon prices, oil, coal, the clean energy index, natural gas, the aviation index, the chemicals index, the food index, cement company, and the metal index. In this timeframe, we also captured significant events such as COVID-19 and the Russia-Ukraine war. Additionally, the connectedness of the assets was significantly impacted by the pandemic and war.

We applied a methodology with two different connectedness measures: static connectedness over the full sample period, and dynamic connectedness with smaller sub-periods of 100 days. Our findings suggest that carbon prices are influenced by shocks originating from

other assets, particularly from the Chemicals index being the main driver in both the returns and volatility systems over the full sample. Moreover, the connectedness of the assets were significantly impacted by the pandemic and war in the dynamic analysis. This paper aims to explore how the thesis connects to international trends and forces, offering a broader context for the research.

10.1.1 International trends and forces

A key part of the EU's strategy to fight climate change is the EU ETS, aligning with other international agreements like the Paris Agreement and the Kyoto Protocol. We are in a phase where it is crucial to reduce global greenhouse gas emissions, which drives the mechanism of carbon markets forward, like the EU ETS. In our study, we focus on carbon markets and demonstrate how these markets develop and operate in light of the international agreements, shaping national policies and influencing cross-border market behaviors. The EU ETS is the biggest carbon market in the world, and sets the standard for other countries and regions creating their own emissions trading systems, underscoring the global interconnection of climate policies. Additionally, the EU ETS has succeeded in reducing emissions and promoting low-carbon technologies. The scheme serve as a powerful tool that should inspire to further globally collaboration and innovation in fighting climate change.

The geopolitical landscape, especially the Russia-Ukraine war, has significant implications for global energy markets and the EU ETS. The war has interrupted the supplies of natural gas to Europe, leading to increased use of coal for electricity production. As a consequence, this has lead to higher carbon prices. This shift highlights how vulnerable energy markets are to geopolitical events, and the resulting international policy responses. Similarly, the COVID-19 pandemic also affected global markets, as the uncertainty led to economic disruptions and periods of high volatility. The pandemic caused significant fluctuations in both energy prices and demand, which were reflected in the volatility observed in carbon and energy markets during the period. The results in our thesis reflect these market dynamics, showing increased volatility in carbon, energy, and other markets during both geopolitical crises like the war and global health emergencies like COVID-19. These fluctuations affect global market stability and influence policy-making. The evolution of these crises, underscores the urgent need for the EU to reduce its dependency on fossil fuel and accelerate the development of renewable energy sources to ensure reliable and sufficient energy security.

Economic globalization has made markets more connected, as seen in the spillover effects between EU carbon markets and global energy commodities. When global markets are integrated, economic activities and policies in one region can impact other regions. Our study shows that industries like chemicals and energy commodities have notable spillovers into carbon markets, highlighting the global nature of these interactions. This emphasizes the need to consider international market dynamics and the role of multinational corporations in shaping and being shaped by these global trends. Moreover, our study reveals that changes in global energy prices, whether caused by geopolitical events or economic disruptions, lead to substantial volatility in carbon markets. This connectedness points to the necessity for coordinated international policies to manage these complex interactions effectively.

Technological advancements play a pivotal role in the shift towards renewable energy sources and the global goal of net zero CO2 emissions by 2050. As countries and companies innovate to reduce their carbon footprints, the demand for carbon allowances and the structure of the carbon markets evolve. This trend is part of the global shift towards more sustainable energy solutions, driven by international efforts to reduce carbon emissions and fight climate change. Furthermore, the adoption of renewable energy sources reduces the worlds reliance on fossil fuels. By further develop renewable sources as solar, water and wind, we contribute to reducing greenhouse gas emissions. This is also supported by the ambitious targets set by the Paris Agreement.

Increasing investments in clean energy projects not only lowers the cost of renewable technologies but also improves their efficiency and integration into the energy grid. These advancements create a competitive market for carbon allowances, prompting companies to balance their emissions through innovation and cleaner production methods. The global push for renewable energy also drives technological research and development, resulting in breakthroughs that further speed up the transition away from carbon-intensive energy sources. This dynamic interplay between technological progress and market mechanisms underscores the important role of innovation in reaching climate goals.

The EU ETS operates within a complex regulatory framework influenced by international standards and practices. Harmonizing regulatory practices across borders is crucial for the effective functioning of global carbon markets, ensuring consistent and reliable carbon pricing

and trading mechanisms. Differences in regulatory approaches can lead to market distortions, creating competitive disadvantages or opportunities for arbitrage, which can undermine the effectiveness of carbon markets. Our thesis highlights the importance of coordinated international policy efforts in addressing these challenges, promoting a more integrated and efficient global carbon trading system. This alignment is essential for achieving the broader objectives of climate policies, facilitating smoother transactions, and enhancing the overall stability and predictability of carbon markets.

The research topic of our thesis focuses on the EU ETS and how it interacts with global energy markets and high-energy demanding sectors within the EU ETS. Our research aims to explore the connectedness and spillovers between these markets, which are shaped by international economic, political, and environmental trends. The study essentially recognizes that carbon trading is a global activity influenced by international market forces.

The findings suggest that there are significant spillovers from the chemical and food sectors and minor spillovers from global energy commodities to carbon prices. This underscores how international market dynamics impact the EU ETS. Events such as geopolitical tensions, technological advancements, and economic policies all play important roles in influencing carbon markets and the EU ETS. By analyzing this, the study demonstrates the importance of considering international factors to understand and predict market behaviors.

The industries and commodities analyzed in the study are relevant worldwide, which highlights the international scope of the research. This means that local market activities can't be looked at in isolation, as they are part of a bigger, global picture. By examining sectors such as chemicals, aviation, cement, metal, and food in addition to global energy markets, within the context of the EU ETS, the study shows how international market forces have cross-border impacts.

Additionally, the operating environment of the EU ETS is heavily shaped by international policies and agreements. Factors such as the COVID-19 pandemic and the Russia-Ukraine war highlight how sensitive carbon and energy markets are to global events. These events create a complex environment where international trends need to be continuously monitored and analyzed to understand their impact on market dynamics.

10.2 Summary & Conclusion

The thesis investigates the dynamic interactions between carbon credits, various high-energy demanding sectors within the EU Emissions Trading System (EU ETS), and global energy markets, using the connectedness approach by Diebold and Yilmaz. The analysis, covering data from July 2017 to February 2024, highlights the significant impact of events such as the COVID-19 pandemic and the Russia-Ukraine war on market volatility and connectedness. The findings show that carbon prices are notably influenced by shocks from other assets, especially the Chemicals index, underscoring the global interdependence of markets. The study emphasizes the critical role of the EU ETS in reducing greenhouse gas emissions and its alignment with international climate agreements. Moreover, it highlights how geopolitical and economic factors shape energy markets. It also emphasizes the need for technological advancements and coordinated international policies to manage these markets effectively and move towards global climate goals. This research relates to the overarching topic of "international" by demonstrating how global trends and events shape and are shaped by the connectedness of carbon and energy markets.

In conclusion, the thesis is closely linked with international trends and forces. Global markets are connected, influenced by geopolitical events, technological advancements, and international regulations. These factors play a crucial role in shaping the behavior of carbon markets. Understanding these international influences is essential for policymakers, businesses, and researchers to navigate and respond effectively to the complexities of global carbon trading. This discussion paper has highlighted the international dimensions of the thesis, emphasizing the importance of considering global trends in analyzing market behaviors and outcomes.

10.3 Responsible by Rex Tim Matthew A. Fonacier

This discussion paper will draw on the knowledge I accumulated during my five years at the University of Agder. Throughout my academic journey, I studied various subjects such as economics, ethics, marketing, math, and programming. I also learned how to collaborate on group projects, act as a leader through my role as an assistant teacher, and I made many lifelong friends. This discussion paper will draw arguments and conclusions from these experiences. Furthermore, I will explore how my final school assignment, the master's thesis, relates to the broad concept of *responsibility*. This paper will approach the topic by decomposing parts of the thesis and discussing aspects related to responsibility. I will address the ethical challenges related to the main topic. Then examine how the concept of responsibility is connected to the research questions. Furthermore, identify potential issues arising from the findings. The paper is structured to first provide a brief presentation of the master's thesis, followed by an exploration of the challenges and issues related to the concept of responsibility. Subsequently, I will present strategies for mitigating these challenges. The paper will conclude with a summary and conclusion.

10.3.1 Summary of the Master's Thesis

Our thesis delved into the relationships between European Union carbon allowances, high-energy-demanding industries included within the scope of the European Emissions Trading System, and global energy commodities. Specifically, we examined price data on carbon futures, Brent crude oil, the Airlines index, natural gas, coal, the global energy index, the chemical commodities index, the metal production index, the food production index, and cement production. The chosen sample period captures significant crises such as the COVID-19 pandemic and the ongoing war between Russia and Ukraine. We focused on how these assets interact during both tranquil and crisis periods.

We applied a methodology designed to uncover the relationships in terms of *connectedness*, both on average over the full sample period and in smaller sub-periods to capture the dynamic aspects of the data. Our findings over the full sample suggest that the chemical commodities index, and to a lesser extent the food production index, were the main drivers of prices and contributed the most in terms of connectedness. The dynamic analysis revealed that connectedness varied over different phases in the sample period, with peaks corresponding to major economic and geopolitical events. Volatility connectedness demonstrated high levels

during crises such as the COVID-19 pandemic and the Russia-Ukraine conflict.

10.3.2 Potential Challenges

One of the main topics of our thesis involves exploring how carbon credits within the European Union Emissions Trading System (EU ETS) influence the industries that are required to participate in this framework, as well as how global energy markets drive these assets. A potential issue that arises is the effectiveness of carbon credits in reducing greenhouse gas emissions, which is the primary goal of the EU ETS implementation. Furthermore, wealthy companies could potentially buy their way to carbon neutrality. If a company has too few carbon allowances allocated to them and needs more quotas, a rich company can simply buy more and still present themselves as a 'green' company.

Additionally, there is the challenge of how carbon credits are allocated fairly. Deciding which industries to prioritize is complex, since energy-intensive industries often generate the most revenue. This raises questions about equity and the real impact of the EU ETS on reducing overall emissions. The allocation process needs to balance economic realities with environmental goals to ensure that the system is both fair and effective.

One of the research problems involves testing whether Brent crude oil plays a pivotal role in driving carbon credits, as suggested by recent literature. A potential issue is that the literature may have misidentified the main driver of carbon prices. Incorrectly identifying the driver can mislead others, potentially causing financial problems through improper diversification of their portfolios.

The primary findings of the analysis over the full sample period indicate that the Chemical index was the main driver of all assets in the study, both in terms of returns and volatility. This concentration of influence in the Chemical index could lead to potential market manipulation, affecting the prices of other assets in the markets. Such a dominant influence by a single index raises concerns about market stability and the integrity of price signals across interconnected markets.

The thesis highlights that markets are highly connected during crisis periods, especially during significant crises such as the COVID-19 pandemic and the ongoing war between Russia and Ukraine. Opportunity seekers might use this information to await crises and

maximize their profits. Hoping for crises to profit from others' losses is ethically wrong. In other words, if a crisis occurs, some people might focus on profit rather than helping others.

10.3.3 Mitigation

A potential solution for evaluating the effectiveness of carbon credits could involve implementing policies and enhanced monitoring to assess whether various sectors are actually reducing their greenhouse gas emissions. A comprehensive guideline requiring industry-wide cooperation, rather than relying solely on individual companies, would ensure collective responsibility in emission reduction. Additionally, imposing strict, weighted penalties on companies that fail to meet the prescribed restrictions would prevent wealthier companies from simply buying their way to carbon neutrality, thus promoting genuine environmental accountability and progress.

Enhanced monitoring could also contribute to identifying which industries could benefit from additional carbon allowances, aiding the European Union in allocating the yearly quota more effectively. This approach ensures that allowances are distributed based on actual needs and performance, promoting a more efficient and fair system for managing carbon emissions across different sectors.

The misidentification of Brent crude oil as the main driver of carbon credits could potentially lead to financial losses. A solution to this issue is to gather researchers with diverse expertise to accurately identify the main driver of carbon credit prices. This collaborative approach can provide more reliable information for policymakers and economic agents, enabling them to implement effective policies, maximize their portfolios, and avert risks related to their investments. Additionally, the proposed strategy of enhanced monitoring can be valuable, as financial markets are dynamic and evolve over time, other words: today's driver might not be tomorrow's driver. This ongoing assessment will help adapt to changing market conditions and ensure continued accuracy in identifying key factors driving carbon credit prices.

The potential issue of the Chemical index having major influence on other markets, and the risk of market manipulation through the Chemical industry, requires careful attention. A possible strategy to mitigate this is for regulatory bodies to enforce greater transparency within the Chemical industry. Firms should be required to undergo audit inspections by reputable auditing firms, with these auditors reporting their findings directly to the govern-

ment. This approach would ensure fair trade practices, prevent manipulation, and maintain market integrity, thereby protecting other sectors from undue influence. However, the implementation of this strategy might be resource-demanding for smaller nations, which could instead allocate those resources to other more critical areas.

Lastly, on the potential issue of opportunity seekers hoping for crises to profit from others' losses, a potential solution could be for governments to enforce strict guidelines on businesses operating during crises. These guidelines could include measures such as limiting the prices of their services or products. This way, businesses would be restricted from profiting excessively during crises, ensuring that the focus remains on helping others rather than exploiting the situation for financial gain.

10.3.4 Summary & Conclusion

This paper presented four potential issues derived from our master's thesis related to the responsible management of markets and carbon credits. First, there is the potential issue of carbon credits' effectiveness in mitigating greenhouse gases across various sectors. Second, the possibility of misidentifying Brent crude oil as the main driver of carbon prices could lead to financial problems by providing misleading information to economic agents seeking to diversify their portfolios. Third, the heavy influence of the Chemical index on other markets raises concerns about potential market manipulation. Fourth, opportunity seekers might exploit our findings that markets are highly connected during crises, using this information to profit unethically.

To address these issues, the paper proposed four potential solutions. A key strategy is to develop a comprehensive guideline that requires industry-wide cooperation to facilitate collective responsibility in emission reduction. Enhancing procedures for monitoring carbon reduction can also contribute to the fair allocation of carbon permits. Additionally, enforcing strict transparency regulations within the Chemical industry can prevent market manipulation. Lastly, implementing strict guidelines on how businesses should operate during crises can prevent opportunistic behavior, ensuring that the focus remains on supporting others rather than exploiting the situation for profit.

These strategies aim to mitigate the identified issues and promote a fair and responsible approach to responsible managing carbon credits and market behavior, ensuring the integrity

and stability of the markets involved.

In summary, through the implementation of carbon allowances and their impact on various industries, the responsible party, namely the European Union, should carefully consider the consequences of this approach. Further down the line, researchers providing valuable insights must also be cautious about the information they present to prevent policymakers and economic agents from making critical mistakes based on their findings. Additionally, firms should not only consider their own benefits but also the potential negative impacts on customers and other industries.

In conclusion, responsibility manifests in many forms and exists at different levels. Thus, while our thesis may not be highly significant on its own, it carries responsibility through its main topic, research problems, insights, and findings, as well as the potential consequences for others.